University of California, Berkeley: DISS-516

SPACE SCIENCES LABORATORY

EFFECT OF WAVE LOCALIZATION ON PLASMA INSTABILITIES

William Kirk Levedahl

Department of Physics
and
Space Sciences Laboratory
University of California
Berkeley, CA 94720

(NASA-CR-184708) EFFECT OF WAVE LOCALIZATION ON PLASMA INSTABILITIES Ph.D. Thesis (California Univ.) 129 p CSCL 20I

N89-[illegible]

Unclas
G3/75 [illegible]

Ph. D. Dissertation

October, 1987

UNIVERSITY OF CALIFORNIA, BERKELEY

Effect of Wave Localization on Plasma Instabilities

William Kirk Levedahl

ABSTRACT

The Anderson model of wave localization in random media is invoked to study the effect of solar wind density turbulence on plasma processes associated with the solar type III radio burst. ISEE-3 satellite data indicate that a possible model for the type III process is the parametric decay of Langmuir waves excited by solar flare electron streams into daughter electromagnetic and ion-acoustic waves. The threshold for this instability, however, is much higher than observed Langmuir wave levels because of rapid wave convection of the transverse electromagnetic daughter wave in the case where the solar wind is assumed homogeneous. Langmuir and transverse waves near critical density satisfy the Ioffe-Riegel criteria for wave localization in the solar wind with observed density fluctuations ~1%. Numerical simulations of wave propagation in random media confirm the localization length predictions of Escande and Souillard for stationary density fluctuations. For mobile density fluctuations localized wave packets spread at the propagation velocity of the density fluctuations rather than the group velocity of the waves.

Computer simulations using a linearized hybrid code show that an electron beam will excite localized Langmuir waves in a plasma with density turbulence. An action principle approach is used to develop a theory of non-linear wave processes when waves are localized. A theory of resonant particles diffusion by localized waves is developed to explain the saturation of the beam-plasma instability. It is argued that localization of electromagnetic waves will allow the instability threshold to be exceeded for the parametric decay discussed above.

Acknowledgments

I thank first and foremost my wife, Barbara, for her encouragement and understanding throughout this project.

The problem I treat here grew out of the work of R. P. Lin and W. Lotko on interpreting ISEE-3 satellite data relating to the type III solar radio burst. My understanding of the problem is the result of many conversations with them. I am indebted to R. P. Lin and my thesis advisor, K. A. Anderson, for guidance and support throughout my graduate studies, and for advice on this project. Conversations with I. Cairns and M. V. Goldman have been fruitful.

My understanding of plasma physics and non-linear dynamics owes much to the lectures and seminars of A. Kaufman, A. Lichtenberg, and M. Lieberman, and many of the ideas here arose out of their work and their presentations, as well as the presentations of their students. In particular, A. Kaufman introduced me to the action principle approach to plasma physics, which has provided natural language for describing plasma wave processes, in addition to being of enormous computational utility. C. K. Birdsall's support, in terms of computer time, and in terms of expertise in plasma simulations, was essential for the completion of this project. The book *Quantum Chaos*, edited by M. Casati, was also a source of much inspiration, and the paper by F. Escande and B. Souillard was seminal. I gratefully acknowledge K. Anderson, A. Kaufman, M. Lieberman and R. P. Lin for their critical reading of this manuscript, which has benefited from their comments.

I am indebted to Marsha Colby for manuscript preparation. To Marge Currie I express gratitude for keeping our world at Space Sciences Lab from total chaos.

This work was supported by NASA grants NAG5-376 and NAGW-516.

Table of Contents

1. Introduction

In the usual picture of weak plasma turbulence theory, the elementary excitations are taken to be plane waves that propagate unimpeded to infinity. These elementary excitations are the standard plasma waves: Langmuir waves, ion-acoustic waves, electromagnetic waves, etc. (*Tsytovich*, 1977). The plasma which supports the waves is assumed uniform, infinite and homogeneous except for the possible inclusion of a constant uniform magnetic field. Density gradients or fluctuations are treated as weak perturbations which refract waves smoothly or cause scattering of one elementary excitation into another.

The picture that waves are freely propagating for times in the remote past and far future, and that interactions all take place in some intermediate time is a fundamental assumption in weak and multiple-scattering theories. On the other hand, a Langmuir or electromagnetic wave which originates and propagates near the critical density will be strongly scattered and modified by relatively small density fluctuations, and the scattering theory picture may not be valid.

In his famous 1958 paper, P. W. Anderson investigated another picture for the elementary excitations in a randomly disordered system. In studying the absence of spin diffusion in silicon at low temperatures, he suggested that spin wave excitations, when the localized site frequencies are randomly distributed, are time-stationary wave packets localized in space with approximately exponential fall-off in amplitude away from the site of localization. The Hamiltonian he considered is equivalent to that of a wave excited in a medium with a random index of refraction, and so is equivalent to the problem of a wave in a plasma with a density that fluctuates randomly about some average density.

In this thesis we adopt the point of view that the elementary excitations of a plasma with turbulent density variations are, in fact, weakly interacting localized (and therefore quantized) waves. The significance of this picture is profound. It suggests that a gentle bump-on-tail instability will excite localized modes with central wave numbers resonant with the beam. Therefore the amount of beam energy extracted should be greatly reduced in comparison with a beam propagating

through a uniform plasma. Wave-wave coupling processes will be modified. First, coupling constants must be reduced by a geometric factor that accounts for the spatial overlap between the coupled waves. Second, there is no wave convection for the localized waves, so the threshold for 3-wave processes is correspondingly modified.

One significant difference between a turbulent plasma and a crystalline lattice with random impurities is that the former does not have a time stationary Hamiltonian. Our point of view is that the turbulence is externally or self-consistently driven and independent of the waves in which we are interested. The effect of time dependent turbulence on localization is therefore an essential consideration.

The motivation for this study is to attempt to clear up certain problems in the understanding of the type III solar radio burst. We adopt the model for this phenomenon presented by *Cairns* (1984) and *Lin et al.* (1986), which is, in brief, the following. High energy electrons, accelerated by solar flares, stream through the solar wind plasma and excite Langmuir waves through a gentle bump-on-tail instability. These Langmuir waves then decay parametrically into an ion-acoustic wave and an electromagnetic wave (at the local plasma frequency). These electromagnetic waves are then observed at the earth by microwave receivers as the narrowband emission that is characteristic of the type III burst. Although there is strong experimental evidence for this process, some theoretical issues remain unresolved.

One remaining issue is the ability of the beam to propagate out to 1 AU without disruption while maintaining a well-defined positive slope. Another is that the electromagnetic decay is a convective instability with growth lengths larger than are consistent with the problem. A third is the spikey nature of the wave envelope of the Langmuir waves. It has been apparent for some time that the resolution of these difficulties must lie in density inhomogeneities in the solar wind plasma. While evidence for the existence of the density turbulence is strong, the details of the turbulence are still unclear. Efforts to understand the effect of the turbulence within the framework of traditional weak turbulence theory have generally required very special assumptions about the nature of the density fluctuations and often more problems are raised than solved. Localization, on the other

hand, is a universal characteristic of random media (for sufficiently strong turbulence), as will be discussed, and any theory must consider the effects of this as well.

The effect of density fluctuations on 3-wave processes has recently been discovered to have a pronounced effect in another context. *Rose et al.* (1987) have shown in plasma simulations that the ion-density fluctuations produced by Stimulated Brillouin Scattering, when sufficiently strong, will spatially localize the Langmuir waves produced by Stimulated Raman Scattering (SRS). Since the allowed Langmuir waves are now quantized, the SRS instability may or may not be suppressed, depending upon whether any of the quantized Langmuir waves satisfy the 3-wave frequency and wave-number matching criterion. In this case, however, the trapping of the Langmuir waves is within a single density depression and can be interpreted semi-classically, which will not be the case for the problem considered in this thesis.

This thesis is organized as follows. In order to motivate this thesis and set the problem in context we begin in section 2 with a review of the type III solar radio burst problem, presenting essential satellite data and current models that attempt to explain these data.

In section 3 we discuss the action principle in plasma theory which will provide the theoretical framework for the remainder of the thesis. In section 4 wave propagation in random media is discussed. Multiple scattering theory is reviewed to explain why it is inadequate for this problem. The Anderson model of wave localization is then discussed. The results of 1-D numerical simulations of the time evolution of gaussian wave packets in random media are presented in section 5. These simulations verify the localization length predictions of *Escande and Souillard* (1984). The effect of mobile density fluctuations is also studied in secion 5.

The bump-on-tail instability in random media is investigated in section 6. A theory for this instability is developed which takes into account that the excited waves are localized by the Anderson mechanism. Results of a 1-D hybrid simulation are presented verifying this model. A theory for the saturation of the bump-on-tail instability by resonant diffusion of beam particles by localized waves is developed and compared with numerical simulation and experiment.

Section 7 begins with a discussion of 3-wave decay processes based on an action principle. Convective effects in homogeneous media and in media with a uniform density gradient are discussed to conclude that the 3-wave process under consideration has too high a threshold. Previous work in 3-wave processes in inhomogeneous media is reviewed. Implications of Anderson localization for the 3-wave process are then developed.

2. Type III Solar Radio Burst — Observations and Current Theory

We begin with a discussion of the type III solar radio burst phenomenon and a presentation of current satellite data. The arguments in favor of a 3-wave decay model for the phenomenon are reviewed, and experimental measurements of density fluctuations in the solar wind are discussed.

The type III solar radio burst is one of the oldest problems in radio astronomy; however, it is not yet understood in theoretical detail. Originally discovered by *Wild and McCready* (1950), the phenomenon is observed by an RF spectrograph at the earth as a narrowband RF emission, starting at ~250 MHz and decreasing over a time period of ~5-15 sec down to ~5 MHz. Observations at lower frequencies using ground-based systems are not possible because of ionospheric reflection. Satellite observations have extended the lower range down to ~10 kHz. Very often emission at or near the 2nd harmonic is observed simultaneously with the above. *Wild* (1950) proposed that the burst was caused by a disturbance which started low in the solar corona and propagated outward, exciting plasma oscillations of progressively decreasing frequency. Later it was established that the disturbance propagates at a velocity ~c/3 from which it was inferred that the disturbance was caused by electron streams (*Wild*, 1954). More recent satellite observations, discussed below, have confirmed that the source of the burst is associated with electrons propagating along open magnetic field lines away from the sun. An interesting peculiarity is that there are some bursts whose frequency decreases and then increases again. These are interpreted as bursts due to electrons traveling on closed field lines associated with coronal loops and returning to regions of higher plasma density near the sun.

IMP-6 satellite observations at 1 AU (*Fainberg and Stone*, 1974) showed that the type III radio emission extends down to ~30 kHz and the burst duration extends to many minutes or hours. *Fainberg and Stone* were also able to show that the emission region follows the Archimedean spiral of the open magnetic field lines predicted by *Parker* (1958). More recent satellite observations in connection with observations from ground-based solar observations have established that electrons with energies from a few keV to ~100 keV, accelerated in solar flares, are responsible for type III

emission.

The most detailed data on the type III solar burst come from the ISEE-3 satellite in orbit at the Lagrange point ~258 R_E upstream (towards the sun) from the earth. The satellite carries the University of California solar electron experiment, which provides electron energy measurements from 2 keV to 1 MeV, and the joint TRW-JPL-Iowa plasma wave instrument which provides electric field measurements in frequency channels from 17.8 Hz to 100 kHz. *Lin et al.* (1981) were able for the first time to measure the electron distribution function parallel to the IMF (interplanetary magnetic field) and show that it develops a well defined bump-on-tail distribution. This study was continued and results more fully interpreted by *Lin et al.* (1986). These results form the basis for the rest of this thesis and are discussed in detail here. For detailed history of type III observations with pertinent references see the review by *Goldstein* (1983). We shall next discuss the data from the *Lin et al.* (1986) study for a typical solar type III radio burst.

Type III Event — 11 March 1979

Table 2.1 shows typical plasma parameters for the event. Figure 2.1 shows the high-energy non-thermal electron flux associated with the event along with electric field measurements for the 11 March 1979 event. The emission in the 100 kHz channel starting at ~10:40 UT is characteristic of the type III emission. It is interpreted as radio emission upstream of the spacecraft which propagates to the spacecraft. Onset of emission at lower frequencies occurs later. Activity in the 17.8 kHz channel, corresponding to the local plasma frequency, occurs with the arrival of electrons in the 8.5 keV channel and corresponds to times when a positive slope bump-on-tail is observed in the reduced parallel electron distribution function shown in Figure 2.2.

Figure 2.3 shows a portion of the same event in high time resolution. The important points to observe are the intense spikiness of the Langmuir waves in the 17.8 kHz channel, and the coincidence of activity in the 100 Hz channel with the most intense spikes of the Langmuir waves. Early on there was some ambiguity about whether the radiation observed by satellite is fundamental or 2nd harmonic emission, but it seems certain from these data that the emission is fundamental

emission.

The following assumptions are made in interpreting the above results. The dominant wave number for the Langmuir waves is given approximately by the beam resonant wave number $k_0 = \omega_p / v_b$ where v_b is the beam velocity. The ion-acoustic waves observed in the 100 Hz channel are actually much lower in frequency and are Doppler shifted by convection past the satellite by the solar wind, i.e., $\omega' = \omega + k\, V_{SW} \cos\theta$ (θ is the angle between the solar wind direction and the interplanetary magnetic field). Assuming $\omega \ll \omega'$, one calculates the wave number for the ion-acoustic waves as

$$k_s \cong \frac{\omega_{\text{observed}}}{V_{SW} \cos\theta} .$$

The actual frequency is then inferred from $\omega_s = k_s c_s$.

Based on the above data *Cairns* (1984) was the first to propose that the important emission mechanism for the type III emission is the parametric decay process L (Langmuir) $\rightarrow T$ (transverse electromagnetic) $+ S$ (ion-acoustic). The argument was based on considering the volume emissivity (brightness temperature) of various 3-wave processes. The weak turbulence process $L \rightarrow T + S$ (random phase approximation) produces emissivities that are far too small. Further evidence for this process was observed in the experiment of *Whelan and Stenzel* (1985). In this experiment Langmuir waves were excited with a weak beam. Electromagnetic radiation at the plasma frequency was observed to occur with growth that closely followed the growth of ion-acoustic waves. The ion-acoustic waves were observed to have a wave number $k_s \cong k_L$, the wave number of the Langmuir waves. This process was also observed in a 2-D numerical simulation (*Pritchett and Dawson*, 1976); however, they interpreted it as a two-step process:

$$L \rightarrow L' + S$$

followed by

$$L + S \rightarrow T .$$

In space, however, the threshold for the process $L \rightarrow L' + S$ is not satisfied by several orders of magnitude (*Lin et al.*, 1986).

A fundamental difficulty with this interpretation is that in homogeneous media the process is in fact a convective instability, since the threshold for absolute instability is not exceeded as a result of rapid convection of transverse wave energy and the high damping rate of the ion-acoustic waves. This is an involved argument and will be taken up again in section 7.2. In fact, the solar wind is not uniform and we will argue that the solar wind density turbulence is fundamental for understanding the type III process.

We note briefly that the frequency and wave matching coupling conditions will give a daughter ion-acoustic wave with wave number $k_s \cong k_L$. The transverse wave will be polarized with the electric field along the direction of the Langmuir pump and propagate transverse to this direction with wave number

$$k_T^2 = \frac{3 v_{th}^2 k_L^2}{c^2} \left[1 - \frac{2}{3} \frac{c_s v_b}{v_{th}^2} \right]$$

(*Lin et al.*, 1986). We note that

$$k_T \ll k_L \quad \text{and} \quad \omega_T = \omega_L + \omega_S \cong \omega_L \, .$$

This is discussed fully in section 7. For the March 11 event this gives $\lambda_T = 360$ km.

Many efforts have been made to understand the type III mechanism as the result of a modulational instability leading to soliton formation and collapse. The experimental evidence does not support this, and furthermore the threshold condition

$$\frac{E_0^2}{8\pi nkT} > 3\,(\Delta k\, \lambda_D)^2 ,$$

where Δk is the half width at half maximum of the spectrum of beam excited Langmuir waves is not satisfied. This is a complex subject with a very extensive literature, and shall not be discussed further here (but see *Lin et al.*, 1986 and references therein).

Solar Wind Plasma Density Fluctuations

Figure 2.4 shows a 3-hour time averaged power spectrum of solar wind density fluctuations that was obtained by *Celnikier et al.* (1981) by measuring the phase shift in a radio beam propagating between the two satellites ISEE-1 and -2. While fluctuations occur at all wavelengths, it is particularly noteworthy that fluctuations with wavelengths of ~100 km have $\delta n/n \gtrsim 1\%$. Little is known in detail about these fluctuations, and there are no results available simultaneous with a type III burst. On the other hand, density fluctuations of this level appear to be a universal feature of the solar wind, confirmed both by scintillation measurements (*Coles and Harmon*, 1978) and by recent Giotto satellite data (*R. P. Lin*, unpublished data). The fluctuations seem to be nearly isotropic with a ratio of fluctuations parallel to the interplanetary magnetic field to those perpendicular to the magnetic field being less than 2:1. Although these fluctuations may be a kinetic drift wave instability (*Mikhailovsky*, 1983) resulting from initial solar wind inhomogeneities at the corona. magnetic field fluctuations suggest that they might be electromagnetic in origin (*M. Goldman*, private communication).

For some time now there has been an awareness that density fluctuations must play a role in the type III problem. The first problem that has bothered people is that Langmuir waves come in clumps or packets ~70 km in extent (see Figure 2.3). Since the electromagnetic radiation is very uniform in time (i.e., Figure 2.1, 100-31.6 kHz channels) one concludes that this clumpiness is spatial rather than temporal. *Smith and Simes* (1977) studied the propagation of Langmuir waves through a turbulent plasma using ray-tracing techniques to conclude that enhancements and reductions would result due to random ray focusing. They concluded, however, that the main cause of the clumping was that the rays would be resonant with the beam leading to growth in certain regions. Implications of this reasoning for 3-wave processes have been examined by *Melrose et al.* (1986). The remainder of this thesis is an effort to understand the effect of density turbulence in detail. In particular we will argue that the correct effects of the density turbulence can only be predicted by studying the full wave equation in random media, and that ray tracing is not a satisfactory approximation when attempting to understand wave behavior near critical density.

It should be noted that much of the effort of solar radio astronomers has employed ray tracing techniques to map observations at the earth back to the source region in the solar wind. Although much of this work is probably valid when identifying source regions, conclusions about the exact size or geometry of source regions is questionable.

3. Theoretical Introduction

In order to make theoretical progress with this problem we use an action principle approach for a wave-plasma system (*Dewar*, 1970, 1972,1973; *Johnston and Kaufman*, 1978*a,b*, 1979; *Kaufman et al.*, 1984; *Crawford et al.*, 1986; *Similon et al.*, 1986; *Kaufman*, 1982, 1987). In this approach we begin with a many particle Lagrangian

$$L = \sum_i \left[\frac{m_i}{2} \dot{\underline{x}}_i^2 - \frac{e}{c} \dot{\underline{x}}_i \cdot \underline{A}(\underline{x}_i) - e_i \phi(x_i) \right] - \frac{1}{8\pi} \int d^3\underline{x} \, [\, |E|^2 - |B^2| \,] \tag{3.1}$$

where $\sum_i$ represents a sum over all particles in the system.

This may be re-written, using a canonical transformation, as

$$L = \sum_i \left[p_i \dot{x}_i - h_i(x_i, p_i; \underline{A}x_i)) \right] - \frac{1}{8\pi} \int d^3\underline{x} \left[|E|^2 - |B|^2 \right] \tag{3.2}$$

where

$$h_i = \frac{1}{2m} \left(p_i - \frac{e_i}{c} A(x_i) \right)^2 + e_i \phi(x_i)$$

is the single particle Hamiltonian. The least action principle with this N-body Lagrangian, in principle, determines the time evolution of any (non-relativistic) system of interacting particles and electromagnetic fields.

We shall divide the particles into groups according to the following distribution functions:

1) $f_{0e}(x,v,t)$ = non-uniform solar wind background electron distribution;

2) $f_{0i}(x,v,t)$ = non-uniform solar wind background ion distribution;

3) $f_{be}(x,v,t)$ = electron beam distribution function.

In the particular type III problem, the beam density is 5-6 orders of magnitude below the solar wind density, and therefore, we make the following separation of terms. We define E^{SC}, B^{SC}, A^{SC}, and ϕ^{SC} to be self-consistent fields arising from strong turbulence associated with non-uniformities in the solar wind, and then define $E^{(1)} = E - E^{SC}$, $B^{(1)} = B - B^{SC}$, $A^{(1)} = A - A^{SC}$, and

$\phi^{(1)} = \phi - \phi^{SC}$.

We use these definitions to expand the Lagrangian as:

$$L = \sum_{i_{BG}} \left[p_i \cdot \dot{x}_i - \frac{p_i^2}{2m_i} + \frac{e_i}{m_i c} p_i \cdot A^{SC}(x_i) - \frac{e_i^2}{2m_i c^2} |A^{SC}(x_i)| - e_i \phi^{SC}(x_i) \right] - \frac{1}{8\pi} \int d^3x \, |E^{SC}|^2 - |B^{SC}|^2$$

$$+ \sum_{i_{BG}} \left[\frac{e_i}{m_i c} p_i \cdot A^{(1)}(x_i) - \frac{e_i^2}{2m_i c^2} |A^{(1)}(x_i)|^2 - e_i \phi^{(1)}(x_i) \right] - \frac{1}{8\pi} \int d^3x \left[|E^{(1)}|^2 - |B^{(1)}|^2 \right]$$

$$+ \sum_i \frac{e_i^2}{m_i c^2} \left| A^{(1)}(x_i) \cdot A^{SC}(x_i) \right| - \frac{1}{8\pi} \int d^3x \, (E^{(1)} E^{SC} - B^{(1)} B^{SC}) \tag{3.3}$$

$$+ \sum_{i_b} \left[p_i \cdot \dot{x}_i - \frac{p_i^2}{2m_i} + \frac{e_i}{m_i c} p_i \cdot A_i^{(1)} - \frac{e_i^2}{2m_i c^2} |A^{(1)}(x_i)|^2 - e_i \phi^2_{(xi)} \right]$$

$$+ \sum_{i_b} \left[\frac{e_i}{m_i c} p_i \cdot A^{SC}(x_i) + \frac{e_i^2}{m_i c^2} A^{(1)}(x_i) A^{SC}(x_i) - \frac{e_i^2}{2m_i c^2} |A^{SC}(x_i)|^2 - e_i \phi^{SC}(x_i) \right]$$

where i_{BG} refers to background particles and i_b refers to beam particles, and $i = i_{BG} + i_b$.

Let us begin to investigate equation 3.3. We choose our definition of the self-consistent fields such that in the absence of beam particles, the first line completely describes the evolution of the solar wind background particles and their self-consistent fields, i.e., variations of the first line with respect to A^{SC}, ϕ^{SC}, x_{BG}, and p_{BG} vanish. In general, for density distributions and magnetic fields present in the solar wind, this is an intractable and unsolved problem in strong turbulence theory which will produce a whole zoo of drift waves, magneto-acoustic waves, etc. We do not discuss this part further, but imagine the problem solved, giving us the turbulently fluctuating background distribution functions and self-consistent fields $f_{0i}(x, v, t)$, $f_{0e}(x,v,t)$, $A^{SC}(x,t)$, and $\phi^{SC}(x,t)$. We shall be concerned with the further evolution of the system due to other waves and the beam particles, having assumed that we can separate out the strong turbulence portion of the problem (not amenable to an order by order perturbation treatment).

In typical approaches to such problems the Lagrangian is divided into a time averaged part and a fluctuating part. The time averaged part is defined as

$$\bar{L} = \frac{1}{T}\int_0^T L$$

and the fluctuating part as

$$\tilde{L} = L - \bar{L} \ .$$

A suitable canonical transformation will transform the fluctuating part to higher order in the expansion, as discussed below. The order of a term in the expansion is given by the sum of the powers of the field quantities. In the approach developed by *Johnston and Kaufman* (1978), this transformation is accomplished by a Lie transform on the particle coordinates x_i, p_i, giving a time averaged (guiding center) part plus a higher order term that will involve the electromagnetic fields. The Lagrangian, expressed in the new variables, is then solved, order by order, using a least action principle.

Thus we define the transform of a function on phase space (x, p) as (*Cary*, 1978; *Lichtenberg and Lieberman*, 1983):

$$e^L = 1 + L + \frac{1}{2}L^2 + \frac{1}{6}L^3 + \ldots$$

where, if $A = A\,(x,p)$, then

$$LA \equiv \sum_i \left[\frac{\partial w}{\partial x_i}\frac{\partial A}{\partial p_i} - \frac{\partial w}{\partial p_i}\frac{\partial A}{\partial x_i}\right] \equiv \{w, A\}$$

for any given $w = w(x,p)$.

In this transformation scheme the new coordinate variables become

$$P = e^L p$$

$$X = e^L x$$

and the particle Hamiltonian is

$$K = e^L H$$

if H is ordered,

$$H = H^{(0)} + H^{(1)} + H^{(2)}$$

then we define terms in the transformed Hamiltonian:

$$\begin{aligned}
K^{(0)} &= H^{(0)} \\
K^{(1)} &= H^{(1)} + LH^{(0)} \\
K^{(2)} &= H^{(2)} + LH^{(1)} + \frac{1}{2} L^2 H^{(0)} \\
K^{(3)} &= \frac{1}{L} L^3 H^{(0)} + \frac{1}{2} L^2 H^{(1)} + LH^{(2)}, \text{ etc.}
\end{aligned} \tag{3.4}$$

In our problem we shall not consider terms over 3rd order. We then have the action

$$S = \int_{t_0}^{t} dt \left(\sum_i p_i \cdot \dot{x}_i - k_i (x_i, p_i, A) - L_{\text{fields}} \right)$$

Where L_{fields} is independent of the particle coordinates and therefore is unchanged by the Lie transform. This transforms to

$$S = \int_{t_0}^{t} dt \left[\sum_i P_i \cdot \dot{X}_i - K_i (X_i, P_i \,;\, A) - L_{\text{fields}} \right] .$$

We choose w such that $K^{(1)}$ vanishes, or $H^{(1)} = -\{w, H^0\}$. Since, in fact, $\{w, H^0\} = \frac{dw}{dt}$ for unperturbed trajectories, $w = -\int^t H^{(1)} dt$, integrated over unperturbed particle trajectories $x = x_0 + \frac{P_0}{m} t$; $P = P_0$.

The third line in equation 3.3 will time average to zero (since we assume that the turbulent spectrum means that there is little self-consistent field energy at a frequency and wave number resonant with the wave under consideration. This is supported by *I. Cairns*'s (1984) argument that random phase processes do not explain the intensities observed. We shall also assume that the last line in equation 3.3 can be ignored. This is equivalent to assuming that the turbulent fields have little energy resonant with the beam electrons, and so therefore the effect on beam propagation can be neglected. When the Lie transform is applied we will get a term of the form

$$\sum_i \frac{e_i^3}{m_i c^3} F(A^{(1)}(x_i), A^{(1)}(x_i), A^{\text{SC}}(x_i)) .$$

where F is a function linear in its arguments. This term is very small compared with those of the 2nd line also quadratic in $A^{(1)}$, and therefore can be ignored. We shall from here on ignore ions in the quantities involving wave-coupling terms since the coupling terms go as $\frac{e^2}{m}$ and $\frac{e^2}{m_e} \gg \frac{e^2}{m_i}$.

Wave Propagation in a Turbulent Plasma

With the beam switched off, the evolution of a wave of sufficiently small amplitude that its effect is negligible on the development of the strong density turbulence, will be governed by the second line of equation 3.3:

$$S^{(1)}=\int_{t_0}^{t_1} dt \left\{ \sum_{i_{BG}} \frac{e_i}{m_i c} p_i A_i^{(1)}(x_i) - \frac{c^2}{2m_i c^2} |A^{(1)}(x_i)|^2 - \frac{1}{8\pi} \int d^2x \, |E^{(1)}|^2 - |B^{(1)}|^2 - e_i \phi^1(x_i) \right\}$$

If we take

$$H^{(1)} = \sum_i \left(\frac{e_i}{m_i c} p_i \cdot A_i^{(1)}(x_i) - e_i \phi^{(1)}(x_i) \right),$$

then $w = -\int^t dt \; H^{(1)}$ (*Johnston and Kaufman*, 1979).

Using this, we find

$$K^{(2)} = \frac{1}{2} \{ w, H^{(1)} \}$$

and

$$S = \int_{t_0}^{t_1} dt \left[\frac{1}{2} \{ w, H^{(1)} \} - \sum_i \frac{c^2}{2m_i c^2} |A^{(1)}(x_i)|^2 - \frac{1}{2\pi} \int d^2x \, |E^{(1)}|^2 - |B^{(1)}|^2 \right]$$

Every term in this expression is quadratic in the fields. If we can use the eikonal representation of a wave, then

$$A = \tilde{A} \, e^{i\theta(x,t)} + \tilde{A}^* e^{-i\theta(x,t)},$$

where θ is a rapidly varying phase and $\tilde{A}(x,t)$ an amplitude that is slowly varying in time and space. *McDonald et al.* (1985) have shown that this is equivalent to

$$S = \int dt \, d^3x \tilde{A}^*(k,\omega;\, x,t) \cdot \overleftrightarrow{D}(k,\omega; x,t) \cdot \tilde{A}(k,\omega;\, x,t)$$

where $\overleftrightarrow{D}$ is the normal dispersion tensor. Variation with respect to the field amplitudes then gives

$$\frac{\delta S}{\delta A} = 0 = \overleftrightarrow{D}(k, \omega) \cdot \underset{\sim}{A}(k, \omega),$$

which is the usual dispersion relation.

For example, if we only consider electrostatic waves of the form

$$\phi = \tilde{\phi}\ e^{i(kx-\omega t)} + cc\ .$$

then

$$w = \sum_j e_j \frac{i\ \tilde{\phi}\ e^{i(k \cdot x_j - \omega t)}}{kv_j - \omega} + cc$$

and

$$S = \int dt\ \frac{1}{2}\ \{w, H^1\} - \frac{1}{8\pi} \int d^2x\ |\nabla \phi|^2$$

$$= -\int dt \sum_i \frac{1}{2} \frac{e_i^2}{m_i} \frac{k^2\phi^2}{(kv_i - \omega)^2} - \frac{1}{8\pi} \int d^3x\ k^2\phi^2\ .$$

Using the Vlasov representation of particle phase space density:

$$\sum_i = \sum_i \int d^3x\, d^3v\, \delta(x - x_i)\, \delta(v - v_i) \equiv \int d^3x\, d^3v\, f(x_i v_i t)$$

we find

$$S = \int dt \int d^3x\ \frac{k^2\phi^2}{8\pi} \left[\int d^3v\ \frac{4\pi e^2}{m}\ \frac{f(x, v, t)}{(kv - \omega)^2} - 1 \right]. \tag{3.4}$$

The quantity in brackets will be recognized as $\varepsilon(k, \omega)$, familiar from the usual plasma kinetic theory (*Lifshitz and Pitaevskii*, 1981). It should be recalled in examining equation 3.4 that this does involve the turbulent particle motions, since $f(x, v, t)$ involves the instantaneous particle positions and velocities.

While the Lagrangian approach does lead nicely to a dispersion relation in k-space in the uniform density case, it does not immediately give us a convenient equation for the time dependence of wave amplitude in the turbulent case. Therefore, we back up a step and redo this part of the problem using fluid equations of motion. (*Nicholson*, p. 27ff). Actually, the fluid equations of motion follow from a Lagrangian such as equation 3.2 by taking suitable moments of the

distribution function and expressing them as fluid quantities (*Dewar*, 1970). For the case of longitudinal waves:

$$\frac{\partial n_e}{\partial t} = -\nabla \cdot (n_e v)$$

$$\frac{\partial v}{\partial t} = -\frac{e}{m} E - \frac{\gamma kT}{m n_o} \nabla n_i$$

$$\nabla \cdot E = -4\pi e (n_e - n_i)$$

We will further assume that $n_i = n_i(x, v, t)$ is already known from the strong turbulence problem and that quasi-neutrality holds. This latter condition is quite good in the type III problem, since $\lambda_D \sim 22$ m, while $\lambda_{\text{Langmuir}} \sim 2.8$ km.

We get

$$\frac{\partial^2}{\partial t^2} (\nabla \cdot E) = \nabla \cdot \left[-\frac{4\pi e^2 n_i}{m} E + \frac{\gamma kT}{m} \frac{\partial^2 E}{\partial x^2} \right] - 4\pi e \nabla \cdot ([\nabla \cdot (n_e v)] v) .$$

The last term is $O(v^2)$ and will therefore be ignored. Therefore, for longitudinal waves

$$\frac{\partial^2}{\partial t^2} E = -\omega_p^2(x) E + 3 v_{th}^2 \frac{\partial^2 E}{\partial x^2}$$

where $\frac{\gamma kT}{m} \equiv 3 v_{th}^2$.

Beginning with Maxwell's equations, it is elementary to derive a similar equation for electromagnetic waves

$$\frac{\partial^2 E}{\partial t^2} = -\omega_p^2(x) + c^2 \frac{\partial^2 E}{\partial x^2}$$

where again $\omega_p^2(x) \equiv \frac{4\pi e^2}{m} n_i(x, t)$ is determined by the strong turbulence problem.

The properties of these wave equations form the content of the next chapter in Anderson localization. Upon concluding with that, we will return in chapters 6 and 7 to our Lagrangian to understand the beam-plasma and wave-wave interactions.

We discuss, finally, our assumptions about the geometry of this problem and the effect of magnetic fields. At 1 AU, the IMF has an average value of 5γ ($1\gamma = 1 \times 10^{-5}$ gauss). An electron plasma wave perpendicular to the magnetic field will have a frequency at the upper hybrid

frequency.

$$\omega_{uh}^2 = \omega_p^2 + \omega_C^2 = 1.000116\ \omega_p^2 .$$

As this is much smaller than the fluctuation in the local plasma frequency (~1-2%), due to density fluctuations, we will ignore this effect. The major effect of the magnetic field will be to constrain the (weak) electron beam to flow along the magnetic field lines, and therefore the wave vector of the Langmuir waves is directed approximately along the magnetic field.

4. Wave Propagation in Random Media

Introduction

A wave with wavelength λ, propagating in a non-dissipative three-dimensional medium with a low density of scatterers with a scattering mean free path l^* such that $\lambda \ll l^*$, will exhibit diffusive behavior when observed at a distance $L \gg l^*$. As the density and strength of the scatterers is increased the diffusivity will decrease until, at some value of $l^* \sim \lambda$, diffusion will cease altogether according to the theory of Anderson localization. The wave will then be localized in space in a time-stationary quantized eigenstate.

Wave propagation in a collisionless turbulent plasma such as the solar wind may provide one of the few observable examples of strong wave localization in a classical system. In general it is difficult to find systems which satisfy the Ioffe-Riegel criterion for localization, namely that the scattering mean free path should be of the same order of magnitude as the wavelength and that the dissipation length be much longer than the mean free path l^* (*Anderson*, 1985). In a weakly collisional plasma, such as the solar wind, the dissipation rate γ for the electromagnetic waves will be of the order of $\frac{\gamma}{\omega_p} \sim 10^{-12}$ and for the Langmuir waves of interest (since $\lambda \gg \lambda_D$) $\frac{\gamma}{\omega_p} \sim 10^{-22}$. Another factor that makes plasma waves attractive for studying localization is that the dielectric contrast $\frac{\Delta\varepsilon}{\varepsilon}$ due to density fluctuations, where ε is the dielectric constant, can be very large, since for plasma waves the ensemble average $<\varepsilon> \equiv 0$ and for electromagnetic waves near the plasma frequency $\varepsilon \sim \frac{\omega^2 - \omega_p^2}{\omega_p^2}$ is very small.

The condition $\lambda \sim l^*$ is in fact a weak condition, and values of l^*/λ as large as 50 have been observed to produce localization as argued by *Trawal et al.* (1986), who attributed the observed vanishing of positron mobility in gaseous helium to localization effects. The ratio l^*/λ appears to be within the appropriate range of values for Langmuir and electromagnetic waves associated with

the type III solar radio burst. This is in contrast to the failure to observe strong localization effects in the propagation of a laser beam through a slurry of small dielectric spheres (*Watson et al.*, 1986). The problem in this experiment was that the dielectric contrast was too low for latex spheres, and so the mean free path was too large.

Before discussing Anderson localization, we begin first with a review of multiple-scattering theory in order to develop some of the language which will be important in localization theory and to show how multiple scattering theory breaks down in the regime where localization is important.

4.1. Multiple Scattering Theory

In discussing multiple scattering theory we rely on standard Green's function techniques discussed, for example, in *Abrikosov et al.* (1975) and applied specifically to the problem of propagation in random media in *Lax* (1981) and *Rickayzen* (1980).

Multiple scattering theory begins with a wave equation of the form

$$\frac{\partial^2 \psi}{\partial t^2} = -\omega_p^2 \psi + c^2 \frac{\partial^2 \psi}{\partial x^2} - V(x)\, \psi(x), \tag{4.1.1}$$

One imagines that as $t \to \pm\infty$ the wave is in a packet which, however extensive, in a region where $V(x) \to 0$, i.e., no scattering takes place. In this region the wave will asymptotically, as $t \to -\infty$, be of a form

$$\psi = \psi_0\, e^{i(kx - \omega_k t)}$$

where $\omega_k^2 = \bar{\omega}_p^2 + k^2 c^2$. One uses perturbation theory to develop solutions which will again be of the same form for $t \to \infty$. A comparison between $\psi(t \to -\infty)$, and $\psi(t \to \infty)$ gives the scattering amplitude.

If we Fourier transform equation 4.1.1, we get

$$[\omega^2 - \omega_p^2 - c^2 k^2]\, \psi(k) = \int v(k - k')\, \psi(k')\, dk' .$$

Let us define a Green's function $G(x, x', t, t')$ such that

$$\left[-\frac{\partial^2}{\partial t^2} - \omega_p^2 + c^2 \frac{\partial^2}{\partial x^2} + V(x) \right] G = \delta(x - x)\, \delta(t - t') .$$

The significance of the Green's function is that if we have some initial condition, $\psi_0(x, t=0)$, then

$$\psi(x,t) \equiv \int d^3x\, G(x, x', t, 0)\, \psi_0(x, t=0)$$

is a solution of the wave equation. We also define $G_0(x, x', t, t')$ such that

$$\left[-\frac{\partial^2}{\partial t^2} - \omega_p^2 + c^2 \frac{\partial^2}{\partial x^2}\right] G_0(x-x', t-t') = \delta(x-x')\,\delta(t-t')$$

In Fourier space this becomes

$$[\omega^2 - \omega_p^2 - c^2k^2]\, G_0(k, \omega) = 1$$

or

$$G_0(k, \omega) = \frac{1}{\omega^2 - \omega_p^2 - c^2k^2}\,.$$

It can be shown that

$$G(k, \omega) = G_0(k,\omega) + \int dk'\, G_0(k,\omega)\, v(k-k')\, G(\omega, k')\,.$$

This can be iterated to for a perturbation expansion in v to obtain

$$G = G_0 + G_0 v G_0 + G_0 v G_0 v G_0 + \ldots \tag{4.1.2}$$

where G_0 and v are integral operators (or matrices).

One represents G diagramatically as $\underset{\omega,\,k}{\Longrightarrow}$ and G_0 diagramatically as $\underset{\omega,\,k}{\longrightarrow}$.

We can represent 4.1.2 as

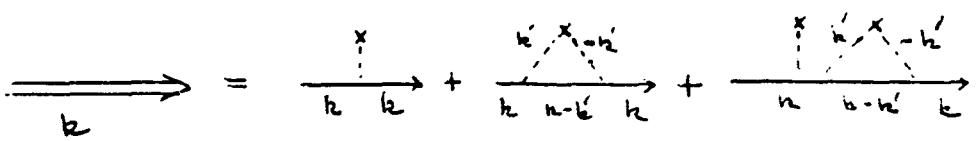

where $\times$ represents the interaction v. One defines a "self energy" $\sum(k, \omega)$ with graph

such that

$$G(k, \omega) = G_0(k, \omega) + G_0(k,\omega) \sum(k,\omega)\, G_0(k,\omega) + G_0 \sum(k)\, G_0(k) \sum(k)\, G_0(k) + \ldots$$

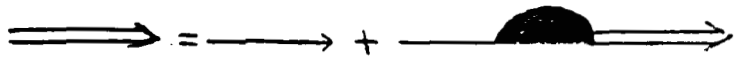

This can be solved as

$$G(k,\omega) = \frac{1}{G_0^{-1}(k,\omega) - \sum(k,\omega)}$$

In order to see how this theory works we consider a simple one-dimensional example. Let us consider a single perturbation in an otherwise uniform medium of the form

$$V(x) = \begin{cases} v_0 & -l_c/2 \le x \le l_c/2 \\ 0 & \text{otherwise} \end{cases}$$

the diagrams for the self-energy are

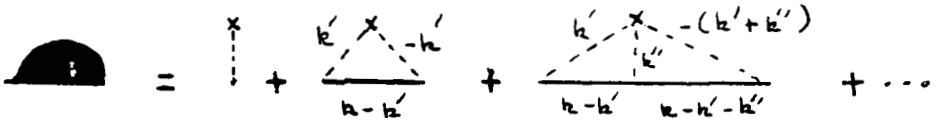

plus terms of higher order in v.

Using the rules in the above cited references, the first order diagram for the self-energy just leads to a shift in the average plasma frequency. The second order diagram in the self-energy may be evaluated as:

$$\sum(k,\omega) = \frac{1}{2\pi L}\int dq\, |v(q)|^2\, G_0(k-q,\omega)$$

where $\frac{1}{2\pi L}$ corresponds to the normalization of the inverse Fourier transform, and where

$$v(q) = \int_{-l_c/2}^{l_c/2} dx\, v_0\, e^{iqx} = \frac{2v_0}{q}\sin\left(\frac{ql_c}{2}\right).$$

Therefore,

$$\sum(k,\omega) = \frac{1}{2\pi L}\int dq \left(\frac{4v_0}{q^2}\right)\frac{\sin^2(ql_c/2)}{\omega^2 - \omega_p^2 - c^2(k-q)^2}$$

and then

$$G(k,\omega) = \frac{1}{\omega^2 - \omega_p^2 - c^2k^2 - \sum(k,\omega)}$$

The pole avoidance procedure is that $\omega \to \omega + i\eta$ corresponding to the retarded propagator. For v_0

sufficiently small, we will only be interested in $\sum$ when $\omega^2 - \omega_p^2 - c^2k^2 \cong 0$. In this case with the approximation $\sum(k,\omega) \cong \frac{i v_0^2 l_c^2}{2kc^2}$ we find

$$G(k,\omega) \cong \frac{1}{\omega^2 - \omega_p^2 - c^2k^2 - \frac{i\, v_0^2\, l_c^2}{2\, kLc^2}},$$

And we see that the self energy then represents a lifetime for the excitation.

For a large system with many scatterers we replace $\frac{1}{L}$ with N, the volume density of scatterers, and we take an ensemble average. Then

$$<G(k,\omega)> \cong \frac{1}{\omega^2 - \omega_p^2 - c^2k^2 - \frac{i\, N v_0^2\, l_c^2}{2c^2k}}.$$

In order to ensure that higher order terms in the expansion may be neglected in the self-energy, we require that $\sum^{(3)} \ll \sum^{(2)}$. But by examining the third diagram in $\sum(k,\omega)$ one estimates that

$$\frac{\sum^{(3)}}{\sum^{(2)}} \sim \frac{v_0\, l_c^2}{c^2}$$

Therefore, we expect that a perturbation theory will break down when $\frac{v_0\, l_c^2}{c^2} \sim 1$. As we shall see in the next section with $v_0 = \delta\omega_p^2$, this is the regime when Anderson localization becomes important, and will be the parameter regime of importance for the type III problem.

If we have an initial amplitude $\psi(x_0, t_0)$, we can compute the transport of probability density as

$$\frac{\partial}{\partial t} |\psi(x,t)|^2.$$

Using the Green's function language

$$|\psi(x,t)|^2 = \psi(x,t)\,\psi^*(x,t) = \int d^3x_0\, d^3x_0'\, G(x,t,x_0,t_0)\,\psi(x_0)\,\psi(x_0')\,G^*(x,t,x_0',t_0) \quad (4.1.3a)$$

The diagram for this is

(4.1.3b)

where $G^R = G = \Longrightarrow$

is the retarded Green's function and

$$G^A = G^* = \Longleftarrow$$

is the advanced Green's function.

Expanding (4.1.3) gives diagrams which include the "ladder" diagrams:

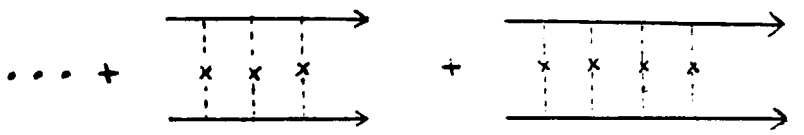

and the maximally crossed diagrams:

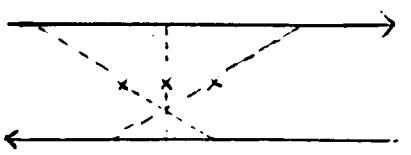

Langer and Neal (1966) showed that in evaluating diffusivity in random media these two sets of diagrams are the most important, and that, in fact, their sum diverges unless one adds in finite lifetimes in the unperturbed propagators (the G_0 or light lines in the diagram).

Particularly important is that the ladder and crossed diagrams interfere constructively for exact backscattering. This is a consequence of the time reversal symmetry of the backscattering processes (*Gor'kov*, 1977). Because this constructive interference is a symmetry that survives ensemble averaging of the above two-particle diagrams it is expected to be a dominant effect and lead to enhanced backscattering. This enhancement has been observed recently by *Van Albeda and Lagendijk* (1986) in an experiment that measured the backscatter of laser light from a slurry of glass beads, and is also important in understanding experiments on electron mobility in thin two-dimensional films. The parameter regime where enhanced backscatter is observable, but behavior is otherwise diffusive, is often referred to as "weak-localization."

One of the major difficulties in studying localization effects analytically is that $<G^A G^R> \neq <G^A><G^R>$. Correlation effects are the essence of Anderson localization theory. Enhanced backscatter, for example, depends upon these correlations. We shall return to the issue of two particle Green's functions later in the next section.

Before concluding this section on multiple scattering theories, we mention the effort of *Muschietti et al.* (1985) to understand the effect of 3-D density fluctuations on beam-plasma instabilities by considering the Fokker-Plank equation

$$\partial_t w_k = 2\gamma_k w_k + \partial_{kj} D_{jl}\, \partial_{kj} w_k + \delta_k$$

with

$$D_{jl} = \omega_{pe}\, \pi \int \frac{d^3 q}{(2\pi)^3}\, c(q)\, q_j\, q_l\, \delta(2k \cdot q),$$

where γ_k is the Langmuir growth rate for wave vector k, w_k is the wave energy density, $c(q)$ is the spectral density of fluctuations of wave number q, and δ_k is the rate of spontaneous emission. It was concluded that the diffusion of Langmuir waves led to the quenching of the beam-plasma process in the case of electron beams in the solar wind unless special assumptions about the anisotropy of solar wind density fluctuations are made. This theory is equivalent to a first order scattering theory, and ignores the possibility that as a result of infinite order scattering effects, a wave may remain in resonance with the beam for a long time.

4.2. Anderson Localization

As mentioned in the introduction, for sufficiently strong random scatterers waves do not diffuse in space, but rather are localized into normalized eigenmodes. The theory of wave localization in random media was first proposed by *P. W. Anderson* (1958) to explain the experimental result that electron spin polarization diffuses very slowly in highly doped silicon at low temperatures. Anderson studied the model Hamiltonian

$$i\dot{a}_j = E_j\, a_j + \sum_k V_{jk}\, a_k \tag{4.2.1}$$

where $a_i(t)$ represents the quantum mechanical amplitude at the site i on a lattice, V_{jk} is a (weak)

coupling between sites and E_j is the local site energy. The crucial point in the Anderson model is that E_j is taken to be a random variable, uncorrelated from site to site. For most of our discussion the probability distribution for E is:

$$p(E) = \begin{cases} \frac{1}{W} & -W/2 \le E \le W/2 \\ 0 & \text{otherwise} \end{cases}$$

although it is argued that the exact nature of the distribution is of little consequence, the width being the important factor.

Equation (4.2.1) can be interpreted as the Hamiltonian for an election in a random lattice in the tight binding model, and therefore has been much studied in the context of solid state theory in order, for example, to understand the low conductivity of amorphous materials. It is relevant to our discussion since it is equivalent to the wave equation for either Langmuir or electromagnetic waves expressed as a finite difference equation.

Localization in One Dimension

Let us start with the wave equation

$$-\frac{\partial^2 \psi}{\partial t^2} = \omega_p^2(x)\,\psi - v^2 \nabla^2 \psi$$

where

$$v^2 = \begin{cases} c^2 & \text{for electromagnetic waves} \\ 3v_{te}^2 & \text{for Langmuir waves} \end{cases}$$

and look for time stationary solutions $-\frac{\partial^2 \psi}{\partial t^2} = \omega^2 \psi$. We rewrite this as a finite difference equation in x where l is some small length:

$$\omega^2 \psi = \omega_p^2(x)\,\psi - \frac{v^2}{l^2}\left(\psi(x+l) + \psi(x-l) - 2\psi(x)\right) \tag{4.2.2}$$

With the following definitions:

$$\psi_j \equiv \psi(jl)$$

$$\psi_j' \equiv \psi_{j+1} - \psi_j$$

and $\delta\omega_{p_j}^2 \equiv \omega_p^2(x_j) - \overline{\omega_p}^2$ where $\overline{\omega_p}^2$ is the square of the average plasma frequency, equation 4.2.2 becomes

$$\omega^2\psi_j = (\overline{\omega_p}^2 + \delta\,\omega_{p_j}^2)\,\psi_j - \frac{v^2}{l^2}(\psi_{j+1}' - \psi_j') \tag{4.2.3}$$

In order to understand the nature of localization in one-dimension, we reproduce an argument, originally due to *Mott and Twose* (1961) and recast by *Escande and Souillard* (1986).

The general rule for solving a second order finite difference equation of the form 4.2.3 is to use a leap-frog method, by which ψ' and ψ are alternately advanced. This gives a solution that is accurate to $O(\Delta x^2)$ rather than just $O(\Delta x)$ (*Birdsall and Langdon*, 1985).

This gives first:

$$-E(1 - \frac{V_j}{E})\psi_j = \psi_{j+1}' - \psi_j' \tag{4.2.4}$$

and second:

$$\psi_{j+1}' = \psi_{j+1} - \psi_j \tag{4.2.5}$$

where we define

$$E = \frac{l^2}{v^2}(\omega^2 - \overline{\omega}_p^2) \equiv k^2 l^2,$$

$$\frac{V_j}{E} \equiv \frac{\delta\omega_p^2(x_j)}{k^2 v^2}$$

and $k^2 \equiv \dfrac{\omega^2 - \overline{\omega}_p^2}{v^2}$. This is strictly a definition and its interpretation as a wave number will be discussed later.

We write (4.2.4) as

$$\begin{pmatrix} \psi_j \\ \psi_{j+1}' \end{pmatrix} = \begin{pmatrix} 1 & 0 \\ -E_j & 1 \end{pmatrix} \begin{pmatrix} \psi_j \\ \psi_j' \end{pmatrix}$$

and (4.2.5) as

$$\begin{pmatrix} \psi_{j+1} \\ \psi'_{j+1} \end{pmatrix} = \begin{pmatrix} 1 & 1 \\ 0 & 1 \end{pmatrix} \begin{pmatrix} \psi_j \\ \psi'_{j+1} \end{pmatrix}$$

which gives

$$\begin{pmatrix} \psi_{j+1} \\ \psi'_{j+1} \end{pmatrix} = \begin{pmatrix} 1-E_j & 1 \\ -E_j & 1 \end{pmatrix} \begin{pmatrix} \psi_j \\ \psi'_j \end{pmatrix} \equiv M_j \begin{pmatrix} \psi_j \\ \psi'_j \end{pmatrix} .$$

In the case where $E_j = E$, a constant, for all j, M_j is easily seen to be a unimodular matrix with eigenvalues $1 \pm i\sqrt{E_j} + 0(E)$. Iteration in this case gives:

$$M_{n-1} \ldots M_0 = M^n$$

with eigenvalues $e^{\pm ikln} = e^{\pm ikx}$, and therefore reproduces the solution expected for a uniform medium.

In the case where the E_j's and therefore the M_j's are random an initial condition, $\begin{pmatrix} \psi_0 \\ \psi'_0 \end{pmatrix}$, is propagated as

$$\begin{pmatrix} \psi_{j+1} \\ \psi'_{j+1} \end{pmatrix} = M_j M_{j-1} M_{j-2} \ldots M_1 M_0 \begin{pmatrix} \psi_0 \\ \psi'_0 \end{pmatrix} .$$

We can define a Liapunov exponent

$$\lambda \equiv \lim_{N \to \infty} \frac{1}{N} Tr\,(M_{j+1} M_j \ldots M_1 M_0)$$

It was first proposed by *Mott and Twose* (1961) and later proven rigorously by *H. Furstenberg* (1963) that for such a set of random matrices $\lambda > 0$ almost everywhere, i.e., except for E taking values on a countable set $\{E_i\}$. The significance of this is that almost any initial condition will developed an exponentially growing wave envelope going as $e^{\lambda |j-j_0|}$ at site j. An exponentially decreasing sequence is developed as follows. If

$$\| \psi_j \| \sim e^{\lambda |j-j_0|} \| \psi_{j0} \|$$

then we define

$$\begin{pmatrix} \phi_j \\ \phi'_j \end{pmatrix} = \begin{pmatrix} \psi_j \\ \psi'_j \end{pmatrix} e^{-\lambda |j-j_0|} .$$

If this is propagated backwards,

$$\begin{pmatrix} \psi_{j_0} \\ \psi'_{j_0} \end{pmatrix} \equiv M_{j_0}^{-1} M_{j_1}^{-1} \ldots M_j^{-1} \begin{pmatrix} \phi_j \\ \phi_j \end{pmatrix}$$

will be an exponentially decreasing sequence, although if continued beyond ψ_{j_0} would again increase exponentially except for certain discrete values of E. We produce exponentially localized states by matching solutions from the left and right following an argument due to *Mott and Twose* (1961). Begin with two initial conditions, say, $\begin{pmatrix} \psi_0 \\ \psi'_0 \end{pmatrix}$ and $\begin{pmatrix} \psi_{2n} \\ \psi'_{2n} \end{pmatrix}$, where n is large. One then finds

$$\begin{pmatrix} \psi_n \\ \psi'_n \end{pmatrix} = M_{n-1} \ldots M_0 \begin{pmatrix} \psi_0 \\ \psi'_0 \end{pmatrix}$$

and

$$\begin{pmatrix} \phi_n \\ \phi'_n \end{pmatrix} = M_n^{-1} \ldots M_{2n-1}^{-1} \begin{pmatrix} \psi_{2n} \\ \psi_{2n} \end{pmatrix}$$

one then adjusts E and $\begin{pmatrix} \psi_{2n} \\ \psi'_{2n} \end{pmatrix}$ such that $\begin{pmatrix} \phi_n \\ \phi'_n \end{pmatrix} = \begin{pmatrix} \psi_n \\ \psi'_n \end{pmatrix}$. Heuristically, one expects that this produces a discrete set of values for E.

The theory of localized states and the nature of the spectrum in one dimension was put on a rigorous mathematical basis by *Kunz and Souillard* (1980). An important point from localization theory is that in one dimension all states are localized. There are no good analytic expressions for localization lengths for $W/V \gtrsim 1$. *Escande and Souillard* (1985) determined the Liapunov exponents numerically for the product of random matrices $\ldots M_n M_{n-1} \ldots M_1 M_0$. The results are shown in Figure 4.1. The relevant parameters are

$$W/E = \delta\omega_p^2/k^2 v_{th}^2$$

and

$$E = k^2 l_c^2 .$$

The Liapunov exponent is

$$\gamma = \frac{l_c}{\xi}$$

where ξ is the localization length, and l_c the "correlation length" is the distance over which $\omega_p^2(x)$ is constant.

We now consider the correct interpretation of the quantity

$$k^2 \equiv (\omega^2 - \omega_p^2)/v^2 .$$

Clearly, when $V_j \equiv 0$ for all j, as we have shown, k is the wave number of a plane wave propagating in the medium. In the case where $k \gg 1/\xi$, i.e., where there are many wavelengths (for the homogeneous case) in a localization length we would expect that the wavelength (measured as twice the average spacing between points where $\psi = 0$, say) would remain the same, since the fluctuating value of the spacing should average to zero, as should be the case when W/E is small. This is not entirely true, since although the fluctuations are uncorrelated, the localized waves are correlated with the fluctuations, but this interpretation is borne out by the simulations in section 5.

The physics of localization in a plasma is as follows for a plasma wave, or for an electromagnetic wave traveling near the critical density. The plasma may be viewed as a collection of weakly coupled harmonic oscillators. Each oscillator has the resonant frequency $\omega_p^2(x) = \bar{\omega}_p^2 + \delta\, \omega_p^2(x)$. If an oscillator is initially set in motion, it will couple to adjacent oscillators. Physically, how well this energy is coupled to adjacent oscillators will depend on two factors:

(1) The dephasing rate $\delta\omega_{pi} - \delta\omega_{pj}$ of the two adjacent oscillators;

(2) The coupling strength $\sim k^2 v^2$ which is a which measure of how well one oscillator can overcome the dephasing tendency of an adjacent oscillator,

and thus the importance of the parameter $\dfrac{\delta\omega_p^2}{k^2 v^2}$.

The other important parameter in localization theory is

$$\frac{E}{V} \equiv \left[\frac{\omega^2 - \omega_p^2}{v^2} \right] l_c^2$$

which measures how near the frequency is to the "band edge." This will be discussed further below.

Another way of viewing localization is that it is an infinite order scattering process in which a localized wave is self-consistently scattered back onto itself while the phases of the waves scattered in the "forward" direction are random and cancel out when viewed far in the forward direction.

Kunz and Souillard (1980) have shown that the spectrum of the equation

$$i\dot{\psi}_i = V_i \psi + [\psi_{i+1} + \psi_{i-1} - 2\psi_i]$$

is

$$[0, 4] + supp\ r$$

where

$$supp\, r \equiv \{ V_0 \mid \mathrm{Prob}\,[V\ \varepsilon\{V_0 - \varepsilon, V_0 + \varepsilon\}] > 0 \quad \text{for all } \varepsilon > 0 \}$$

This is equivalent to the set

$$\{ \omega^2 \mid \omega^2 = \omega_p^2 + [-\delta\omega_p^2, \delta\omega_p^2] + [0, 4v^2/l^2] \}$$

for equation 4.2.3. For waves in a continuous medium, $l \rightarrow 0$ and the upper limit of this set has no meaning.

This tells us nothing about the probability of finding a state located within a finite region of size much greater than the localization length. For example, for weak perturbations, a wave with approximate wave number k will have an energy which is near the value $\omega^2 = \omega_p^2 - \delta\omega_p^2 + k^2 v^2$ with very small probability, since the probability of almost every wave peak aligning itself with a density minimum is very small.

In localization theory an important parameter is how close ω^2 is to the "band edge," $-\delta\omega_p^2$. The concept "band center" does not have strict meaning since there is no upper band limit as is the case for a crystalline lattice. By making k^2 sufficiently large, we can make the localization length in one dimension arbitrarily large provided the condition $k^2 \lambda_D^2 \ll 1$ remains met for plasma waves.

Localization in Higher Dimensions

So far we have only considered localization effects in one dimension, and higher dimensionality effects must be considered. Anderson's original approach was to take the Laplace transform of (4.2.1) which was written as

$$f_j(s) = \frac{i\,\delta_{0j}}{is - E_j} + \sum_{k \neq j} \frac{1}{is - E_j} v_{jk} f_k(s)$$

where the initial condition is $a_j(t=0) = \delta_0 j$. Solving for f_0 gives

$$f_0(s) = \frac{i}{is - E_0} + \sum_k \frac{1}{is - E_0} V_{0k} \left(\frac{V_{0k}}{is - E_k} + \sum_l \frac{1}{is - E_k} V_{kl} \frac{1}{is - E_l} V_{l_0} + \ldots \right)$$

The question whether energy remains localized is equivalent to the question whether $\lim_{t \to \infty} a_0(t) \geq \varepsilon$ for some $\varepsilon > 0$. This is equivalent to $\lim_{R_e(s) \to 0} f_0(s) \geq \varepsilon$. This will in fact be the case provided that the self energy at site $i = 0$

$$\sum(0) = \sum_k \frac{(V_{0k})^2}{is - E_k} + \sum_{kl} \frac{V_{0k} V_{kl} V_{l0}}{(is - E_k)(is - E_l)} + \ldots \tag{4.2.6}$$

converges. Anderson studied this by considering the probability of the value of very long sequences when the E_i's are random variables. Anderson argued that the self-energy would converge with probability 1 whenever $W/V > (W/V)_c$, where $(W/V)_c$ is to be determined. Anderson's estimate was that $(W/2V)_c = 2K \ln (W/2V)_c$ where K is the connectivity of the lattice (from percolation theory) and is approximately $z - 1.5$ where z is the number of nearest neighbors. *Thouless* (1979) argued that this estimate is high because Anderson assumed that the contribution of each sequence was independent. Accordingly, a better estimate is

$$\left(\frac{W}{V} \right)_c = 4K \,.$$

A more transparent, but less rigorous argument for this is the following: The amplitude on a neighboring site will be

$$a_j \sim \frac{v}{E_j - E_i} a_i \,.$$

Since the values in the denominator can range between $\pm W/2$, a typical value is $W/4$. If there are z neighbors then we require

$$\frac{a_j}{a_i} \cong \frac{V}{W/4} < \frac{1}{Z} > \text{ or } \frac{W}{V} > 4Z .$$

Even this estimate, it turns out, is high. The most convincing numerical work on this was done by *Yoshino and Okazaki* (1977), who solved the Hamiltonian $Ea_i = E_i\, a_i - v \sum_j a_j$, where the sum is over nearest neighbors, by diagonalizing the Hamiltonian on a 100×100 grid. They found that for $W/V > 6.5$ a transition occurred between extended and strongly localized states. *Thouless* (1979) later argued that when $W/V \sim 6.5$ the state is localized with a localization length on the order of the size of the system.

Actually, it is believed that $W/V = 6.5$ is a transition point between strongly and weakly localized waves in 2-D. According to scaling arguments (*Abrahams et al.*, 1979) all states in 1-D and 2-D are localized, and for 3-D there is a critical value, $(W/V)_c$ above which states are localized. *Licciardello and Thouless* (1978), looking at the sensitivity to changes in boundary values, concluded that 3-D wave functions are apparently localized for the diamond lattice for $9 \leq (W/V)_c \leq 12$ but the localization is slower than exponential. For the cubic lattice, localization occurs for $W/V \cong 15$. This was confirmed in a numerical study by *McKinnon* (1985) who studied the scaling with M of the localization length of long 1-dimensional chains when M^2 adjacent chains were coupled together using nearest-neighbor coupling. His localization estimates were again based on a Liapunov exponent estimate. Also of great importance is that the normalized localization length $\Lambda \equiv \xi(M)/M$ in fact was found to follow the behavior $\Lambda \sim 1/M$ for strong localization ($W/V \gtrsim 25$), thus suggesting that for strong localization, the localization length is only weakly dependent on dimensionality.

A significant difference between our wave equation and that of the Anderson theory is that in our case there is no natural discrete lattice. In a crystalline lattice there is an upper limit on the wave vector in the unperturbed case corresponding to the first Brillouin zone. For Langmuir waves or electromagnetic waves there is no upper band edge, and for frequencies high enough, the wave

will be delocalized (ignoring Landau damping for the moment).

It is not straightforward to compare parameters in the solar wind plasma with the critical ratio $(W/V)_c$ to determine dimensionality effects. The difficulty is a result of l in (4.2.3) being much smaller than the scale length of the change in ψ, i.e., much smaller than a typical wavelength. But on this scale the density fluctuations may not be (and in the solar wind plasma are not) decorrelated, so that $\omega_p^2(x = jl)$ is not independent from one lattice site to the next. Therefore, this situation is significantly different from the solid state case where perturbations are (assumed to be) coincident with lattice sites.

We can approximate the situation by imagining that our plasma is divided into a lattice with pieces of size l_c where l_c is the correlation length of the density fluctuations. Each piece is then a separate harmonic oscillator.

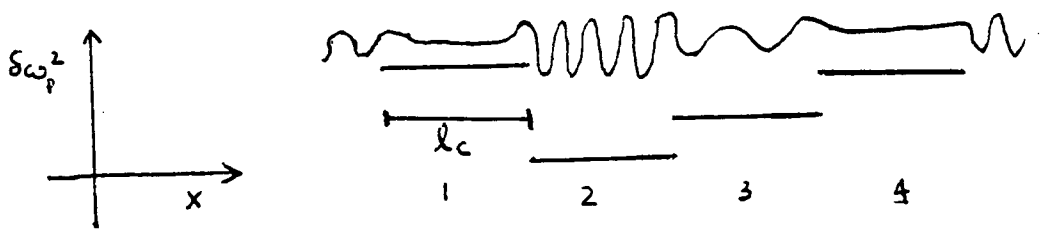

For a state with frequency ω, the wave number in each piece will be a function of the $\omega_{p_i}^2$. The coupling between, say, oscillator 1 and 3 through 2 will be $\frac{v_g}{l_c}$ where v_g is the group velocity for piece 2. Therefore,

$$W/V \cong \frac{\delta\omega_p^2 l_c^2}{v_g^2}$$

We use v_g rather than v when looking at the plasma on a scale $l \geq \lambda$. When observed at small scales $l \ll \lambda$, the weak coupling v leads to propagation at the group velocity for distances $\geq \lambda$. Further rescaling will not change the group velocity. Dividing the plasma into pieces larger than $l \sim l_c$ will smooth out the density fluctuations. On the other hand, on these larger scale lengths, the coupling between pieces becomes a complicated function to account for scattering and decreased transmission which are strongly dependent on frequency at this scale length.

Using an average group velocity given by

$$v_g = \begin{cases} \dfrac{3k\, v_{th}^2}{\omega_p} & \text{for Langmuir waves} \\ \dfrac{kc^2}{\omega_p} & \text{for electromagnetic waves} \end{cases}$$

and using the parameters for the 11 March event, estimating $l_c \sim 100$ km, and $\dfrac{\delta\omega_p^2}{\omega_p^2} = .01$, for the Langmuir waves:

$k = 2.3 \times 10^{-5}\ \text{cm}^{-1}$;

$v_g = 2.4 \times 10^7$ cm/sec

$W/V = 10^7$

for the electromagnetic waves:

$k = 1.7 \times 10^{-7}\ \text{cm}^{-1}$

$v_g = 1.9 \times 10^8$ cm/sec

$W/V = 1800$

In both cases, this greatly exceeds even the largest estimates of $(W/V)_c$. Our estimates for W/V here may be too large because of overestimating l_c and l_c^2 could conceivably be smaller by as much as a factor of 25 or greater.

Once establishing that $W/V > (W/V)_c$ so that waves are strongly localized, of more practical importance will be estimates of W/E and E, the parameters used in the *Escande and Souillard* (1985) study.

For the Langmuir waves

$$W/E = \frac{\delta\omega_p^2}{\omega_p^2}\,\frac{v_b^2}{3v_{th}^2} \cong 1.4$$

for the March 11 event where v_b is the beam velocity. Likewise, if we could treat the transverse waves 1-dimensionally (which we cannot) we would get, using $\lambda_T = 360$ km for the March 11 event:

$$\left(\frac{W}{E}\right)_{\text{Transverse}} = 2.43$$

If $l_c = 100$ km, $E = 3.00$, and plot 4.1 gives approximately $\gamma = .2$. So $\xi = 500$ km.

A difficulty in making localization estimates for the type III problem comes from the nature of the turbulent density spectrum, as discussed in section 2, which is that there are large amplitude long-wavelength fluctuations simultaneous with smaller amplitude, shorter wavelength fluctuations. If the localization length from the latter is smaller than the correlation length of the former, then it is the small amplitude short wavelength fluctuations that are important. That this may be so for the Langmuir waves is evident from the following. Using the 11 March 1979 parameters, if density fluctuations have a scale length $l_c = 2$ km, then $E = 21$. If the localization length $\xi \sim 70$ km, then we estimate from Figure 4.2 that $W/E \cong .5$, which gives $\frac{\delta n}{n} \cong .003$, required to give this localization length. The actual localization is therefore dependent upon the fluctuation spectrum.

Scaling Theory of Localization

The first successful scaling theory of localization was proposed by *Abrahams et al.* (1979) who used the scaling of the conductance of a sample with scaling of size to find that all one- and two-dimensional waves are localized in a random system and that a mobility edge exists in these dimensions, delimiting a transition between extended and localized states. This scaling theory was verified numerically by *McKinnon* (1985), discussed earlier in this section. Although all states in one- and two-dimensions are localized, Figure 4.2 and the numerical work of *Yoshino and Okazaki* (1977) indicate that there is a transition between weakly and strongly localized states.

Another way of viewing the localization problem mathematically is to look at the Green's functions which are solutions of

$$[-c^2 \nabla^2 + v(r) - E]\, G(r, r_0) = \delta(r - r_0)\,.$$

They may be written as

$$G_{A/R}(r - r_0, E) = \sum_{\alpha} \frac{\psi_\alpha^*(r)\, \psi_\alpha(r_0)}{E - E_\alpha \pm i\eta}$$

where A/R determines whether it is the advanced (retarded) Green's function, and α is an eigenstate label. Now $G(r-r_0) \to 0$ as $|r-r_0| \to \infty$ if all the wave functions are localized.

As discussed in the previous section, the quantity

$$D \sim \langle G^A(r-r_0,E)\,G^R(r-r_0,E)\rangle$$

where the average is an average over the statistical ensemble $[v(x)]$ is important in the study of wave localization. For localized states

$$G(r-r_0,E) \sim \frac{e^{-|r-r_0|/\xi}}{r^{(d-1)}}$$

where $d \geq 1$ is the dimensionality. An important property of this Green's function is that as the disorder, W/E, approaches a critical value the correlation length ξ becomes infinite. This sudden transition of the correlation length is a universal property of phase transitions, in this case called the Anderson transition. By applying techniques from renormalization group theory and the theory of critical phenomenon *Wegner* (1982, and references contained therein) argued that the rate of diffusion for frequencies above the mobility edge scales as

$$E \sim \left[(E-E_c)/E_c\right]^{\nu}$$

where ν is some exponent (called the critical exponent). In 3-D one gets a "phase diagram" (*Stephen*, 1983)

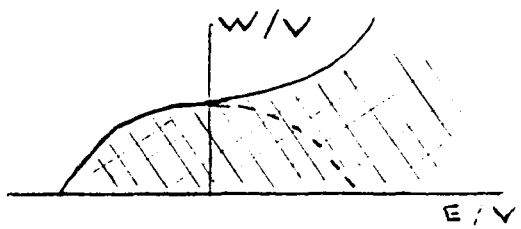

where states lying within the hatched area are extended. In a solid, the boundary is determined by the dashed line, but as we have discussed, for a plasma, there is no upper band edge, and for sufficiently large values of E/V states will be extended.

An important conclusion from this is that in 3-D, for any disorder there is some energy $E_c > \overline{\omega_p^2} - \delta\omega_p^2$, i.e., above the band edge, below which the states are localized. To see how this

might be the case we return to Anderson's argument and consider the probability of convergence of the series 4.2.6. As $is \rightarrow E + i\eta$, where $\eta \rightarrow 0$ and $E \rightarrow -W/2$, the probability of small denominators decreases and therefore the probability of convergence increases.

We consider the implications of this for the type III problem. The difference between the frequencies for the waves in the 11 March case are

$$f_L - f_{\text{plasma}} \cong 45 \text{ Hz}$$

and

$$f_T - f_{\text{plasma}} \cong 25 \text{ Hz}.$$

Therefore, even if we greatly overestimated W/V for the transverse waves for typical solar wind parameters, f_T may be below the mobility edge in any case, since f_T is so near the "band edge." In the second place, if f_T were in fact above the mobility edge, it would be expected that the rate of diffusion would be very small. The consequence of this is that a transverse wave that originated in a given region would still be "approximately" quantized, resembling a given stable bound state in quantum theory, and therefore, the implications for the type III problem would be little different than what is discussed in section 7.

Localization and Mobile Density Fluctuation

By applying normalization group techniques *Vollhardt and Wölfe* (1980, 1982) argued that the ladder and maximally crossed diagrams (4.1.7) are responsible for the Anderson transition. If these diagrams are the most important for localization then this provides an estimate for the effect of the mobility of density fluctuations. The destruction of enhanced backscattering in the weak localization limit was studied by *Golubentsev* (1983) who concluded that the loss of phase coherence due to the destruction of time reversal symmetry for the backscattered wave is important when $\tau > \tau_\phi$ where τ is the mean time between wave-scattering and $\tau_\phi = (3\tau\,\tau_\lambda^2)^{1/3}$ is a measure of phase coherence time when the scatterers are mobile with τ_λ the average time for a scatterer to travel a distance λ, the wavelength of the wave. In this computation *Golubentsev* assumed that the scatterers had independent random velocities with a Maxwellian distribution. We estimate $\tau = \xi/V_g$ and

$\tau_\lambda = \lambda / c_s$ and define

$$\alpha_G = \frac{\tau_\phi}{\tau} = \left[\frac{3\tau_\lambda^2}{\tau^2} \right]^{1/3} = \left[\frac{3\lambda^2 V_g^2}{\xi^2 c_s^2} \right]^{1/3}$$

where c_s is the velocity of a density fluctuation. Then we expect localization will be preserved for $\alpha_G \gg 1$, and destroyed for $\alpha_G \lesssim 1$.

If we use the ion-acoustic velocity for c_s, then for the 4 March event, for the Langmuir waves $\alpha_G = .9$ and for the transverse electromagnetic wave $\alpha_G \sim 100$. This would indicate that the Langmuir waves may not be localized, but that the transverse waves probably are. We mention the following points:

(1) As we shall see in numerical simulations in section 5.2., when localization is very strong, waves will become localized by a co-moving group of fluctuations and scattered by the remainder.

(2) Although little is known about the source of the turbulence in the solar wind, very often in plasma turbulence there is an average drift along or across the magnetic field relative to which other turbulent motion is slow. Therefore phase coherence may be preserved longer since the random component of the velocity can be much less than the average velocity.

(3) This estimate is based on only the destruction of time reversal symmetry of the enhanced backscattering. In fact, for strong localization, the phase reinforcement comes from a fortuitous coincidence in the scattering off of different fluctuations in the neighborhood of the localization peak.

Density of States

Also of importance to us will be the density of states. In this problem we are primarily interested in waves which are resonant with a particle beam. For this to be the case, we expect that the waves of interest will have a localization length that extends over many wavelengths. The density of states will determines how many states/volume the beam can resonate with and therefore how much beam energy will be lost in exciting localized waves.

For any finite homogeneous system of length L, the density of states is given by the usual formula

$$\frac{d^d n}{dk^d} = \left[\frac{L}{2\pi} \right]^d \tag{4.2.7}$$

where d is the dimension of the system. For a disordered system and for $E < E_c$, the density of states corresponding to bound states is discrete while for $E \geq E_c$ there is a continuum of states corresponding to the freely propagating waves. The question is how closely we can approximate the density of states by the expression 4.2.7. As numerical work by *Dean* (1961) has shown, away from the band edge, the density of states will closely resemble that of 4.2.7, while for frequencies near the band edge the density of states is highly perturbed. We expect that for waves whose localization length is many wavelengths in extent, the frequency will not be near the lower band edge (since the probability that the minimums of that density will correlate with an extended wave is very small). Therefore, we expect 4.2.7 will be close to the actual density of states.

Using the parameters for the March 11 event, the number of states in one dimension in a localization length $\xi \cong 70$ km, resonant with the beam with $\frac{\Delta v_b}{v_b} = .05$, the apparent width of the positive slope region, is approximately

$$\frac{k_b \xi}{2\pi} \frac{\Delta v_b}{v_b} = 1.25 .$$

Finally we consider the conditions under which localized states are resolvable. The density of states in 1-D is given by

$$\frac{dn}{dk} = \frac{L}{2\pi} , \tag{4.2.8}$$

which gives $dk = \frac{2\pi}{L} dn$. In order to determine the separation in frequency of modes contained within a localization length ξ, we start from:

$\omega^2 = \overline{\omega_p^2} + k^2 v_{th}^2$, then

$d\omega = v_g \, dk$ where v_g is the group velocity. Using 4.2.8 gives

$\Delta\omega \equiv \frac{2\pi v_g}{\xi}$. The length of time τ_R to resolve two such states is given by the requirement $\tau_R \Delta\omega \gtrsim 2\pi$, which gives $\tau_R \gtrsim \frac{\xi}{v_g}$, which might have been guessed heuristically.

Summary

We have reviewed Anderson localization theory which leads us to expect that electromagnetic and possibly Langmuir waves will be localized by the density fluctuations in the solar wind plasma. Theoretical predictions are consistent with experimental observations. The theory in this section will be used in interpreting the numerical simulations of the next section.

5. Numerical Simulations — Propagation of Gaussian Wave Packets in Random Media

We present the results of a series of numerical simulations of the time development in a random medium of an initially Gaussian wave packet. While numerical work has been done by others, in order to study localization the usual approach has been to diagonalize the Hamiltonian to find the eigenstates of a random lattice. This has usually been in the context of solid state theory and lattice sizes have usually been small (100×100 grid points) (*Dean*, 1961; *Yoshino and Okazaki*, 1977). To our knowledge time development with mobile fluctuations has not been studied numerically.

Here we investigate the time development of an initial wave which presumably is the overlap of many localized eigenstates. In section 5.2 we also investigate the effect of mobile density fluctuations. This study has used the program PERLOC, discussed in detail in Appendix B. This program propagates an initial Gaussian wave packet according to the wave equation

$$\frac{\partial^2 \psi}{\partial t^2} = -\omega_p^2(x)\,\psi + c^2 \frac{\partial^2 \psi}{\partial x^2}$$

with the initial conditions:

$$\frac{\partial \psi}{\partial t}(x, t=0) = 0$$

$$\psi(x,0) = \psi_0 \cos k_0(x - x_0)\, e^{-(x-x_0)^2/\Delta x^2}$$

periodic boundary conditions

$$\psi(0,t) = \psi(x_{\max}, t)\,.$$

and where

$\omega_p^2(x)$ is a random variable on the interval $[1 - dn, 1 + dn]$.

In most of the simulations shown $dn = .01$, corresponding to a 1% density variation. The simulations are done on a spatial grid of 2048 or 4096 grid points. The fluctuations in ω_p^2 are constant on steps typically of 4 or 8 grid points. A typical plot of the value of $\omega_p^2(x)$ is shown in Figure B.1.

We plot the following quantities at various times.

Psi: $\psi(x,t)$ = amplitude. Since this is a linear problem, the units of this quantity are arbitrary.

Energy: $E(x,t) \equiv \frac{1}{2}\,\omega_p^2(x)\,\psi^2(x,t) + \frac{1}{2}\left(\frac{\partial\psi(x,t)}{\partial t}\right)^2 + \frac{c^2}{2}\left[\frac{\partial\psi(x,t)}{\partial x}\right]^2$

This is the numerical value of the Hamiltonian density which generates the wave equation. This should be a slowly varying quantity, and therefore a better indicator of localization than ψ or $\frac{\partial\psi}{\partial t}$ individually, which oscillates in time as ω_p.

The following symbols are used in describing each simulation. The quantities are discussed in section 4.2 and values of W/E and E are used to enter Figure 4.1 to determine the predicted localization length ξ.

$k_0 =$	central wave number of the initial Gaussian wave packet
$c =$	velocity in the dispersion relation $\omega^2 = \omega_p^2 + c^2k^2$; $\omega_p^2 \equiv 1$
$n_c =$	number of grid points in a density fluctuation step
$l_c =$	length of density fluctuation step (correlation length)
$E \equiv$	$k_0^2\, l_c^2$
$W/E \equiv$	$\delta\omega_p^2/k_0^2c^2$
$\gamma =$	Liapunov exponent from plot 4.1
$\xi =$	l_c/γ = predicted localization length from the theory of *Escande and Souillard* (1984)
dn:	the plasma frequency ω_p^2 is a random variable on the interval $[1-dn, 1+dn]$
$v_g =$	$\frac{kc^2}{\omega_p}$ (group velocity)
$v_g t =$	total distance propagated at the group velocity at the end of the run.

In interpreting these simulations the following general remarks pertain.

1) If $\psi \sim e^{-\kappa|x|}$, then energy $\sim e^{-2\kappa|x|}$. Therefore, the localization length will be the ½ width of the wave packet at the amplitude $E = E_{\max}\, e^{-2}$.

2) Although it might be expected that results would only be valid after a time t such that $v_g t \gg \xi$; in fact we find very good agreement with theory when $v_g t \gtrsim \xi$.

3) An important qualitative difference between a freely propagating and a localized wave can be seen in the energy. For a propagating wave, $\psi \sim \cos(kx - \omega_p t)$, and so, for small c^2, $E \sim \frac{\omega_p^2}{2}\,[\cos^2(kx-\omega_p t) + \sin^2(kx-\omega_p t)] \sim$ constant. For a standing wave, on the other

hand, $\psi \sim \cos kx \cos \omega t$ and so for small c^2, $E \sim \omega_p^2 \cos^2 kx(\cos^2 \omega t + \sin^2 \omega t) \sim \cos^2 kx$. For a propagating wave the energy density will have a smooth envelope, while for a standing wave it will be modulated with wave number k.

Free Propagation

Figures 5.1 and 5.2 show freely propagating waves (constant density). These are to be compared with the other simulations in this section which are all with randomly fluctuating densities.

These two runs show the free propagation at the group velocity of two initial Gaussian wave packets. The initial excitation of the form

$$\psi(x) = \psi_0 e^{-\kappa |x - x_0|} \cos k_0 (x - x_0); \ \dot{\psi}(x) = 0$$

is seen to split in two and propagate in opposite directions. The dispersion relation is

$$\omega^2 = \omega_p^2 + c^2 k^2 \quad \text{with} \quad \omega_p^2 = 1$$

in both cases $v_g t$ is very close to the distance which the peak of the envelope propagates. The parameters in these simulations are the following.

Figures 5.1.1—5.1.5	Figures 5.2.1—5.2.5
$k_0 = .16$	$k_0 = 1.7$
$c = .2$	$c = .05$
$v_g = .0064$	$v_g = .0043$
$v_g t = 51.2$	$v_g t = 34.4$
$n_g = 4096$	$n_g = 4096$
$dt = .2$	$dt = .2$

5.1. Localization Length Studies

The following series of simulations shows the effect of time-stationary random density fluctuations for a wide set of parameters. The observed localization lengths are consistent with the values from Figure 4.1.

Figures 5.3.1—5.3.6

Parameters:

$k_0 = .16$
$c = .2$
$dn = .01$
$n_c = 16$
$l_c = 1.22$
$E = .04$
$W/E = 9.8$
$v_g = .0064$
$n_g = 4096$
$d_t = .2$

This set shows the time development for the same Gaussian wave packet as for the freely propagating case shown in plots 5.2.1—5.2.5. In this case, however, the density fluctuations are strong and localization is quite evident. In plot 5.3.2 we see the high wave number small amplitude signal propagating at the velocity c. This is the Sommerfeld precursor (*Jackson*, p. 9, p.313 ff.). With $W/E = 9.8$ this is far removed from the plotted region. We might estimate $\gamma \sim .1$ and therefore $\xi \sim 12$, which is of the same order as the observed localization length. In this case, however, we do not expect $k_0 l_c$ to be a meaningful quantity since the wave is so strongly distorted.

Figures 5.4.1—5.4.4

Parameters:

$k_0 = .32$
$c = .2$
$dn = .01$
$n_c = 16$
$l_c = 2.54$
$E = .66$
$W/E = 2.44$
$v_g = .0128$
$v_g t = 307$
$\gamma = 8 \times 10^{-2}$
$\xi = 31$

We have run this for 120,000 time steps to $t = 24{,}000$. Despite the very strong localization, there is still very good agreement between the predicted and the observed localization lengths. γ is estimated since $W/E = 2.44$ is not on the graph of Liapunov exponents Note that localization is very strong even though $v_g t/\xi \cong 10$.

Figures 5.5.1—5.5.6

Parameters:

$k_0 = .85$
$c = .15$
$dn = .01$
$n_c = 3$
$l_c = .46$
$E = .154$
$W/E = .61$
$\gamma = 3 \times 10^{-3}$
$\xi = 153$
$v_g = .019$
$v_g t = 570$

We show the time development of this in some detail. This shows a case where the final localized wave packet is ~40 wavelengths long. The initial wave packet is confined to a region much smaller than the final localized wave. The wave packet splits and begins to propagate, as seen at $t = 2{,}000$, however, there is evidently already significant reflection and a significant amount of wave

energy remains in the initial region. By $t = 12{,}000$, the outward propagating portion has been significantly depleted and by time $t = 18{,}000$ there seems to be little propagation. It is evident in the energy plots at $t = 20{,}000$ and $t = 22{,}000$ that the observed localization length is ~150, consistent with predictions at $t = 28{,}000$. It is more confused since propagated energy does wrap around due to the periodic boundary conditions.

The initial and "final" conditions are exhibited for the following sets of parameters.

Figures 5.6.1—5.6.3

Parameters:

$k_0 = 1.28$
$c = .07$
$dn = .01$
$n_c = 8$
$l_c = .306$
$E = .15$
$W/E = 1.24$
$v_g = .0062$
$v_g t = 50$
$\gamma = 8 \times 10^{-3}$
$\xi = 38$

Figures 5.7.1—5.7.3

Parameters:

$k_0 = 1.7$
$c = .05$
$dn = .01$
$n_c = 8$
$l_c = .306$
$E = .27$
$W/E = 1.37$
$v_g = .004$
$v_g t = 34$
$\gamma = 1.5 \times 10^{-2}$
$\xi = 20$

Figures 5.8.1—5.8.3

Parameters:

$k_0 = 1.28$
$c = .1$
$dn = .01$
$n_c = 8$
$l_c = 1.23$
$v_g = .013$
$v_g t = 230$
$E = 2.47$
$W/E = .61$
$\gamma = 1.2 \times 10^{-2}$
$\xi = 100$

Figures 5.9.1—5.9.3

Parameters:

$k_0 = 1.7$
$c = .05$
$dn = .01$
$n_c = 8$
$l_c = .3$
$v_g = .004$
$v_g t = 34$
$E = .27$
$W/E = 1.38$
$\gamma = 2 \times 10^{-2}$
$\xi = 15.3$

5.2. Effect of Time Varying Density Fluctuations on Localization

In a real plasma the density turbulence is not time stationary, and therefore the effect of motion of the density fluctuations on localization must be studied. As discussed in section 4.3 we expect that the parameter

$$\alpha_G \equiv \left(3 \frac{v_g^2 \lambda^2}{c_s^2 \xi^2} \right)^{1/3}$$

will be important in studying the effect of the mobility of density fluctuations.

One would expect that for $\alpha_G \gg 1$ waves will remain localized, but might spread at a rate corresponding to the velocity spread of the density fluctuations. As α_G decreases to $\alpha_G \sim 1$ one might expect to reach a point at which the wave is no longer localized and therefore the wave packet will spread diffusively. In fact, in the numerical work presented, for strongly localized waves, this does not seem to be the case.

Density fluctuations moving uniformly with a velocity $v < v_g$, the group velocity of the waves, are stationary in a co-moving frame and should not affect localization. This has been verified numerically, but is not presented here.

A second possibility for one-dimensional turbulence is that density fluctuations have a constant speed and may be directed either to the left or to the right. To investigate the effect of this we form two random independent distributions $\delta n_1(x)$ and $\delta n_2(x)$ on the interval $[.5 - dn/2, .5 + dn/2]$ and form the time dependent distribution

$$\delta n(x,t) = \delta n_1(x - c_s t) + \delta n_2(x + c_s t) .$$

The results of these simulations are shown in Figures 5.10.1—5.10.6 and 5.11.1—5.11.6. In these cases one has to remember that the sum of two uniform distributions is not a uniform distribution, and so the results of previous localization length predictions do not apply directly.

For these we use parameters as before except that:

$$\frac{\partial^2 \psi}{\partial t^2} = -\omega_p^2 + 3 c_s \frac{\partial^2 \psi}{\partial x^2}$$

so $v_g = \dfrac{3k\, c_s^2}{\omega_p}$.

Figures 5.10.1—5.10.6

Parameters:

$dn_1 = dn_2 = .004$
$k_0 = .64$
$l_c = 1$
$v_g = .003$
$v_g t = 42$
$E = 1.6$
$W/E = 2.0$
$\gamma \sim .1$
$\xi \cong 10$
$\alpha_G = 1.2$
$c = .04$
$c_s = .004$

In this case we see that the initial wave packet splits and separates at the velocity c_s, and seems to be localized by the co-moving density fluctuations. Spreading appears to occur due to scattering by the oppositely directed wave packet.

Figures 5.11.1—5.11.6

Parameters:

$k_0 = .426$
$c = .2$
$dn = .05$
$n_c = 35$
$l_c = 10.7$
$v_g = .05$
$v_g t = 1635$
$E = 18.5$
$W/E = 1.6$
$\gamma =$
$\xi = 50$
(from Fig. 5.11.2)

In this set we show the resulting distribution of E in the cases of oppositely moving density profiles with:

Figure 5.11.1—5.11.2
$c_s = 0$ (stationary profiles)
$\alpha_G = \infty$
Figure 5.11.3—5.11.4
$c_s = .005c$ ($c_s/v_g = 1/50$)
$\alpha_G = 8.7$
Figure 5.11.5—5.11.6
$c_s = .01c$ ($c_s/v_g = 1/25$)
$\alpha_G = 5.4$

In these cases the wave packet spreads at the speed c_s. Most of the wave energy seems to remain confined within a space determined by $x_0 \pm (\xi + c_s t)$, although we do see indication of some additional spread of wave energy, especially in Figure 5.11.6 in the regions $x < 185$ and $x > 415$.

In the following simulations we assume density fluctuations with widths l_c, amplitudes, random on the interval $[-dn, dn]$, and velocities random on the interval $[-c_s, c_s]$. In other words, each density fluctuation has an independent random velocity.

Figures 5.12a.1—5.12c.1

Parameters:

$k_0 = .426$
$c = .2$
$dn = .02$
$n_c = 14$
$l_c = 4.29$
$v_g = .05$
$v_g t = 480$
$E = 3.3$
$W/E = .92$
$\gamma = .06$
$\xi = 75$

Figure 5.12a.1—5.12a.2
$c_s = 0$ (stationary density fluctuations)
Figure 5.12b.1—5.12b.2
$c_s = .01c$ $(c_s/v_g = 1/25)$
$\alpha_G = 4.14$
Figure 5.12c.1—5.12c.2
$c_s = .01c$ $(c_s/v_g = 1/2.5)$
$\alpha_G = .9$

In this case again the spreading of the wave packet seems limited by $c_s t$.

Figures 5.13a.1—5.13c.3

Parameters:

$k_0 = .854$
$c = .12$
$dn = .028$
$n_c = 8$
$l_c = 2.45$
$v_g = .037$
$v_g t = 1180$
$E = 4.7$
$W/E = .89$
$\gamma = .03$
$\xi = 85$

Figure 5.13a.1—5.13a.6

In this sequence we show the time development for stationary density fluctuations.

Figure 5.13b.1—5.13b.3
As above, but $c_s = .0025c$ $(c_s/v_g = 1/3333)$
$\alpha_G = 6.8$
Figure 5.13c.1—5.13c.3
As above, but $c_s = .01c$ $(c_s/v_g = 1/31)$
$\alpha_G = 2.7$ Note that the vertical scale is different in 5.13c.1 and that the localization region is the same as the others.

Figure 5.13d.1—5.13d.3. As above, but $c_s = .05c$ $(c_s/v_g = 1/16)$ $\alpha_G = .93$

Figure 5.13e.1—5.13e.3. As above, but $c_s = .1c$ $(c_s/v_g = 1/3)$ $\alpha_G = .58$

Again, in this sequence the spreading of the wave packet seems to be limited by $c_s t$, despite small values of α_G. In order to decrease α_G further, it would be necessary to increase $c_s \sim v_g$. At this point localization ceases to have any meaning.

Conclusions

We have found excellent agreement between the localization length predictions of *Escande and Souillard* and the confinement of waves observed in numerical simulations. The interpretation of

$$k_0 \equiv \sqrt{(\omega^2 - \bar{\omega}_p^2)/c^2}$$

as the central wave number of the confined wave packet is borne out, and does lead to, the correct localization length predictions.

Strong localization seems to depend weakly on global properties of the medium and strongly upon local properties. By this it is meant that the structures and spectrum of a localized packet is largely determined by the properties of the medium where most of the wave energy is confined, and the effect of the medium far from this seems only to insure that what little wave energy does reach distant points is scattered back. It is this property which seems responsible for the fact that a localized packet, in the presence of mobile density fluctuations, spreads at the speed c_s characteristic of the speed of the density fluctuations rather than at, for example, v_g.

We see for example, in the early simulations and in 5.13a.2, that initial spreading occurs at the group velocity, despite the existence of density fluctuations up to the point where the wave is confined.

It must be kept in mind that the results shown here for mobile density fluctuations are not necessarily valid for higher dimensions, and in particular it might be expected that waves near the mobility edge in three-dimensions are delocalized by time dependent density fluctuations. On the other hand, the apparent lack of dependence of localization in one dimension on the motion of density fluctuations provides hope that things will not be radically different, and the argument is further supported by the weak dependence of localization length on dimensionality for strong localization as discussed in section 4.

6. Beam-Plasma Processes in Random Media

In section 6.1 we develop a theory for the weak-beam plasma instability in random media. In section 6.2 the results of numerical simulations of this instability are presented. In section 6.3 we develop a theory for the saturation of the instability.

6.1. Theory of Beam-Plasma Processes in a Turbulent Plasma

If waves are localized in a turbulent plasma as theory and our simulations suggest, then a beam-plasma instability could be expected to excite localized waves with a central wave number $k_0 = \frac{\omega_p}{v_b}$ resonant with the beam particles.

In order to understand how this interaction comes about, we return to the Lagrangian discussion of section 3. We shall concern ourselves with the portion of the Lagrangian

$$L = \sum_{i_{BG}} e_i \, \phi(x_i) + \sum_{i_b} \left[p_i \, \dot{x}_i - \frac{p_i^2}{2m} - e_i \, \phi(x_i) \right] - \frac{1}{8\pi} \int |\nabla \phi|^2 \, d^3x$$

We make the assumption that we can represent the fields in this expression as a sum over localized waves whose representation is an exponentially localized wave packet, i.e.,

$$\phi(x,t) = \sum_m \phi_m(x,t)$$

where

$$\phi_m(x,t) = \phi_m \cos \omega_m t \cos k_m(x - x_m) \, e^{-\kappa_m |x - x_m|}$$

where $\kappa_m = 1/\xi_m$.

As seen from the simulation in the previous section, this is only an approximate representation; however, it will allow us to make some theoretical predictions, and it should be reasonable for waves where the localization length is much greater than the central wave length.

We can rewrite this as

$$\phi_m(x,t) = \frac{\tilde{\phi}_m}{2\pi} \int dk \, S_m(k) \left[\cos[\, k(x - x_m) - \omega_m t \,] + \cos[\, k(x - x_m) + \omega_m t \,] \right]$$

where

$$S_m(k) \equiv \frac{\kappa_m}{(k-k_m)^2+\kappa_m^2}$$

From this we readily obtain the generator for the Lie transform

$$w = -\sum_i e_i \int dt\, \phi(x_i,t)$$

$$= -\sum_{i,m} e_i \frac{\tilde{\phi}_m}{2\pi} \int dk\, S_m(k) \left[\frac{\sin[k(x_i-x_m)-\omega_m t]}{kv_i-\omega_m} + \frac{\sin[k(x_i-x_m)+\omega_m t]}{kv_i+\omega_m} \right]$$

If $k^{(1)} = \sum_i e_i\, \phi(x_i)$ where the sum is over all beams and plasma particles, then

$$K^{(2)} = \frac{1}{2}\{w, K^{(1)}\} = -\frac{1}{2} \sum_{j,m,n} \frac{\tilde{\phi}_m \tilde{\phi}_n}{(2\pi)^2} \int dk'\, dk''\, S_m(k')\, S_n(k'') \left\{ \frac{\sin[k'(x_i-x_m)-\omega_m]}{k'v_i-\omega_m} + \frac{\sin[k'(x_i-x_n)+\omega_m t]}{k'v_i+\omega_m}, \right.$$

$$\left. \cos[k''(x_i-x_n)-\omega_m t] + \cos[k''(x_i-x_m)+\omega_n t] \right\}$$

Evaluating the Lie bracket and taking a time average over the rapid phases $\omega_m t$, $\omega_n t$

$$\bar{K}^{(2)} = \sum_{i,m} \frac{e_i^2 \tilde{\phi}_m^2}{8 m_i \pi 2} \int dk'\, dk''\, S_m(k')\, S_m(k'')\, k'\, k''$$

$$\times \left[\frac{\sin k'(x_i-x_m) \sin k''(x_i-x_m)}{(k'v_i+\omega_m)^2} + \frac{\sin k'(x_i-x_m) \sin k''(x_i-x_m)}{(k'v_i-\omega_m)^2} \right]$$

Next we assume that, in this representation, we may replace the sum over particles by a spatially uniform average. Using the Vlasov representation:

$$\sum_i \equiv \sum_i \int d^3x\, d^3v\, \delta^3(x-x_i)\, \delta^3(v-v_i) = \int d^3x\, d^3v\, n_0\, g(v)\,.$$

The assumption that we make here is that once we have taken into account the effect of density fluctuations on the wave propagation which is to localize the waves in the problem, we can use average medium properties (such as averages of the dielectric function) to account for wave-wave and medium-wave coupling effects. The simulation results that will be presented in section 6.2

bear out this assumption.

This gives

$$\bar{K}^{(2)} = \frac{1}{2} \sum_m \frac{|\phi_m|^2}{2\pi} \frac{n_0 e^2}{m} \int d^3v\, g(0)$$

$$\times \int d^3k'\, d^3k''\, k'\, k''\, S_m(k')\, S_m(k'') \frac{\delta(k'+k'') - \delta(k'-k'')}{2}$$

$$\left[\frac{1}{(k'v+\omega_m)^2} + \frac{1}{(k'v-\omega_m)^2} \right]$$

$$= \frac{1}{2} \sum_m \frac{|\phi_m|^2}{2\pi} \int dk'\, S_m^2(k')\, k'^2$$

$$\times \frac{n_0 e^2}{m} \int dv\, g(v) \frac{1}{(k'v+\omega_m)^2} + \frac{1}{(k'v-\omega_m)^2}$$

Likewise we can write

$$L_{\text{fields}} = \frac{1}{8\pi} \int d^3x\, |\nabla\phi|^2 = \frac{1}{8\pi^2} \sum \tilde{\phi}_m^2 \int dk\, k^2 S_m^2(k)$$

We can then write our Lagrangian as

$$L^{(2)} = \bar{K}^{(2)} + L_{\text{fields}}$$

$$= \int dk \sum_m \tilde{\phi}_m^2 \frac{k^2}{2\pi} S_m^2(k) \left[\frac{n_0 e^2}{2\pi} \left\{ \int d^3v \frac{g(v)}{(k'v+\omega)^2} + \frac{g(v)}{(k'v-\omega_n)^2} \right\} - \frac{1}{4\pi} \right]$$

$$= -\sum_m \frac{\tilde{\phi}_m^2 k_m^2}{8\pi^2} \left[-\frac{1}{2} (\varepsilon(k_m, \omega_m) + \varepsilon(-k_m, \omega_m) \right]$$

where $\varepsilon(k, \omega)$ is the usual plasma dielectric function for a plasma with uniform density n_0 and velocity distribution $g(v)$.

But then the action is

$$S^{(2)} = \int dt\, L^{(2)}[\tilde{\phi}_n;\, \theta_m].$$

Varying the action with respect to ϕ_m, and setting it to zero:

$$0 = \frac{\delta S^{(2)}}{\delta \tilde{\phi}_m},$$

gives

$$[\varepsilon(k_m, \omega) + \varepsilon(-k_m, \omega)] = 0 .$$

We note that with the beam present,

$$\varepsilon(k_m, \omega) \neq \varepsilon(-k_m, \omega) .$$

Following the standard analysis this will give a growing wave mode provided

$$\left.\frac{\partial g}{\partial v}\right|_{v=\frac{\omega_p}{k_m}} + \left.\frac{\partial g}{\partial v}\right|_{v=-\frac{\omega_p}{k_m}} > 0 .$$

For all the cases we are interested in the beam velocity $v_b \sim 10\ v_{te}$. The damping from the Maxwellian is negligible. Therefore, ϕ_m should grow at a rate ½ the standard Landau growth rate.

We therefore expect that in a turbulent plasma those localized modes which are resonant with the positive slope portion of the beam will grow with the same growth rate as a plane wave with the same central wave number in the homogeneous case. A major difference between the two will be that the localized waves will remove much less energy from the beam for any given maximum wave amplitude.

For the sake of completeness, we can also look at single particle motion. If we have the new single particle Hamiltonian $\overline{K}_i^{(2)}$, then the guiding center motion of particles is $\dot{P}_i = -\frac{\partial \overline{K}^{(2)}}{\partial X_i}$.

$$\overline{K}_i^{(2)} = \frac{1}{2}\{w, k_i^{(1)}\} =$$

$$-\frac{1}{2}\sum_n \frac{e_i^2}{m_i}\frac{|\phi_n|^2}{(2\pi)^2}\int dk'\, dk''\, S_n(k')\, S_m(k'')\, k'\, k''$$

$$\sin k'(x_i - x_m)\sin k''(k_i - x_m)\left[\frac{1}{(k'v_i + \omega)^2} + \frac{1}{(k'v_i - \omega)^2}\right] .$$

This can be evaluated noting that:

$$\int dk''\, k''\, S_m(k'')\sin k''y = -\pi\frac{\partial}{\partial y}\left[\cos k_m y\, e^{-\kappa_m |y|}\right]$$

and near resonance for v_i,

$$\int dk'\, k'\, S_m(k')\frac{1}{(\omega_m - k_m v_i)^2}\sin k'y$$

$$\cong \frac{\pi}{v_i^2} \frac{\partial}{\partial\left(\frac{\omega}{v_i}\right)} \left[\left(\frac{\omega}{v_i}\right) S_m \left(\frac{\omega}{v_i}\right) \cos\left(\frac{\omega}{v_i}\right) \right] \left[\Theta(y) - \Theta(-y)\right]$$

where

$$\Theta(y) = \begin{cases} 1 & \text{if } y>0 \\ 0 & \text{if } y<0 \end{cases}$$

Far from resonance when $\left|\omega_n - |k_n v_i|\right| \gg \kappa_m$

$$\bar{K}_i^{(2)} = \frac{e_i^2}{16\, m_i} \sum_n k_m^2 \phi_n^2 e^{-2\kappa_n |x - x_n|} \left[\frac{1}{(k_n v_i - \omega_n)^2} + \frac{1}{(k_n v_i + \omega_n)^2} \right].$$

This is just the usual ponderomotive potential (*Schmidt*, 1979, p. 51).

Near a resonance, $\left|\omega_n - |k_n v_i|\right| \leq \kappa_n$

$$\bar{K}_i^{(2)} = \frac{1}{2} \frac{e_i^2 \phi_n^2}{m_i (2\pi)^2} \left[-\pi \frac{\partial}{\partial y} \cos k_n (k - x_n) e^{-\kappa_n |x - x_n)} \right]$$

$$\left[\frac{\pi}{v_i^2} \frac{\partial}{\partial\left(\frac{\omega}{v_i}\right)} S_n \left(\frac{\omega}{v_i}\right) \cos \frac{\omega_n}{v_i} (x - x_n) \right] \left[\Theta(x - x_n) - \Theta(x_n - x)\right]$$

$$\cong \frac{e_i^2}{8 m_i v_i^2} e^{-\kappa_n |x - x_n|} \phi_n^2 \frac{k_n}{\kappa_n} \frac{\partial}{\partial\left(\frac{\omega_n}{v_i}\right)} \left\{ \left(\frac{\omega_n}{v_i}\right) \frac{1}{\left(\omega_n/v_i - k_n\right)^2/\kappa_n^2 + 1} \right.$$

$$\left. \sin\left[\left(\frac{\omega_n}{v_i} - k_n\right)(x - x_n) \right] \left[\Theta(x - x_n) - \Theta(x_n - x)\right] \right\}$$

$$\cong \left[\frac{e_i^2 k_n^2 \phi_n^2}{8 m_i v_i^2 \kappa_n} \right] e^{-\kappa_n (x - x_n)} \frac{\left[\frac{\omega_n}{k_n v_i} - 1\right]}{\left(\omega_n/v_i - k_n)^2/\kappa_n^2 + 1\right)} \cos\left[\left(\frac{\omega_n}{v_i} - k_n\right) \left(x - x_n\right) \right]$$

$$\times \left[\Theta(x - x_n) - \Theta(x_n - x)\right]$$

We note the following points. Everything outside of the braces is dimensionless. $K_i^{(2)} \sim \frac{1}{\kappa_n}$ and therefore is strongly dependent on the localization length. It also changes sign with $\omega_n - k_n v_n$, i.e., as the particle is faster, or slower than the resonant velocity. We will return to this subject when we discuss saturation mechanisms for the beam-turbulent plasma instability in section 6.3.

6.2. Simulation of Beam-Plasma Processes

In this section we show the results of a series of simulations of beam-plasma instabilities. The method of simulation and the program are described fully in Appendix A, but briefly is as follows:

The beam is simulated by particles which obey the equations of motion:

$$\frac{d^2x_i}{dt^2} = \frac{e}{m} E(x_i)$$

$$n_{\text{beam}}(x,t) = \sum_i \delta\,(x - x_i(t))$$

For the background, define

$$\psi(x,t) = -e\left(n_e(x,t) - n_i(x,t)\right)$$

with equation of motion

$$\frac{\partial^2\psi}{\partial t^2} = \omega_p^2(x)\,\psi + 3v_t^2\,\frac{\partial^2\psi}{\partial x^2}$$

where $\omega_p^2(x) \equiv 4\pi n_t\,(x,t)\,e^2/m_e$ is a random variable.

For the fields: $\nabla \cdot E = 4\pi\rho$, where $\rho = -en_{\text{beam}}(x,t) + \psi(x,t)$.

We plot E and ψ as before, except that ψ now represents the background charge density perturbations due to plasma oscillations. The plot parameters are as in section 5 with the following additions and exceptions.

v_{t_1} = effective electron thermal velocity of background plasma

n_b/n_p = beam density/effective background plasma density

v_b = beam drift velocity

v_{t_2} = beam thermal velocity

k_0 = beam resonant wave number

$v_g = \dfrac{3k_0\,v_{t_1}^2}{\omega_p}$ = group velocity of beam resonant waves in the background plasma

# of states $\equiv \dfrac{k_0 L}{2\pi}\left(\dfrac{v_{t_2}}{v_b}\right)$, which represents the expected number of localized states which should be excited by the beam. (See the discussion in section 4.2 on density of states.)

The initial conditions for all of these simulations are $\psi(x)=0$, $\dot{\psi}(x)=0$, and beam particles uniformly distributed in space with average velocity v_b and a Maxwellian distribution with thermal velocity v_2.

Figures 6.1.1—6.1.3

Parameters:

$v_{t_1}=.07$
$v_b=1.5$
$v_{t_2}=.15$
$n_b/n_{pl}=9\times10^{-6}$
$k_0=.67$
$v_g=.01$
$dn=0$

This set shows a system without density fluctuations and should be compared with 6.3.1—6.3.6 which has 1% density fluctuations. The noteworthy points in this are the smooth variations in the envelope of ψ, and the purity of the harmonic content. The envelope modulation can be understood as the beating of a narrow spectrum of waves excited by a beam of finite temperature. If we take $\xi\Delta k=2\pi$, where ξ is the characteristic length of the modulation and $\Delta k=\Delta\left(\omega/v\right)\cong\omega_p\, v_{t_2}/v_b^2=.066$. Therefore $\xi=94$, consistent with the characteristic length of the modulation of ψ. The other noteworthy point is that the energy density plot is characteristic of a traveling wave. Furthermore, comparing the positions of the peaks at $t=3{,}000$ and $t=4{,}800$, it is apparent that they have moved a distance $v_g\,\Delta t=18$ between these two times, as one would predict.

Figures 6.2.1—6.2.15

Parameters:

$v_{t_1}=.035$
$v_b=1.0$
$v_{t_2}=.1$
$n_b/n_{pl}=9\times10^{-6}$
$dn=.01$
$n_c=4$
$k_0=1.0$
$l_c=.61$
$E=.38$
$W/E=2.77$
$\gamma\cong.06$
$\xi=8.7$
$v_g=.0036$
$v_g t=20$
states=5

6.2.1 shows the distribution of density fluctuations.

6.2.2 shows the initial beam-particle phase space (velocity vs. position).

6.2.3 shows the initial beam distribution function.

At $t=0$, $\psi=0$, and Figures 6.2.4—6.2.15 show the subsequent time development of the beam-plasma instability.

At $t=200$, ψ is approximately uniform in space, and the energy shows that the wave is a traveling wave. By $t=1200$ the localized structure is beginning to show. Between times $t=4{,}000$ and

$t = 5{,}000$, the mode structure is reasonably stable and the growth has saturated.

Figures 6.3.1—6.3.6

Parameters:

$v_{t_1} = .07$
$v_b = 1.5$
$v_{t_2} = .15$
$n_b/n_{pl} = 9\times10^{-6}$
$dn = .01$
$k_0 = .67$
$n_c = 8$
$l_c = 2.34$
$E = 2.46$
$W/E = 1.5$
$\gamma = 6\times10^{-2}$
$\xi = 27$
$v_g = .01$
$v_g t = 58$
states = 13

Simulation shows the same initial conditions as in 6.1.1—6.1.3 except that 1% density fluctuations were introduced. The energy density plots are consistent with standing waves.

Figure 6.4.1—6.4.6

Parameters:

$v_{t_1} = .1$
$v_b = 1.26$
$v_{t_2} = .12$
$n_b/n_{pl} = 9\times10^{-6}$
$dn = .02$
$k_0 = .79$
$n_c = 4$
$l_c = 1.17$
$E = .854$
$W/E = 1.06$
$\gamma = 2\times10^{-2}$
$\xi = 59$
$v_g = .024$
$v_g t = 142$
# of modes = 15

Figure 6.5.1—6.5.2

Parameters:

$v_{t_1} = .04$
$v_b = .7$
$v_{t_2} = .1$
$dn = .01$
$n_b/n_{pl} = 9\times10^{-6}$
$k_0 = 1.43$
$n_c = 4$
$l_c = .6$
$E = .77$
$W/E = 1.0$
$\gamma = 2\times10^{-2}$
$\xi = 30$
states = 10
$v_g = .006$
$v_g t = 26$

Figure 6.6.1—6.6.2

Parameters:

$v_{t_1} = .05$
$v_b = .7$
$v_{t_2} = .08$
$dn = .01$
$n_b/n_p = 9\times10^{-8}$
$k_0 = 1.43$
$n_c = 4$
$l_c = .61$
$E = .77$
$W/E = 1.9$
$\gamma \cong 5\times10^{-2}$
$\xi = 12.2$
states = 8
$v_g = .0036$
$v_g t = 13.6$

Figure 6.7.1—6.7.2

Parameters:

$v_{t_2} = .15$
$v_b = 1.5$
$v_{t_1} = .1$
$dn = .01$
$n_b/n_p = 9\times10^{-6}$
$k_0 = .66$
$n_c = 4$
$l_c = .61$
$E = .16$
$W/E = 2.3$
$\gamma \cong 6\times10^{-2}$
$\xi = 10$
states = 2
$v_g = .0067$
$v_g t = 13.2$

Growth rates and levels at saturation

The peak energy density (E) versus time is plotted in Figure 6.11 for the simulation presented in Figures 6.2.1-6.2.15, giving an observed growth rate between $t = 200$ and $t = 1200$ as $\gamma/\omega_p = .0015$. The growth rate between $t = 1200$ and $t = 3500$ is $\gamma/\omega_p = .00024$. (Note that the

growth rate for E is 2γ.) The standard expression for the Landau growth rate of a weak beam is

$$\frac{\gamma}{\omega_p} = \frac{\omega_{p_b}^2}{\omega_p^2} \frac{1}{n_b} \frac{\partial f_b}{\partial v_\parallel} \bigg|_{v_\parallel = \omega/k}$$

(*Chen*, 1976), and gives for the fastest growing wave resonant with a Maxwellian beam:

$$\frac{\gamma_{\max}}{\omega_p} \cong .38 \frac{\omega_{p_b}^2}{\omega_p^2} \frac{v_\parallel^2}{v_{th_b}^2} = .00034$$

for the fastest growing wave for the parameters of this simulation. We had predicted that the observed growth rate for a localized wave should be $\gamma/2 = .00017$. We note that the observed growth rate between $t = 1200$ and $t = 3500$ lies between $\gamma/2$ and γ. That the observed growth is larger than $\gamma/2$ is to be expected since the growth time $1/\gamma \sim \xi/v_g$ and so the resonant wave is only partially reflected during the growth time. The very large growth rate for $t < 1200$ is a result of discrete particle effects early on and the "quiet start" beam initialization (*Birdsall and Langdon*, 1985). Resolving these difficulties would require many more particles and a much slower growth rate, straining available computer time.

We can scale the levels of saturation in our simulation to values for the type III solar radio burst in *mks* units as follows. Let primed units refer to type III parameters in *mks* units and unprimed quantities to simulation values. Then from the equation of motion $\ddot{x} = (q/m)E$ the scaling is

$$\frac{E'}{E} \sim \frac{(m'/q')}{(m/q)} \frac{v'}{v} \left[\frac{t}{t'} \right]$$

We use $t/t' \sim \omega_p'/\omega_p$, m'/q' = electron charge/mass ratio in *mks* units and

$$\frac{v'}{v} = \frac{\text{Type III beam velocity } (mks)}{\text{Simulation beam velocity}} .$$

Since $E = 4\pi\rho/k = \psi/k$; $k = 1$; and at saturation (Figure 6.2.12) $\psi = 2 \times 10^{-4}$, the saturation field is

$$E' = 3 \ mV/\text{m}$$

which should be compared with the 1 mV/m observed field for the March 11 event. This scaling, it should be noted, is only valid for the case that n_b/n_{pl}, $v_b/v_{th_{BG}}$, and v_b/v_{th_b} are the same for both

plasmas. This is not exactly the case, and furthermore, as discussed in the summary to this section, the distribution function for the solar wind is not a Maxwellian.

6.3. Saturation of the Beam-Plasma Instability

A fundamental problem in understanding the type III solar burst is the mechanism for saturation of the beam-plasma instability, limiting growth to the observed levels, despite the persistence of the observed positive slope at a distance of 1 AU. An extensive study of this problem was done using quasi-linear theory (*Magelssen*, 1976; *Magelssen and Smith*, 1977). These authors concluded that an important effect in the persistence of the beam is that at a given point in space, the beam velocity decreases with time. Slower beam electrons later in time reabsorb plasma waves which were resonant with the faster electrons that produced them earlier in time. At 1 AU the ISEE-3 data do not support the quasi-linear relaxation hypothesis, since a strong positive slope is observed on the electron distribution function.

Papadopolous (1974) has proposed that the oscillating two-stream instability is responsible for removing resonant Langmuir waves, thereby limiting the growth rate of the beam-plasma instability. Observed wave levels at 1 AU are below the threshold for this process, however (*Lin et al.*, 1986). As discussed in section 4.1, *Muschietti* (1985) examined the effect of Langmuir waves being scattered out of resonance with the beam electrons by solar wind density fluctuations and concluded that the process was "too efficient." They found that unless special assumptions are made about the anisotropy of the density fluctuations the beam plasma instability will be suppressed.

In the *Whelan and Stenzel* experiment (1984), the beam was observed to travel the length of the experiment with no evidence of quasi-linear relaxation, although Langmuir waves from the beam-plasma instability were observed only in the first few centimeters of the experiment. They concluded that particle trapping was responsible for saturating the instability. In their simulation of this problem, *Pritchett and Dawson* also concluded that trapping was responsible for saturation of the instability. In both cases, however, the beam was relatively cold.

Davidson (1972, p. 55 ff.) gives the characteristic trapping time for a particle resonant with a Langmuir wave with electric field E and wave vector k as

$$\tau_{tr} \equiv \omega_B^{-1} \equiv (m_e/ekE)^{1/2} .$$

for the 11 March event this gives

$$\tau_{tr} = .0016 \text{ sec} . \tag{6.3.1}$$

On the other hand, the transit time through a localized wave packet of 70 km extent using v_b from the 11 March event is $t = \xi/v_b = .002$ sec. It should be kept in mind that in 6.3.1 we have used the peak field. Not only is the average trapping time much larger due to the lower average field, but the bounce frequency changes radically on transit through the localized structure. Therefore, particle trapping does not occur, and we propose another saturation mechanism in what follows.

We show the distribution functions at saturation for two cases. The runs are similar to those of runs 6.1 through 6.7, however, we have used a short simulation volume ($L = 150$ vs. $L = 1200$) in order to increase the phase space density of simulation particles. This results in much smoother distribution function.

Figures 6.8.1—6.8.3 Parameters:	Figures 6.9.1—6.9.3 Parameters:
$v_{t_1} = .15$	$v_{t_1} = .13$
$v_b = 2.2$	$v_b = 1.8$
$v_{t_2} = .15$	$v_{t_2} = .15$
$n_b/n_p = 9\times10^{-6}$	$n_b/n_p = 9\times10^{-6}$
$dn = .02$	$dn = .03$
$n_c = 12$	$n_c = 12$
$\gamma = .06$	$\gamma = .09$
$\xi = 30$	$\xi = 20$
$k_0 = .45$	$k_0 = .55$
$l_c = 1.8$	$l_c = 1.8$
$E = .65$	$E = 1.0$
$W/E = 1.5$	$W/E = 1.8$

The important result is that in both cases the distribution function is flattened in the vicinity of the wave-resonant velocity. There appears to be no overall heating or diffusion of the beam, a characteristic shared with every simulation that we have done.

The crucial difference between our condition and quasi-linear diffusion is that here the particles see only one wave at a time. Furthermore, the localized wave, although having a width in k space is not well approximated by the random phase approximation, since, in fact, it is a coherent structure, the phases are well determined, and first order changes to the particle velocity are enough to maintain a certain phase relationship between the wave and a particle.

Velocity space diffusion of particles by localized wave packets

In order to investigate the effect of a localized wave packet on the distribution function, a simple program was run. We followed the orbits of an initial particle distribution governed by the equation of motion

$$\frac{d^2x}{dt^2} = E_0 \cos t \cos x \; e^{-\kappa |x|}$$

where κ is a variable parameter. E_0 was chosen so that the trapping velocity

$$v_{tr} \equiv \sqrt{\frac{2e\,E_0}{mk}} = \sqrt{2E_0} = .1\,,$$

meaning that a particle of velocity $v_0 \pm .1$ would be trapped by the wave if $\kappa = 0$. The results were as follows:

Figure 6.10.2 the initial distribution function for the numerical experiment was:

$$f(v) = \begin{cases} \text{constant} & .8 \le v \le 1 \\ 0 & \text{otherwise} \end{cases}$$

Figure 6.10.2 distribution function after passing through the wave packet for $\kappa = .1$.

Figure 6.10.3 as above but $\kappa = .2$

Figure 6.10.4 as above but $\kappa = .4$

It is clear that the particles have diffused in velocity space around the resonant velocity $v_{res} = 1.0$. The diffusion is significant in the neighborhood of velocity $v = 1.0$ with width approximately $\cong \pm\,\kappa$. In the case (not shown) where

$$f(v) = \begin{cases} \text{constant} & .8 \le v \le 1.2 \\ 0 & \text{otherwise} \end{cases},$$

no distortion of the distribution after passage through the wave was noted.

In order to explain this we begin with the Vlasov equation:

$$0 = \frac{df}{dt} \equiv \frac{\partial f}{\partial t} + \{f, H\}. \tag{6.3.2}$$

We expand f and H by order in the field:

$$f = f^{(0)} + f^{(1)} + f^{(2)}$$

$$H = H^{(0)} + H^{(1)} = \sum_i \left[\frac{p_i^2}{2m_i} + e_i\, \phi(x_i) \right]$$

Then 6.3.2 becomes

$$\frac{\partial t^{(1)}}{\partial t} = -\{f^{(0)}, h^{(1)}\} \quad \text{or,}$$

$$f^{(1)} = \{w, f^{(0)}\} \text{ and}$$

$$\overline{\frac{\partial f^{(2)}}{\partial t}} = \overline{\{f^{(1)}, h^{(1)}\}}$$

where the bar indicates time-averaging.

Using our previous expression for w,

$$w_i = -\frac{e\phi_0}{\pi} \int dk \left[\frac{\kappa}{(k-k_0)^2 + K^2} \right] \left[\frac{\sin(kx_i + \omega t)}{kv_i + \omega} + \frac{\sin(kx_i + \omega t)}{kv_i - \omega} \right]$$

we find

$$\begin{aligned}
\overline{\frac{\partial f^{(2)}}{\partial t}} &= \overline{-\{f^{(1)}, h^{(1)}\}} \\
&= \overline{-\{\{w, f^{(0)}\}, k^{(1)}\}} \\
&= \frac{-e^2\phi^2}{2\pi^2} \int dk'\, dk'' \, \frac{\kappa^2 k''}{[(k_0-k')^2 + \kappa^2]\,[(k_0-k'')^2 + \kappa^2]} \\
&\quad \times \overline{\left\{ \left[\frac{\cos(k''x + \omega t)}{k''v + \omega} + \frac{\cos(k''x - \omega t)}{k''v - \omega} \right] \frac{\partial f_0}{\partial p}, \cos k'x \cos \omega t \right\}}. \\
&= \frac{-e^2\phi^2}{4\pi^2} \int dk'\, dk'' \, \frac{\kappa^2 k' k'' \sin k'x \cos k''x}{\left[(k_0-k')^2 + \kappa^2\right]\left[(k_0-k'')^2 + \kappa^2\right]} \frac{\partial}{\partial p} \left[\left(\frac{1}{k''v + \omega} + \frac{1}{k''v - \omega} \right) \frac{\partial f_0}{\partial p} \right]
\end{aligned}$$

Keeping resonant terms and ignoring ponderomotive effects, this can be evaluated as

$$\frac{\partial f}{\partial t} = -\left(\frac{e\,k_0\,\phi}{m}\right)^2 \frac{\partial}{\partial v}\left[\frac{\kappa v \sin k_0 x \sin\left|\frac{\omega}{v}x\right| e^{-\kappa|x|}}{(\omega - k_0 v)^2 + \kappa^2 v^2}\,\frac{\partial f_0}{\partial v}\right]$$

This is the standard form for a diffusion equation. Although we might try to integrate this numerically, it is instructive to examine this expression and make some estimates of the diffusion rate. We note first that $D(v)$ will be significantly different from zero only in a region

$$\frac{\omega}{k_0}\left(1 - \frac{\Delta\kappa}{k_0}\right) \lesssim v \lesssim \frac{\omega}{k_0}\left(1 + \frac{\Delta\kappa}{k_0}\right)$$

and

$$-\frac{1}{\kappa} \lesssim x \lesssim \frac{1}{\kappa}.$$

agreement with the computational results of plots 6.12.1—6.12.4.

We attempt to estimate the maximum electric field to which a wave can grow by assuming the growth stops when the distribution is flattened in the region resonant with the wave. To flatten the original slope of the beam distribution function f we require that $\Delta t\,\frac{\partial f}{\partial t} \sim (v - v_r)\,\frac{\partial f}{\partial v}$.

Noting that the transit time $\Delta t \sim \frac{1}{\kappa v}$, taking

$$\frac{\partial f_0}{\partial v} \sim \frac{1}{v_{th}} f_0,$$

and assuming

$$<\sin k_0 x \sin\left|\frac{\omega}{v}x\right|> \sim \frac{1}{2}$$

where the average is over the trajectory of a nearly resonant particle. We obtain

$$\frac{v - v_r}{\kappa v\,\Delta t} = \left(\frac{e k_0 \phi}{m}\right)^2 \frac{2\,(v - v_r)\,k_0^2 + 2\kappa^2 v}{[(\omega - k_0 v)^2 + \kappa^2\,v^2]^2}$$

from this we estimate

$$E = \left[m_e\,\frac{\kappa^2}{k_0^2}\,v^2\right] k_0. \tag{6.3.3}$$

As an example we use the 11 March 1979 parameters. For $v = .1\,c$, $\kappa = 1/7 \times 10^4$m (20 wavelengths/localization length), and $k_0 = 2 \times 10^{-5}$/cm which are values typical of a type III burst, we obtain $E_{max} \cong .5$ mV/m. This number should not be taken too seriously, but is close to the observed ~ 1 mV/m of the 11 March 79 event.

Likewise for our simulations (Figures 6.2.1-6.2.15), equation 6.3.3 with $kE = \psi$ gives us $\psi = \frac{m}{e}\kappa^2 v^2$. Using the simulation parameters $m/e = 1$, $\kappa = 1/\xi = 1/8.7$, $v = .1$, we predict at saturation $\psi = 1.3 \times 10^{-4}$, which is within a factor of 2 of the values in Figure 6.2.12.

This theory for resonant diffusion is similar to quasi-linear theory (*Davidson*, 1972, p. 151, ff.), except that we do not make the assumption $<\phi_k\,\phi_{k'}> = |\phi_k|^2\,\delta_{kk'}$, as is usual in weak turbulence theory, but keep the Fourier representation of the waves in the system and integrate over that.

Summary

The consequences of wave localization in one dimension as presented in this section are consistent with satellite observations of the weak-beam plasma instability in the solar wind. Two considerations have been ignored in this section:

i) The solar wind is three-dimensional. This is discussed further in the conclusions (section 8).

ii) The solar wind plasma has a non-thermal tail (see figure 2.3). Among other things this reduces the positive slope of the distribution function reducing the growth rate. The growth time $1/\gamma$, in our simulation are $\lesssim$ the localization times, while growth times in the solar wind plasma are ~1 sec.

For the 11 March event $v_g = 2.4 \times 10^7$ cm/sec. If $\xi \sim 70$ km, the localization time $\sim \tau = .3$ sec. So $\gamma\tau = .3$. If anything, this should mean that localization is even more evident in the solar wind plasma.

Simulating the non-thermal tail on the background distribution function is a very difficult problem because of limitations on the number of simulation particles (see Appendix A). The experiment done by *Whelan and Stenzel* (1985) suggests that this non-thermal tail may result from a strong turbulence mechanism, which would have significant implications for the mechanisms discussed here. These mechanisms may be important far upstream in or near the solar corona, but as discussed in section 2, are inconsistent with satellite observations at 1 AU.

7. Three-Wave Processes

Although this section is last in the thesis, the considerations in it were the motivation for studying everything so far presented. In section 7.1 we will review the theory of 3-wave processes in homogeneous media, and then in section 7.2 discuss the convective problem as it applies to the type III problem. We conclude that wave convection in homogeneous media inhibits the $L \to T + S$ decay process. We review previous work on 3-wave processes in inhomogeneous media. In section 7.3. we develop theory for 3-wave processes when wave localization occurs.

7.1. Three-Wave Decay Processes

In the absence of density fluctuations, the second and third order terms in the action can be written as

$$S^{(2)} + S^{(3)} = -\int dt \left\{ K^{(2)} + \frac{1}{8\pi} \int d^3x \left(|E|^2 - |B|^2 \right) \right\} - \int dt\, K^{(3)}$$

where the first integral on the right is of second order in the fields and the second is of third order.

Starting from the expansion (3.4)

$$K^{(3)} = \frac{1}{6} L^3 H^{(0)} + \frac{1}{2} L^2 H^{(1)} + L H^{(2)} .$$

and using

$$L H^{(0)} = -H^{(1)}$$

we obtain:

$$K^{(3)} = \frac{1}{3} L^2 H^{(1)} + L H^{(2)} . \tag{7.1.1}$$

If we can use the eikonal approximation to express the potentials

$$\Phi = \sum_k \tilde{\Phi}_k\, e^{i\theta_k(x,t)} + cc \quad \text{(complex conjugate)}$$

and

$$\underset{\sim}{A} = \sum_k \hat{\varepsilon}_k \tilde{A}_k\, e^{i\theta_k(x,t)} + cc$$

then, as *Kaufman* has shown

$$S^{(2)} = -\sum_a \int d^3x\, dt\, \varepsilon_a(k,\omega;x,t)\,\hat{\Phi}_a^2(x,t) + \sum_b \int d^3x\, dt\, \hat{\varepsilon}_b^* \overleftrightarrow{D}(k,\omega,xt)\,\hat{\varepsilon}_b(k,x)\, \left|\tilde{A}_b(x,t)\right|^2$$

where ε is the dielectric function for electrostatic waves, $\overleftrightarrow{D}$ is the electromagnetic dispersion tensor, and $\hat{\varepsilon}_b$ is the polarization vector of the electromagnetic wave, b.

We have made this separation because we shall be concerned with electrostatic and transverse electromagnetic waves. As *Kaufman* has shown, one can use this to find the variable canonically conjugate to $\theta_a(x,t)$, the phase of the wave in the eikonal approximation localizing $k_a = \nabla\theta_a$ and $\omega_a = \dfrac{-\partial\theta_a}{\partial t}$, one finds

$$J_a(x,t) \equiv \frac{\delta S}{\delta[\partial\theta_a/\partial t]} = -\frac{\delta S}{\delta\omega} = \left[\frac{\partial\varepsilon_a(x,t;k_a,\omega_a)}{\partial\omega}\right] \left|\phi_a(x,t)\right|^2$$

Likewise

$$J_b(x,t) \equiv \frac{\delta S}{\delta[\partial\theta_b/\partial t]} = -\frac{\delta S}{\delta\omega_b} = \left(\frac{\partial}{\partial\omega_b}\left[\hat{\varepsilon}_b^* \overleftrightarrow{D}(x,t;k,\omega)\,\hat{\varepsilon}_b\right]\right) |A_b(x,t)|^2$$

These expressions will be recognized as the standard action densities with the Hamiltonian

$$\sum_\alpha \int d^3x\, dt \quad \omega_\alpha J_\alpha .$$

We may also use these variables to re-express the fields in $S^{(3)}$. We will then have

$$K^{(2)} + K^{(3)} = \sum_a \int d^3x\, \omega_a(x,t)\, J_a(x,t) + \sum_{\mu\nu\lambda} \beta_{\mu\nu\lambda} \sqrt{J_\mu J_\nu J_\lambda}\, e^{i(\theta_\mu + \theta_\nu + \theta_\lambda)}$$

In Appendix B, we show that

$$K^{(3)} = i\sqrt{J_S J_L}\, \sqrt{\frac{\omega_L\, \omega_S\, E_L^2}{16\pi n_0 k\, T}}\, \sin\alpha\, e^{i(\theta_L - \theta_T - \theta_D)} + cc$$

We define

$$\beta = \sqrt{\frac{\omega_L\, \omega_S}{16\pi\, n_0 kT\left(\partial\varepsilon_L/\partial\omega\right)}}\, \sin\alpha$$

and obtain

$$K^{(3)} = 2\beta \sqrt{J_S J_L J_T} \cos\phi$$

where

$$\phi \equiv \theta_L - \theta_T - \theta_S$$

We will also define

$$\gamma_0 \equiv \beta \sqrt{J_L}$$

The factor of 2 comes from the fact that the growth rate for the action is twice the growth rate for the fields, as computed by *Shukla et al.* (1983).

Going back to the action $S^{(2)} + S^{(3)}$, and varying with respect to $\theta(x,t)$, we get

$$\frac{dJ_a}{dt} = \frac{\partial J_a}{\partial t} + v_g \cdot \nabla J_a = -2\beta \sqrt{J_a J_v J_\lambda} \sin\Phi \tag{7.1.1}$$

We also get:

$$\frac{\partial \theta_a}{\partial t} = -\frac{\partial K}{\partial J_a} = -\omega_a + \beta \sqrt{\frac{J_v J_\lambda}{J_a}} \sin\Phi$$

From 7.1.1 we can see that $\overline{\frac{dJ}{dt}} \cong 0$ unless $\overline{(\theta_a + \theta_v + \theta_\lambda)}$ does not vanish when the bar indicates a time average. This gives us the resonance conditions

$$\omega_a - \omega_b - \omega_c = 0 \quad \text{and} \quad \underset{\sim}{k}_a - \underset{\sim}{k}_b - \underset{\sim}{k}_c = 0 \tag{7.1.1a}$$

If one wave, J_a, initially has large amplitude and the other two J_b, J_c have very small amplitude, then initially we may take J_a as almost constant. Furthermore, the relative phase Φ will quickly evolve so that $\sin\Phi \cong 1$, and so we use $\sin\Phi = 1$ in what follows. (For this and a discussion of the general time development of such a system of equations see *Meiss*, 1979, and *Bergmann*, 1985.)

We define $a_1 = \sqrt{J_S}$ $\quad a_2 = \sqrt{J_T}$ and obtain

$$\left[\frac{\partial}{\partial t} a_1 + v_{g_1} \cdot \frac{\partial a_1}{\partial \underset{\sim}{x}} \right] = \gamma_0 a_2$$

$$\left[\frac{\partial}{\partial t} a_2 + \underset{\sim}{v}_{g_2} \cdot \frac{\partial a_2}{\partial \underset{\sim}{x}} \right] = \gamma_0 a_1$$

If waves 1 and 2 are damped, we can put in the damping heuristically to obtain the WKB equations:

$$\left[\frac{\partial}{\partial t} + \underset{\sim}{v}_{g_1} \cdot \frac{\partial}{\partial x} + \gamma_1\right] a_1 = \gamma_0 a_2 \tag{7.1.2a}$$

$$\left[\frac{\partial}{\partial t} + \underset{\sim}{v}_{g_2} \cdot \frac{\partial}{\partial x} + \gamma_2\right] a_2 = \gamma_0 a_1 \tag{7.1.2b}$$

which were first obtained by *Rosenbluth* (1972).

In the cases where the damping is of kinetic origin (ion Landau damping for example), this would have come out of the solution of $\varepsilon(k, \omega) = 0$. In the case of the transverse waves, however, where the damping is dominated by collisional effects, it is not deriveable from an action principle.

A brief word about the damping rates of the ion-acoustic and electromagnetic waves is in order. For the transverse waves we use the Dawson-Oberman impedance

$$\frac{\Gamma_T}{\omega_{pe}} \leq \frac{2 \ln \Lambda - 1}{\sqrt{18\pi}\, \Lambda} \quad \text{where} \quad \Lambda = 4\pi n \lambda_D^3$$

(*Dawson*, 1968). This may actually be as much as a factor of 2 larger due to enhancement from ion density perturbations in the solar wind.

$$\frac{\Gamma_T}{\omega_{pe}} \sim 2.5 \times 10^{-11} \text{ for the 11 March 1979 event.} \tag{7.1.3}$$

For the ion-acoustic wave, the damping rate as determined by *Lin et al.* (1986), is

$$\gamma_S \cong .1\, \omega \tag{7.1.4}$$

due to Landau damping of the ion-acoustic waves. For the 11 March 79 event $T_e/T_i \sim 5$.

The damping of ion-acoustic waves leads to a dissipative "localization" in space. The dissipation length will be

$$\frac{\xi}{\lambda_S} \equiv \frac{c_S}{\gamma_S \lambda_S} = \frac{1}{.1\, k_S \lambda_S} = 1.5\,.$$

7.2. Space-Time Evolution

If we assume that $a_1(x,t) = \tilde{a}_1 e^{\underset{\sim}{K}\cdot\underset{\sim}{v} - \omega t}$, and $a_2(x,t) = \tilde{a}_2 e^{\underset{\sim}{K}\cdot\underset{\sim}{v} - \omega t}$, and substitute these into 7.1.2*b*, then $(\omega - \underset{\sim}{K}\cdot\underset{\sim}{v}_1 + \gamma_1)\tilde{a}_1 = \gamma_0 \tilde{a}_2$, and $(\omega - \underset{\sim}{K}\cdot\underset{\sim}{v}_2 + \gamma_2)\tilde{a}_2 = \gamma_0 \tilde{a}_1$, which can be combined to yield the "disperson relation"

$$(\omega - \underset{\sim}{K}\cdot\underset{\sim}{v}_1 + \omega_1)(\omega - \underset{\sim}{K}\cdot\underset{\sim}{v}_2 + \gamma_2) - \gamma_0^2 = 0 . \tag{7.2.1}$$

The spatial and temporal development of a 3-wave system governed by 7.2.1 have been thoroughly studied and reviewed by *A. Bers* (1983) whose analysis we follow in the remainder of this section. In order to simplify the analysis, we first transform to a frame moving with velocity V such that $v_1 = v_1' + V$, $v_2 = v_2' + V$, and $\omega' \equiv \omega - \underset{\sim}{K}\cdot\underset{\sim}{V}$, where V is chosen such that v_1', v_2' are (anti-) parallel. We will take wave 1 to be the ion-acoustic daughter wave and wave 2 to be the transverse electromagnetic daughter wave. The general vector relationship of $\underset{\sim}{v}_T$ and $\underset{\sim}{v}_S$ are shown in 7.2.2, along with our choice for V, which will reduce the problem to one-dimension with the vector relation shown in 7.2.3.

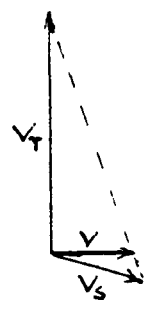

7.2.2

7.2.3

In the frame of reference shown in 7.2.3, one obtains the "dispersion relation"

$$(\omega' - K\, v_T' + \gamma_1)(\omega' - K v_S' + \gamma_2) - \gamma_0^2 = 0$$

If $\gamma_1 = \gamma_2 = 0$, this would be an absolute instability (positive growth rate for a fixed position in space) with the growth rate

$$\omega = \frac{2\,|v_T'\, v_S'|}{|v_T'| + |v_S'|}\,\gamma_0 .$$

There are, however, two thresholds associated with $\gamma_1 \neq 0$ and $\gamma_2 \neq 0$:

1) $\gamma_0^2 > \gamma_1 \gamma_2$ for there to be an instability at all, and (7.2.4)

2) $\gamma^2 > \dfrac{[\gamma_1 \mid v_g \mid + \gamma_2 \mid v_T \mid]^2}{4 \mid v_S v_T \mid}$ for the instability to be absolute. (7.2.5)

If (7.2.4) is satisfied, but (7.2.5) is not, then the instability is convective, meaning that at a fixed point, x, in space $a(x,t) \to 0$ as $t \to \infty$, but there is a moving pulse that will grow in time.

The growth rate of a convective pulse moving with velocity u parallel to v_S. and v_T' 7.2.3 is given by

$$\omega_0'' = \frac{2[(v_T - u)(v_S + u)]^{1/2}}{v_T + v_S} \gamma_0 - \frac{\gamma_1 (u + v_S) + \gamma_2 (v_T - u)}{v_S + v_T} \tag{7.2.6}$$

For the March 11 case $\gamma_0 = 1.8/\mathrm{s}$, as was determined by *Lin et al.* (1986). Using 7.1.3 and 7.1.4, $\gamma_0^2 > \gamma_S \gamma_T$ so the process is unstable. On the other hand it is the case in this problem that $\gamma_T v_S' \ll \gamma_S v_T'$, and so,

$$\frac{(\gamma^T \mid v_S' \mid + \gamma_S \mid v_T' \mid)^2}{4 \mid v_S' v_T' \mid} \to \gamma_S^2 \frac{v_T'}{4 v_S'} = 4 \times 10^6$$

Therefore the condition (7.2.5) is not satisfied by 6 orders of magnitude. When $\gamma_1 \to 0$, (7.2.6) becomes

$$\omega_0'' = \frac{2[(v_T' - u)(v_S' + u)]^{1/2}}{v_T' + v_S'} \gamma_0 - \frac{\gamma_2 (v_T' - u)}{v_S' + v_T'}$$

It is easy to show that the fastest growing pulse will be when

$$(v_T' - u) \equiv \frac{v_T' \gamma_0^2}{\gamma_S^2}$$

which gives

$$\omega_0'' = \frac{\gamma_0^2}{\gamma_S} .$$

The growth length for the 11 March 79 event will be

$$l_g \equiv \frac{1}{K} = \frac{u}{\omega_0''} \cong \frac{v_T \gamma_S}{\gamma_0^2} \cong 7 \times 10^4 \text{ km} .$$

This presents a distinct problem for growth. An ideal, non-turbulent solar wind plasma would have a density gradient (due to conservation of the solar wind flux)

$$\Delta n_{S\omega} = -\frac{2n_{S\omega}}{R}.$$

where R is the distance from the sun to the point of interest (1 AU). The eikonal equation for the wave vector $\hat{n}$ of a wave propagating in media with inhomogeneities with a scale length much longer than the wavelength of the wave is:

$$\frac{d\hat{n}}{dl} = \frac{1}{v}\nabla v + \frac{\hat{n}(\hat{n}\cdot\nabla v)}{v} \tag{7.2.7}$$

where v is the group velocity of the wave (*Landau and Lifshitz*, vol. 6, para. 66). Since k_L is approximately parallel to the density gradient in the solar wind, v_T will be transverse to it. The dominant term in 7.2.7 is therefore $\frac{1}{v}\nabla v$, and we find that

$$\frac{d\hat{n}}{dl} \cong \frac{\omega_p^2}{c^2k^2}\frac{1}{R} = 1.6\times10^{-6}/\text{km}.$$

In one growth length the wave will be displaced a distance along the density gradient given by

$$\nabla R = \frac{d\hat{n}}{dl}\frac{l_g^2}{2} = 3920 \text{ km}.$$

The resonance condition for growth is such that growth will cease when $v_g\Delta k = \gamma_0$. But

$$v_g\Delta k = v_g\nabla k\ \Delta R = \frac{d\hat{n}}{dl}\frac{c^2k^2}{\omega_p}\Delta R = 2$$

and so the transverse wave will be refracted out of the resonance region within oen growth length. The consequence of this is that because of the low level of the Langmuir pump and the high damping rate of the ion-acoustic daughter wave, the instability is convective instead of absolute, but because of refractive effects the convective instability is suppressed.

By contrast, we apply the same considerations to the *Whelan and Stenzel* (1985) experiment. Using their results we estimate

$$\gamma_0 \cong 3\times10^8/\text{sec}^2,\ \gamma_i^2 \cong 1\times10^{13}/\text{sec}^2$$

$$v_T = 4.5\times10^9 \text{ cm/sec} \quad \text{and}$$

$v_S = 2.6 \times 10^5$ cm/sec

We see that $\gamma_0^2 \gg \gamma_t^2 \frac{v_T}{4v_S}$, and therefore in this case the absolute threshold is greatly exceeded.

If the discussion in this section has so far cast doube that a 3-wave process is involved, the following argument gives strong support for it. If we write down eq. 7.1.1 for each wave in the type III process, assuming no wave damping, we get

$$\frac{dJ_L}{dt} = -2\beta \sqrt{J_L J_S J_T} \sin\Phi$$

$$\frac{dJ_S}{dt} = 2\beta \sqrt{J_L J_S J_T} \sin\Phi$$

$$\frac{dJ_T}{dt} = 2\beta \sqrt{J_L J_S J_T} \sin\Phi$$

Adding the first two gives us

$$\frac{d}{dt}(J_L + J_S) = 0 \tag{7.2.8}$$

This is one of the Manley-Rowe relations (*Sagdeev and Galeev*, 1969). Again ignoring damping and convective effects, we would expect from eq. 7.2.8 that at saturation of the 3-wave decay $J_L \equiv J_S$. Using the standard expression for $\varepsilon_S(k, \omega)$ and $\varepsilon_L(k, \omega)$ gives us

$$\frac{J_S}{J_L} = \frac{1}{k_S^2 \lambda_D^2} \left(\frac{E_S}{E_L}\right)^2 = 1.02$$

when we substitute parameters for the 11 March 1979 event. *Bergman* (1985) did an extensive numerical study of the time evolution 3-wave systems when one of the daughters is damped and found that the damped daughter wave and pump wave will oscillate in amplitude 180° out of phase with each other, between zero and nearly equal maximum amplitude, which, however, decay with the damping rate of the damped daughter wave. Actually, this argument ignores another effect which is that the electron beam will replenish the Langmuir pump wave as the latter is depleted by the 3-wave decay.

Because all other factors seem to support the 3-wave process we next examine how density turbulence modifies the convective process and what effect this modification would have. We begin with a review of the considerable effort that has been made to understand the effect of spatial

plasma inhomogeneities on parametric instabilities, much of which has been directed towards understanding laser-induced plasma instabilities for laser fusion applications.

The usual approach to this problem begins with the following equations for the slowly evolving amplitudes

$$\frac{\partial a_1}{\partial t} + v_1 \left(\frac{\partial a_1}{\partial x}\right) = \gamma_0 a_2^* \quad \exp\left(i \int_0^x K\, dx\right)$$

$$\frac{\partial a_2^*}{\partial t} + v_2 \left(\frac{\partial a_2^*}{\partial x}\right) = \gamma_0 a_1 \quad \exp\left(-i \int_0^x K\, dx\right)$$

where $K = \sum_i \Delta \tilde{k}_i$ (*Rosenbluth*, 1972; *Nishikawa*, 1968). For a linear density profile such that $K(x) \sim K' \cdot (x - x_0)$, *Rosenbluth* concluded that for $v_1 v_2 < 0$, when both waves propagate along the density gradient, the gradient leads to convective growth of the instability. *DuBois et al.* (1974) showed, however, that this effect was due to the unphysical assumption of an infinite length plasma with constant density gradient, and finite lengths lead to temporal growth for normal modes of the system.

Klein et al. (1973) considered the case of the Raman side-scatter instability, the geometry of which is similar to the type III problem. A laser pump propagating along the density gradient decays into a Langmuir wave propagating approximately along the density gradient and another electromagnetic wave propagating transverse to the density gradient. The authors did a 2-D numerical simulation and discovered that this instability is not stabilized by a strong density gradient as is the Raman backscatter instability. This was attributed to the side-scattered wave remaining in the resonance region until refracted out, allowing for a much longer growth length.

Further theoretical progress on the Raman backscatter instability was made by *Drake et al.* (1973), after *Forslund et al.* (1973) discovered through computer simulation that a temporally growing mode (absolute instability) existed in the Raman backscatter problem. *Drake et al.* pointed out that the beating of the pump and the backscattered wave caused a bunching of electrons which would partially reflect the backscattered wave back into the region of the instability. Temporal growth became possible for waves which were quantized by the well formed between the two

turning points.

M. Mostrom (1975) considered this effect for the Raman side-scatter problem using WKB techniques. The conclusion was that the reflection due to the inhomogeneities produced by the beating of the pump and side-scattered wave could balance the effect of refraction, thereby allowing for absolute rather than convective growth.

The first study of the effect of *random* inhomogeneities on parametric instabilities was done by *Tamoikin and Fainshtein* (1972). The effect of random inhomogeneities considered in this study is to cause the phases of the three waves to fluctuate randomly, and to be scattered. The major effect is shown to be an exponential damping of the pump wave, due to scattering by the inhomogeneities. This depletion of the pump damps the parametric decay.

Nicholson and Kaufman (1974) studied the effect of random density fluctuations superimposed on a linear density profile. The suppression of a temporally growing mode, as discussed by *Rosenbluth* (1972) and mentioned above, was due to phase cancellations which, as *Nicholson and Kaufman* showed, is destroyed by random fluctuations. They therefore showed that a temporally growing mode can occur. *Nicholson* (1976) also studied the effect of a sinusoidal density modulation on parametric decays. The effect of this density modulation was discovered to suppress growth rates, but a large density modulation was required to provide substantial suppression.

The effect of random wave phase caused by time varying random density fluctuations was studied by *Laval et al.* (1976) using the Bouret approximation, who concluded that the effect was to suppress growth.

In summary, the major effects that have been considered are the effects of inhomogeneity in the phase relationship between the waves. Only in the studies of Drake and Mostrom has the effect of reflection and partial trapping by inhomogeneities been considered, yet for the cases studied the daughter waves propagate near the critical density where even small inhomogeneities will have major effects.

For long wavelength large amplitude density fluctuations, on the other hand, waves near critical density will be completely trapped. Although such a trapped region will be very irregular in

shape, leading to chaotic ray trajectories, a large body of work has been done which shows that in such cases, waves will in fact be quantized. This was studied by *McDonald* (1983). There is also a large body of work in quantum chemistry studying the quantization of classically chaotic systems (see *Casati*, 1983, and references therein).

The effect of wave-trapping on a parametric instability is two-fold. The first is that since there is no wave convection, the instability will be temporally growing rather than spatially growing. The second is that the trapped wave will be quantized. The discrete spectrum for k and ω will limit the possible waves in the instability and may slow or inhibit the growth due to phase mismatches. The effect of smaller amplitude shorter scale length fluctuations is not so easily treated in this scheme, and for this situation we return to localization effects.

7.3. Localization and Three-Wave Processes

We are nearly at the end of the story. The effect of wave localization on the 3-wave process is to prevent wave convection out of the region of interaction non-dissipatively. Localization of the Langmuir waves is unnecessary for this, but as we saw in section 7.2, prevention of convection of the transverse wave is necessary. In order to make theoretical progress we assume, again, that once localization effects on wave propagation are included, we can use averaged plasma properties to compute coupling constants. We assume therefore that the Langmuir and transverse waves are exponentially localized so that we may use a modified eikonal representation of the waves as follows:

$$\underset{\sim}{E}_T = \tilde{E}_T\, \hat{\varepsilon}\,(k,x)\, e^{-\kappa_T |x - x_T|} \quad e^{i\theta_T} + cc$$

$$E_L = \tilde{E}_L\, e^{-\kappa_L |x - x_L|} \quad e^{i\theta_L} + cc$$

Then,

$$S^{(2)} + S^{(3)} = \int d^{3x}\, dt \left[\varepsilon_L(k_L, x)\, \tilde{E}_L^2\, e^{-2\kappa_L |x - x_L|} + D_T\,(k_T, x)\, \tilde{E}_T^2\, e^{-2\kappa_T |x - x_T|} \right.$$

$$\left. + \varepsilon_S\,(k_S, x)\, \tilde{E}_S^2\,(x,t) \right.$$

$$+ \beta \int d^3x\, dt\, \sin\alpha(x)\, \tilde{E}_L\, \tilde{E}_T^*\, \tilde{E}_S^*\, e^{-\kappa_T |x - x_T|} \quad d^{-\kappa_L |x - x_L|} \quad e^{i(\theta_L - \theta_L - \theta_S)}$$

$$+ cc$$

where

$$\beta = \frac{n_0 e^3}{m\sqrt{kTM}\ \omega_L^2\ \omega_S}$$

as determined in Appendix B. Again

$$\sin\alpha(x) \equiv \frac{k_L \cdot \hat{\varepsilon}_T}{|k_L|}$$

where in this case it may be a function of position. Take variations

$$\frac{\delta}{\delta\theta_L} : 0 = \frac{d}{dt}\frac{\partial\varepsilon}{\partial\omega} E_L^2\, e^{-2\kappa_L|x-x_L|} + i\beta\ \sin\alpha(x)\,\tilde{E}_L\,\tilde{E}_T^*\,\tilde{E}_S^*\, e^{-\kappa_L|x-x_L|}\ e^{-\kappa_L|x-x_L|} \tag{7.3.1a}$$

$$e^{i(\theta_L-\theta_T-\theta_S)} + cc$$

$$\frac{\delta}{\delta\theta_T} : 0 = \frac{d}{dt}\frac{\partial D}{\partial\omega} E_T^2\, e^{-2\kappa_T|x-x_T|} + i\beta\ \sin\alpha(x)\,\tilde{E}_L\,\tilde{E}_T^*\,\tilde{E}_S^*\, e^{-\kappa_L|x-x_l|}\ e^{-\kappa_T|x-x_T|} \tag{7.3.1b}$$

$$e^{i(\theta_L-\theta_T-\theta_S)} + cc$$

$$\frac{\delta}{\delta\theta_S} : 0 = \frac{d}{dt}\frac{\partial\varepsilon}{\partial\omega} E_S^2 - i\beta\ \sin\theta(x)\,\tilde{E}_L\,\tilde{E}_T^*\,\tilde{E}_S^*\, e^{-\kappa_L|x-x_L|}\ e^{-\kappa_T|x-x_T|} \tag{7.3.1c}$$

$$e^{i(\theta_L-\theta_T-\theta_S)} + cc$$

If we define the total wave action

$$J_L \equiv \int d^3x\ |\tilde{E}_L^2|\left(\frac{\partial\varepsilon_L}{\partial\omega}\right) e^{-2\kappa_L|x-x_L|} = \frac{|\tilde{E}_L|^2}{\kappa_L^3}\frac{\partial\varepsilon}{\partial\omega}$$

$$J_T \equiv \int d^3x\ |\tilde{E}_L|^2\frac{\partial D}{\partial\omega}\, e^{-2\kappa_T^3|x-x_T|} = \frac{|\tilde{E}_T|^2}{\kappa_T^3}\frac{\partial D}{\partial\omega}$$

where we have assumed that $\int d^3x\, e^{-2\kappa|x|} = \frac{1}{\kappa^3}$, and therefore that the localization is isotropic.

Then

$$\tilde{E}_L = \sqrt{\frac{\kappa_L^3 J_L}{(\partial\varepsilon/\partial\omega)}}\ e^{-\kappa_L|x-x_L|}$$

and

$$\tilde{E}_T = \sqrt{\frac{\kappa_T^3 J_T}{(\partial D/\partial\omega)}}\ e^{-\kappa_T|x-x_T|}$$

Since the ion-acoustic wave convects and is damped, we must retain the action density

$$J_S(x) = \frac{\partial \varepsilon_S}{\partial \omega} |\tilde{E}_S|^2$$

If we integrate 7.3.1*a-c*

$$\frac{d}{dt} J_L = \left\{ -2\beta \sqrt{\frac{\kappa_L^3 \kappa_{Ti}^3}{(\partial\varepsilon_L/\partial\omega)(\partial\varepsilon_S/\partial\omega)(\partial D_T/\partial\omega)}} \int d^3x \sin\alpha(x) \cos\phi(x)\, e^{-\kappa_L|x-x_L|}\, e^{-\kappa_T|x-x_T|} \right.$$
$$\left. \times \sqrt{J_L J_T J_S(x)} \right\} - \gamma_L J_L$$

$$\frac{d}{dt} J_T = \left\{ 2\beta \sqrt{\frac{\kappa_L^3 \kappa_T^3}{(\partial\varepsilon_L/\partial\omega)(\partial\varepsilon_S/\partial\omega)(\partial D_T/\partial\omega)}} \int d^3x \sin\alpha(x) \cos\phi(x)\, e^{-\kappa_L|x-x_L|}\, e^{-\kappa_T|x-x_T|} \right.$$
$$\left. \times \sqrt{J_L J_T J_S(x)} \right\} - \gamma_T J_T$$

$$\frac{d}{dt} J_S(x) = \left\{ 2\beta \sqrt{\frac{\kappa_L^3 \kappa_T^3}{(\partial E_L/\partial\omega)(\partial E_S/\partial\omega)(\partial D_T/\partial\omega)}} \sin\alpha(x) \cos\phi(x)\, e^{-\kappa_L|x-x_L|}\, e^{-\kappa_T|x-x_T|} \right.$$
$$\left. \times \sqrt{J_L J_T J_S(x)} \right\} - \gamma_S J_S(x)$$

As before, we consider the case where at $t = 0$, E_L is large and E_T, E_S are at fluctuation levels, so that initially we can take E_L a constant. Then we use the definition

$$\gamma_0 = \beta \sqrt{\frac{\kappa_L^3 J_L}{(\partial\varepsilon_L/\partial\omega)(\partial\varepsilon_S/\partial\omega)(\partial D_T/\partial\omega)}}\,.$$

With this definition γ_0 will be of the same form as in section 7.1 where E_L is now the peak value of the electric field. Again we have

$$\left(\frac{d}{dt} + \gamma_T\right) \sqrt{J_T} = \gamma_0 \sqrt{\kappa_T^3} \int d^3x \left\{ \sin\alpha(x) \cos\phi(x)\, e^{-\kappa_L|x-x_L|}\, e^{-K_T|x-x_T|} \sqrt{J_S(x)} \right\}$$

and

$$\left(\frac{d}{dt} + \gamma_S\right) \sqrt{J_S(x)} = \gamma_0 \sqrt{\kappa_T^3} \sin\alpha(x) \cos\phi(x)\, e^{-\kappa_L|x-x_L|}\, e^{-\kappa_T|x-x_T|} \sqrt{J_T}\,.$$

Combining these gives

$$\left(\frac{d}{dt}+\gamma_T\right)\left(\frac{d}{dt}+\gamma_S\right)\sqrt{J_S(x)}=\kappa_T^3\gamma_0^2\sin\alpha(x)\cos\phi(x)\,e^{-\kappa_L|x-x_L|}\,e^{-\kappa_T|x-x_T|}$$
$$\left\{\int d^2x'\,\sin\alpha(x')\cos\phi(x')\,e^{-\kappa_L|x-x_L|}\,e^{-\kappa_T|x-x_T|}\sqrt{J_S(x')}\right\}$$

Although we could attempt to integrate this numerically over assumed forms for the localized waves, we can make some estimates as follows.

Experimentally, it appears that the envelope of the ion-acoustic wave is similar to that of the Langmuir wave. Furthermore we assume

$$\sin\alpha(x)\sim 1 \quad\text{and}\quad \cos\phi(x)\sim 1\,.$$

Therefore, we assume we can write

$$J_S(x)=\kappa_L\tilde{J}_S(t)\,e^{-2\kappa_L|x-x_L|}$$

We make the WKB assumption

$$\sqrt{\tilde{J}_S(t)}=e^{\omega t}\sqrt{\tilde{J}_S}\,.$$

Then

$$(\omega+\gamma_T)(\omega+\gamma_S)=\kappa_L^3\,\kappa_T^3\,\gamma_0^2\left[\int d^2x\,e^{-\kappa_L|x-x_T|}\right]$$
$$\times\left[\int d^3x\,e^{-2\kappa_L|x-x_L|}\,e^{-\kappa_T|x-x_T|}\right]$$

Let us further assume that $\kappa_T \ll \kappa_L$ and that $|x_L-x_T|\ll\frac{1}{\kappa_T}$. Then

$$(\omega+\gamma_T)(\omega+\gamma_S)\cong\left(\frac{2\kappa_T}{\kappa_L}\right)^3\gamma_0^2$$

which gives us the requirement for positive growth that

$$\gamma_0^2>\left[\frac{\kappa_L}{2\kappa_T}\right]^3\gamma_T\gamma_S\,. \tag{7.3.2}$$

For the 11 March event

$$\kappa_L\sim\frac{1}{70\text{ km}}\,;\ \kappa_T\sim\frac{1}{500\text{ km}}\,;\ \frac{\gamma_T}{\omega_{pe}}\sim 2.5\times10^{-11}\,;\ \frac{\gamma_S}{\omega_S}\sim .1$$

The instability requirement (7.3.2) is $\gamma_0^2 > 9 \times 10^{-4}/\text{sec}^2$. The actual value of $\gamma_0^2 \cong (1.8/\text{sec})^2 = 3.24/\text{sec}^2$ and we see that the instability threshold is exceeded by more than 3 orders of magnitude. The effects of phase decorrelations, etc., might be estimated at 1 to 2 orders of magnitude.

The following considerations are of possible significance:

i) Because the Langmuir localization length is much less than a transverse wavelength, wave number matching is not significant. We should merely have $k_S \cong k_L$. On the other hand, frequency matching is significant. It is necessary that the frequency mismatch be less than the growth rate γ_0. The frequency matching will be determined by the frequency levels of localized states.

ii) Other than assuming that $\underset{\sim}{k}_T$ is perpendicular to $\underset{\sim}{k}_L$, we have not really considered the effects of the 3-dimensionality of the problem. Although a one-dimensional model may be adequate for the Langmuir waves, the transverse wave is certainly a 3-dimensional problem, and the localization length predictions from the 1-dimensional theory are certainly shorter than in reality. Furthermore, the electromagnetic wave is a vector wave and consideration of the effects of scattering on the wave polarization is important.

8. Concluding Remarks

We have argued that wave localization effects can be important whenever a wave propagates near the wave cut-off in a plasma with superimposed density turbulence. The effect of localization will be to stop propagation and limit wave spreading to a velocity approximately that of the density fluctuations. Furthermore, the confinement of the wave and possible daughter waves can change the nature and threshold of plasma instabilities.

We have discussed beam-plasma interactions at length because this problem is easily treated by one-dimensional simulations. The localization of Langmuir waves in itself would seem to be a curiosity with little importance other than proving that density fluctuations do not suppress the beam-plasma instability. On the other hand the localization of the transverse waves allows an instability to reach threshold which otherwise would not occur.

We have only simulated those parts of the problem amenable to a one-dimensional treatment. To treat the full problem, including 3-wave decay and non-linear effect in even two dimensions, by computer simulation would be very difficult. Because effects happen on both electron and ion time scales, a two component model of the background fluid would be needed, this leads unfortunately to charge separation and noise for warm fluids. A large number of grid points would be needed since the system needs to be large enough to include several electromagnetic wave wavelengths. When beam particles are included one obtains a memory requirement of $\sim 4 \times 10^6$ words. This would be prohibitively expensive in Cray time.

Although the existence of wave localization in 3-dimensions is well established theoretically for fixed scatterers, the problem of mobile scatterers in 3-dimensions is not settled. This problem is amenable to study using an extension of the methods used in Chapter 5 on, say, a $100 \times 100 \times 100$ lattice. In this case, only waves localized to a small number of lattice points could be studied.

Within the context of the type III problem, the arguments we present are consistent with observations at 1 AU. We make no claim as to their importance or validity in other regions, in the

solar corona, for example, where strong turbulence effects may in fact be important. On the other hand it seems improbable that if the solar wind is turbulent at 1 AU that is is not also turbulent in other and perhaps all regions closer to the sun. In this case, localization will still occur for small amplitude waves. For waves of large amplitude, strong turbulence effects including soliton formation and collapse are probably of more importance, although wave localization may cause a faster onset of these processes.

A final word for those who would argue that wave localization is unnecessary for understanding the behavior of the Langmuir waves. To a certain extent, we would agree. As the scale length, L, of the shortest wavelength density fluctuations increases to the point that $L \gg \lambda_L$, semi-classical or WKB techniques become valid. As *McDonald* (1983) showed, the closed, quantized trajectories are of special significance. Since we are ultimately concerned with wave behavior, however, we argue that one cannot just use ray trajectories and ignore quantization effects. This is the import of the work by *Bezzerides* (1986), discussed in the introduction. Even if, because of particular anisotropies in the turbulence, most trajectories are not trapped, some will be, and when closed and quantized, lead to long-lived quasi-stationary states. Once the Langmuir waves are confined and quantized, whether through localization or semi-classical effects, much of the discussion of Chapter 6 holds. Because of the length scales involved, the properties of the transverse waves can only be understood through the properties of the full wave equation in random media, i.e., localization theory, since dispersive effects are as important as refractive effects. The advantage of using localization theory, on the other hand, is that one can be very ignorant about the turbulence involved and still make very powerful statements about the consequences.

Appendix A. Simulation Techniques and Code Listing

The simulation codes developed for this study are based on standard plasma simulation techniques as discussed in *Birdsall and Langdon* (1985), which is the reference for the numerical techniques discussed below, and some of the code is taken directly from the program ES1 by Bruce Langdon.

For the localization studies we have used two programs, BEAMLOC, and PERLOC. BEAMLOC is used for the beam-plasma interaction, and is listed following this discussion. PERLOC was used for the Gaussian wave packet propagation, and is similar to BEAMLOC except that the unnecessary particle mover and field solver were eliminated, resulting in a very much faster running program.

In the remainder of this section we discuss BEAMLOC; however, the discussion of PERLOC, suitably restricted, would be the same.

Our techniques for simulating the background plasma is to use a linearized one-fluid plasma. Our rationale for this is the following.

In this problem we wish to simulate the effect of a very weak beam with physical density $\frac{n_b}{n_{\text{plasma}}} \sim 10^{-5}$. If we tried to use particles, in order to observe the fields that arrive from the beam plasma interaction, we would certainly expect that the statistical fluctuations in the background density would be significantly less than the beam density.

Let n_p = number of background simulation particles in the box Δx; n_b = number of beam simulation particles. The charge of a simulation particle is

$$e = \frac{\omega_p^2}{4\pi (e/m) n_p}$$

(e/m) is established by the particle type.

If we require that the fluctuations in the background particles produce fields significantly less than those arising from the beam-plasma interaction, then

$\tilde{E}$ = fluctuating electric field

$\tilde{n}$ = fluctuating density

$$\tilde{n} \equiv \sqrt{n_p}$$

$$E_b \sim \frac{en_b}{k} = \frac{\omega_b^2}{e/m}\,\frac{1}{k}$$

$$\nabla \tilde{E} \equiv 4\pi e\tilde{n}$$

$$\frac{\tilde{E}_p}{\Delta x} = \frac{\omega_p^2}{(e/m)} \approx \frac{\omega_p^2}{e/m}\sqrt{n_p}$$

We require

$$\tilde{E}_p \ll E_b$$

We get

$$\frac{\omega_p^2\sqrt{\tilde{n}_p}}{(e/m)\,n_p}\,\Delta x \ll \frac{\omega_b^2}{(e/m)}\,\frac{1}{k}$$

or

$$n_p \ll (k\Delta x)^2\left[\frac{\omega_p^2}{\omega_b^2}\right]^2 \sim 10^{10}$$

It is quite impossible to use particles for the background in this case.

A further problem, which also restricts the ability to use a two-component fluid for the background is that since we have significant density gradients because of our fluctuating background fields, we will get strong electric fields due to charge separation unless we have $\Delta x \ll \lambda_D$. However, for our problems we want to follow several hundred wavelengths and want 100 Debye lengths per wavelength. In order to satisfy all of this, we should then require $\gtrsim 10^6$ grid points.

By using the equation of motion

$$\frac{\partial^2\psi}{\partial t^2} = -\omega_p^2(x)\psi + 3v_t^2\,\frac{\partial^2\psi}{\partial x^2}$$

for the turbulent background plasma we gain in simulation quietness and isolation of the effect we are interested in (the effect of density fluctuation on wave propagation). On the other hand, we

completely eliminate any effects which are non-linear in the background plasma. This could be significant since the density fluctuations are large.

SPERLOC uses the following equations. We assume a grid with $n_g + 1$ grid points, equally spaced over a length L giving $\Delta x = \frac{L}{n_g}$. Quantities defined on the grid are advanced by time steps Δt.

The equations of motion we solve are:

Particles:

$$\frac{d^2 x_i}{dt^2} = \frac{e}{m} E(x_i)$$

$$n_{\text{beam}}(x_1 t) \equiv \sum_i \delta(x - x_i(t))$$

Fluid:

Define $\psi(x,t) = -3\,[n_e(x,t) - n_i(x,t)]$

$$\frac{\partial^2 \psi}{\partial t^2} = -\omega_p^2(x)\,\psi + 3 v_t^2 \frac{\partial^2 \psi}{\partial x^2}$$

where $\omega_p^2(x) \equiv \dfrac{4\pi n_i(x) e^2}{m_e}$

Field:

$\nabla \cdot E = 4\pi\rho$ where $\rho = -e n_{\text{beam}} + \psi$

Initial conditions:

$$\psi(x,0) = 0$$

$$\frac{\partial \psi}{\partial t}(x,0) = 0$$

$\omega_p^2(x) = \left[1 \pm \dfrac{\delta n(x)}{n_0} \right]$ where $\delta n(x)$ is a randomly distributed variable

$x_i(t=0)$ is uniformly distributed in space

$v_i(t=0) =$ drifting maxwellian distribution

We use a time centered leap-frog scheme to solve these equations. We define the quantities:

$v_j^{n+1/2} \equiv \frac{\Delta t}{\Delta x} v_j\,(t = (n + 1/2)\Delta t)$ the velocity for the jth particle

$\dot{\psi}_j^{n+1/2} \equiv \frac{\partial \psi}{\partial t}\,(x = j\Delta x;\, t = (n + 1/2)\Delta t)$

$x_i^n \equiv x_i(t = n\Delta t)$ the position of the jth particle

$\psi_j^n \equiv \psi(x = j\Delta x;\, t = n\Delta t)$

$\omega_{pi}^2 = \omega_p^2(x = i\Delta x)$

We first solve for the electric fields in Fourier space from the following.

$$\rho_i^n = \psi_i^n + \rho_{i\,\mathrm{beam}}^n$$

$$\Delta \cdot E_i^n = 4\pi\rho_i^n$$

and then advance quantities in time:

$$v_j^{n+1/2} = \frac{-e_j \Delta t}{m_j} E_{i=x_j}^n + v_j^{n-1/2}$$

$$\dot{\psi}_i^{n+1/2} = \Delta t \left[-\omega_{pi}^2 \left[x_i \psi_i^2 + \rho_{\mathrm{beam}\,i}^n \right] \right] + 3v_t^2 \frac{\Delta t^2}{\Delta x^2} \left[\psi_{i+1}^n + \psi_{i-1}^n - 2\psi_i^2 \right] + \dot{\psi}_i^{n-1/2}$$

$$\psi_i^{n+1} = \psi_i^2 + \Delta t\, \dot{\psi}_i^{n+1/2}$$

$$x_i^{n+1} = x_i^n + v_i^{n+1/2} \Delta t$$

We then find ρ_i^{n+1}, then E_i^{n+1} and so on. The advantages of a time centered leap-frog scheme to solve differential equations which are 2nd order in time is that the solutions are of accuracy $0\,(\Delta t^2)$.

Plots:

In addition to plotting the quantities ψ_i^n and $\dot{\psi}_i^{n-1/2}$ we are also interested in the "energy density," which we define as

$$E_i^n = \frac{1}{2}\,\omega_{pi}^2\,\psi_i^{n^2} + \frac{1}{2}\,\dot{\psi}_i^{n+1/2^2} + \frac{3}{2} v_t^2 \frac{[\psi_{i+1} - \psi_{i-1}]^2}{4\Delta x^2}$$

This is the Hamiltonian density which will generate the equations of motion for ψ and $\dot{\psi}$. Plotting this has the advantage that the quantity is phase independent, unlike ψ and $\dot{\psi}$.

Model for background density fluctuations

In most cases the model we use for density fluctuations is that of *Escande and Souillard*, which is that $\omega_p^2(x)$ is a step function, constant on a specified number of gridpoints, n_c, which is 4, 8, or 16 in most of the simulations presented. The value at each step is generated by a random number generator and is uniform on the interval.

$$[1-\delta\,\omega_{p_{max}}^2\,,\quad 1+\delta\,\omega_{p_{max}}^2\,].$$

We show the power spectrum of density fluctuations in this model in Figure B.2. In this figure $l=314$, $n_g=512$. According to this,

$$\delta n_k=\int_0^L dx\, e^{ikx}\,\delta n(x)=\sum_{j=0}^{n_c} e^{i(kl_c j)}\,\delta n_j \int_{l_c/2}^{l_c/2} e^{ikx}\,dx\, e^{ikl_c/2}$$

This gives

$$|\,\delta n_k\,|^2=\left[\sum_{jj'=0}^{n_c} e^{ikl_c(j-j'0}\,\delta n_j\,\delta n_{j'}\right] 4l_c^2\left[\frac{\sin^2 kl_c/2}{(kl_c/2)^2}\right]$$

For moderate k, the sum vanishes unless $j=j'$ and so

$$|\,\delta n_k\,|^2\rightarrow\sum_j l_c^2\,\delta n_j^2\left[\frac{\sin^2 kl_c/2}{(kl_c/2)^2}\right]$$

As $k\rightarrow 0$ however,

$$|\,\delta n_k\,|^2\rightarrow\left[\sum_j \delta n_j\right]\left[\sum_{j'}\delta n_{j'}\right]\cong 0$$

The peak occurs for $kl_c=.55\left[\frac{4}{512}\times 100\pi\right]=1.227$ and decreases approximately as k^{-2} up to $kl_c=2\pi$. The detailed structure, however, is of course a specific manifestation of the statistics of the ensemble, since the sample is finite, and it is this that gives rise to the localization.

Notes on units:

We use the following convention for units in this program. We choose units of time so that the background plasma frequency $\omega_{p_{bg}}=1$. We choose units of mass so that $e/m=1$. Once we specify the number of simulation particles n_{beam} in a box of length Δx, we have set the charge of a

beam particle

$$e_b = \frac{\omega_{p\,\mathrm{beam}}^2}{4\pi(e/m)\,n_{\mathrm{beam}}} .$$

Typically we take

$$\frac{\omega_{p\,\mathrm{beam}}^2}{\omega_{p_{bg}}^2} = \frac{n_{\mathrm{beam}}}{n_{bg}} = 9 \times 10^{-6}$$

As it is, we find that 4,096 grid points is the largest number necessary, and 8,192 particles gives us two simulation particles per grid point.

A typical length of the system is $L \sim 314$, and $v_t \sim .05$. With $\omega_p = 1$, $\lambda_D = \frac{v_t}{\omega_p} = .05$. With $n_g = 4{,}096$ the number of gridpoints, we have $\Delta x/\lambda_D = 1.5$. As none of the physics of our simulation relies on being able to resolve a Debye length this is sufficient. Also a typical beam velocity will be $v_b = 1.0$. Then

$$k_0 = \frac{\omega_p}{v_b} = 1.0 \qquad \lambda \sim \frac{2\pi}{k_0} = 6.28 \qquad \frac{\lambda}{\Delta x} = 82,$$

therefore a typical wavelength is very well resolved.

The typical CRAY run time for BEAMLOC with $n_g = 4{,}096$, $n_{\mathrm{beam}} = 8{,}192$, $n_t = 4{,}000$ was 10 minutes. The typical run time for PERLOC with $n_g = 4{,}096$, $n_t = 80{,}000$ was 4 minutes.

Appendix B. Computation of the 3-Wave Coupling Constant

In this appendix we calculate the 3-wave coupling constant between a Langmuir wave, an ion-acoustic wave and a transverse electromagnetic wave, used in Chapter 7. We begin with eq. 7.1.1,

$$K^{(3)} = \frac{1}{3} L^2 H^{(1)} + LH^{(2)} \tag{B.1}$$

In this particular case we note that $LH^{(2)}$ will contain no term of the form $e^{i(\theta_L - \theta_T - \theta_S)}$ since $H^{(2)} \sim |\underset{\sim}{A}|^2$ and the only wave with non-vanishing $\underset{\sim}{A}$ in our choice of gauge is the transverse wave.

Let us write

$$H_\alpha^{(1)} = \sum_i \frac{e_i}{m_i c} P_i \cdot \tilde{A}_i^\alpha(x,t)\, e^{i\theta_\alpha(x,t)}$$

where α is a wave index and $H_{\bar{\alpha}}^{(1)} \equiv [H^{(1)}]^*$ (complex conjugate), and where we have defined the "non-relativistic" 4-vectors

$A = (0, \underset{\sim}{A}_T)$ for the transverse wave

$A = (\phi_\alpha, 0)$ for the ion-acoustic or Langmuir waves

and $p_i = (m_i c, m_i \underset{\sim}{v}_i)$.

Then $w_\alpha = \int dt\, H_\alpha^{(1)} = \dfrac{H_\alpha}{i\dot{\theta}_\alpha}$

where $\dot{\theta}_\alpha = k_\alpha v_i - \omega_\alpha$. Eq. B.1 becomes

$$K^{(3)} = \frac{1}{3} \sum_\alpha \{ w, \{ w, H_\alpha^{(1)} \} \}$$

If we use the Vlasov approximation

$$f(x,p) = \sum_i \delta(x - x_i)\, \delta(p - p_i)$$

then

$$\sum_i \int_{x_0}^{t_1} dt\, \frac{1}{3} \{ w_i, \{ w_i, H_\alpha^{(1)} \} \} = \sum_i \int_{t_0}^{t_1} dt \int d^3x\, d^3p \sum_i \delta(x - x_i)\, \delta(p - p_i) \{ w, \{ w, H_\alpha^{(1)} \} \}$$

$$= -\int d^3x\, dt\, d^3p\, n_0\, g(p)\, \frac{1}{3} \{ w, \{ w, k_i^{(1)} \} \}$$

Integration by parts gives

$$K^{(3)} = \frac{1}{3} \sum_{\alpha} \int d^3x\, d^3p\, n_0 \{w, g(p)\} \{w, H_\alpha^{(1)}\}$$

$$= \frac{1}{3} \sum_{\alpha} \int d^3x\, d^3p\, n_0 \left(\frac{\partial w}{\partial \underline{x}} \cdot \frac{\partial g}{\partial \underline{p}} \right) \{w, H_\alpha^{(1)}\} .$$

If $g(p)$ is a Maxwellian distribution, then

$$\frac{\partial g}{\partial p} = \frac{p}{mkT} g(P)$$

and we find

$$S^{(3)} = \frac{1}{3} \sum_{\alpha} \int d^3x\, dt\, d^3p\, g(p) \frac{n_0}{mkT} p \cdot \frac{\partial w}{\partial x} \{w, H_\alpha^{(1)}\}$$

We take

$$w = \sum_{\alpha} \frac{H_\alpha}{i\dot{\theta}_\alpha}$$

which gives

$$p \cdot \frac{\partial w}{\partial x} = \sum_{\alpha} \frac{H_\alpha}{\dot{\theta}_\alpha} (k_\alpha \cdot p)$$

$$\{w, H^1\} = \sum_{\alpha\beta} \left\{ \frac{H_\alpha}{i\dot{\theta}_\alpha}, H_\beta \right\} = \sum_{\alpha\beta} \left[\frac{1}{i\dot{\theta}_\alpha} \{H_\alpha, H_\beta\} + H_\alpha \{ \frac{1}{i\dot{\theta}_\alpha}, H_\beta \} \right]$$

Combining the above gives

$$K^{(3)} = \frac{1}{3} \int d^3x\, d^3p\, \frac{n_0 g(p)}{mkT} \left[\sum_{\alpha} \frac{H_\alpha}{\dot{\theta}_\alpha} (k_\alpha \cdot p) \right] \left[\sum_{\beta\gamma} \left[\frac{1}{i\dot{\theta}_\beta} \{H_\beta, H_\gamma\} + H_\beta \{ \frac{1}{i\dot{\theta}_\beta}, H_\gamma \} \right] \right]$$

Now, we note that for $v_b \gg v_{T_e}$,

$$\omega_L - k_L \cdot v \cong \omega_L \left(1 - \frac{v}{v_b} \right) \cong \omega_L$$

$$\omega_T - k_T \cdot v \cong \omega_L \text{ since } k_T \ll k_L$$

and we assume that we may use $\omega_S - k_S v \sim -k_S \cdot v$ when integrated over the thermal distribution.

We write $K_{\{L\bar{S}\bar{T}\}}$ to represent the sum over all permutations of $\alpha\beta\gamma$ where one of the waves is a Langmuir wave, one ion-acoustic, and one transverse.

$$K^{(3)}_{\{LS\bar{T}\}} = \frac{1}{3}\int d^3x\, d^3p\, \frac{n_0\, g(p)}{mkT} \left(\frac{e^3}{mc}\right) \left(\tilde{\phi}_L\, \tilde{\phi}_S^*\, \tilde{A}_T^*\right) e^{i(\theta_L - \theta_S - \theta_T)}$$

$$\left\{ \underbrace{\frac{k_S \cdot p}{\dot{\theta}_S} \left(\frac{k_L \cdot \hat{\varepsilon}_T}{\dot{\theta}_L} + \frac{p \cdot \hat{\varepsilon}_T\, (k_L \cdot k_T)}{n\dot{\theta}_L^2} \right)} + \frac{(k_T \cdot p)(k_L \cdot k_S)}{\dot{\theta}_T} \left[\frac{1}{\dot{\theta}_S^2} + \frac{1}{\dot{\theta}_L^2} \right] \right.$$

$$+ \underbrace{\frac{k_L \cdot p}{\dot{\theta}_L} \left(\frac{k_S \cdot \hat{\varepsilon}_T}{\dot{\theta}_S} + \frac{(p \cdot \dot{\varepsilon}_T)\, k_S \cdot k_T}{m\dot{\theta}_S^2} \right)} + \frac{k_L \cdot p}{\dot{\theta}_L} \left[\frac{k_S \cdot \hat{\varepsilon}_T}{\dot{\theta}_T} + \frac{k_T \cdot k_S}{m\dot{\theta}_T^2} \right]$$

$$\left. + \underbrace{\frac{k_S \cdot p}{\dot{\theta}_S} \left[\frac{k_L \cdot \hat{\varepsilon}_T}{\dot{\theta}_T} + \frac{p \cdot \hat{\varepsilon}_T}{m} \frac{(k_L \cdot k_T)}{\dot{\theta}_T^2} \right]} \right\}$$

Since $\underset{\sim}{k}_L \cong \underset{\sim}{k}_S$ and $\dot{\theta}_L \cong \dot{\theta}_T \gg \dot{\theta}_S$, the underlined terms are approximately equal and are dominant, cancelling the $\frac{1}{3}$. If we define

$$\sin\alpha = \frac{k_S \cdot \hat{\varepsilon}_T}{|k_S|}$$

then

$$S^{(3)} = \int dt\, d^3x\, d^3p \sin\alpha\, \frac{n_0\, g(p)}{kT} \frac{e^3}{mc}\, \hat{\phi}_L \tilde{\phi}_S^*\, \tilde{A}_T^*\, e^{i(\theta_L - \theta_S - \theta_T)} + \text{c.c.}$$

$$= \int dt\, d^3x\, \frac{n_0}{kT} \left(\frac{e^3}{mc}\right) \frac{k_S}{\omega_L} \sin\alpha\, \tilde{\phi}_L\, \tilde{\phi}_S^*\, \tilde{A}_T^*\, e^{i(\theta_L - \theta_S - \theta_T)} + \text{c.c.}$$

We evaluate the quantity β defined as

$$\beta \equiv \frac{n_0}{kT} \left(\frac{e^3}{mc}\right) \frac{k_S}{\omega_L} \sin\alpha$$

as follows:

Noting that

$$\tilde{E}_T = i\, \frac{\omega_T}{c}\, \tilde{A}_T \cong i\, \frac{\omega_L}{c}\, \tilde{A}_T$$

$$\tilde{E}_S = ik_S\, \tilde{\phi}_S$$

$$\tilde{E}_L = ik_L\, \tilde{\phi}_L$$

and using the definitions

$$J_L = \frac{|E_L^2|}{4\pi} \frac{\partial\varepsilon}{\partial\omega} = |E_L|^2 \frac{2}{\omega_L}$$

$$J_S = \frac{|E_S|^2}{4\pi} \frac{\partial \varepsilon}{\partial \omega} = |E_S|^2 \frac{2\omega_i^2}{\omega_S^3}$$

where we have used the standard expression for the dielectric response functions ε_L and ε_S. Then we find

$$\beta \phi_L \tilde{\phi}_S^* \tilde{A}_T^* = \sqrt{J_S J_T} \sqrt{\frac{\omega_L \omega_S E_L^2}{16\pi\, n_0\, kT}} \sin\alpha$$

The factor

$$\gamma_0 \equiv \sqrt{\frac{\omega_L \omega_S E_L^2}{16\pi\, n_0 kT}}$$

is the same as that derived by *Shukla and Yu* (1983) using fluid equations. We can also write β in the form

$$\beta \phi_L \tilde{\phi}_S^* \tilde{A}_T^* = \frac{i n_0 e^3}{m \sqrt{kTM}\, \omega_L^2\, \omega_S} E_L \tilde{E}_S^* \tilde{E}_T^*$$

References

Abrahams, E., P. W. Anderson, D. C. Licciardello, and T. V. Ramakrishnan, Scaling theory of localization: Absence of quantum diffusion in two dimension, *Phys. Rev. Lett.*, *42*, 10. 1979.

Anderson, P. W., Absence of diffusion in certain random lattices, *Phys. Rev.*, *109*, 5, 1958.

Anderson, P. W., Local moments and localized states, *Reviews of Modern Physics*, *50*, 2, 1978.

Anderson, P. W., A question of classical localization: A theory of white paint? *Phil. Mag. B.*, *52*, 505, 1985.

Bergman, R., Linear generation and non-linear decay of electrostatic hydrogen cyclotron waves on auroral field lines, Ph.D. thesis, U.C. Berkeley, 1985.

Bers, A., "Space-time evolution of plasma instabilities—absolute and convective," in *Handbook of Plasma Physics*, M. N. Rosenbluth and R. Z. Sagdeev, eds., North Holland, 1983.

Birdsall, C. K., and A. B. Langdon, *Plasma Physics via Computer Simulation*, McGraw-Hill, New York, 1985.

Cairns, I. H., Arguments for "Fundamental emission by the parametric process $L \rightarrow T + S$ in interplanetary type III bursts," in *Proceedings of the Varenna Workshop on Plasma Astrophysics*, Varenna, Italy, ESA SP-207, p. 141.

Cary, J., Lie transforms and their use in Hamiltonian perturbation theory, *DOE/ET-0074*, 1978.

Casati, G., ed., *Chaotic Behavior in Quantum Systems*, Plenum Press, New York, 1983.

Celnikier, L. M., C. C. Harvey, R. Teagou, M. Kemp, and P. Moricet, A determination of the electron density fluctuation spectrum in the solar wind, *Astron. Astrophys.*, *126*, 293, 1983.

Coles, W. A., and J. K. Harmon, Interplanetary scintillation measurements of the electron density power spectrum in the solar wind, *J. Geophys. Res.*, *83*, 1413, 1978.

Crawford, J. D., S. Johnston, A. N. Kaufman, and C. Oberman, Theory of beat-resonant coupling of electrostatis modes, *Phys. Fluids*, *29*, 3219, 1986.

C-2

Davidson, R. C., *Methods in Non-Linear Plasma Theory*, Academic Press, New York, 1972.

Dawson, J. M., Radiation from plasmas, *Advances in Plasma Physics, 1*, 1, 1968.

Dewar, R. L., Interaction between hydrodynamic waves and a time dependent, inhomogeneous medium, *Phys. Fluids, 13*, 2710, 1970.

Dewar, R. L., A Lagrangian theory for non-linear wave packets in a collisionless plasma, *J. Plasma Physics, 7*, 267, 1972.

Dewar, R. O., Oscillation center quasi-linear theory, *Phys. Fluids, 16*, 1103, 1973.

Deylon, F., H. Kunz, and B. Souillard, One dimension wave equations in disordered media, *J. Phys. A., 16*, 25, 1983.

Drake, J. F., and Y. C. Lee, Temporally growing backscatter instabilities in an inhomogeneous plasma, *Phys. Rev. Lett., 31*, 1197, 1973.**

DuBois, D. F., D. W. Forslund, and E. A. Williams, Parametric instabilities in finite inhomogeneous media, *Phys. Rev. Lett., 33*, 1013, 1974.

Edwards, J. T., and D. J. Thouless, Numerical studies of localization in disordered systems, *J. Phys. C., V.*, 807, 1972.

Elliott, R. J., J. A. Krumhansl, and P. L. Leeth, The theory and properties of randomly disordered crystals and related physical systems, *Reviews of Modern Physics, 46*, 3, 1974.

Escande, D. G., and B. Souillard, Localization of waves in a fluctuating plasma, *Phys. Rev. Lett., 5*, 1296, 1984.

Fainberg, J., and R. G. and Stone, *Space Sci. Rev., 16*, 145, 1974.

Fried, B. C., "Statistical Mechanical Foundations," in *Plasma Physics in Theory and Applications*, W. Kunkel, ed., McGraw-Hill, New York, 1966.

Furstenburg, H., Non-commuting random products, *Journal of the American Mathematical Society, Sept.*, 377, 1963.

Goldman, M. V., Progress and problems in the theory of type III solar radio emission, *Solar Phys.*,

89, 403, 1983.

Golubsntsev, A. A., Suppression of interference effects in multiple scattering of light, *Sov. Phys. JETP*, *59*, 26, 1984.

Gorikov, L. P., A. I. Larkin, D. E. Khmelnitskii, Particle conductivity in two-dimensional random potential, *JETP Lett.*, *30*, 229, 1979.

Jackson, J. D., *Classical Electrodynamics*, John Wiley and Sons, 1975, p. 313ff.

John, S., Localization and absorption of waves in a weakly dissipative disrodered medium, *Phys. Rev. B*, *31*, 304, 1985.

Johnston, S., A. N. Kaufman, and G. L. Johnston, Beat hamiltonians and generalized ponderomotive forces in hot magnetized plasmas, *J. Plasma Phys.*, *20*, 365, 1978*a*.

Johnston, S., and A. N. Kaufman, Lie-operator approach to mode coupling in non-uniform plasma, *Phys. Rev. Lett.*, *40*, 1266, 1978*b*.

Johnston, S., and A. N. Kaufman, Oscillation centres and mode coupling in non-uniform Vlasov plasma, *J. Plasma Phys.*, *22*, 105, 1979.

Kaufman, A. N., Natural Poisson structures of non-linear plasma dynamics, *Physica Scripta*, *T2/2*, 517, 1982.

Kaufman, A. N., The phase-space-Lagrangian action principle and the generalized K-χ theorem, submitted to *Phys. Rev. Lett.*, 1987.

Kaufman, A. N., and D. D. Holm, The Lie transformed Vlasov action principle: relativistically covariant wave propagation and self-consistent ponderomotive effects, *Phys. Lett.*, *105A*, 277, 1984.

Kaufman, A. N., and L. Stenflo, Action conservation in the presence of a high-frequency field, *Plasma Physics*, *17*, 403, 1975.

Kaufman, A. N., S. W. McDonald, and Eliezer Rosengaus, Transition of a coherent classical wave to phase incoherence, in *Chaotic Behavior in Quantum Systems*, G. Casati, ed., Plenum Press, New York, 1983.

Khor, K. E., and P. U. Smith, Localization of electron states in two-dimension disordered potential arrays, *J. Phys. C.*, *4*, 2029, 1971.

Klein, H. H., W. M. Manheimer, and E. Ott, Effect of side-scatter instabilities on the propagation of an intense laser beam in an inhomogeneous plasma, *Phys. Rev. Lett.*, *31*, 1187, 1973.

Kramer, B., A. Bergman, and Y. Bruynseraede, Localization, interaction, and transfer phenomena in input metals, in *Localization, Interaction and Transport Phenomena*, Vol. 61, Springer Verlag, New York, 1985.

Kunz, H., and B. Souillard, Sur le spectre des opèrateurs aux différences finies aléatoires, *Commun, Math. Phys.*, *788*, 201, 1980.

Landau, L. D., and E. M. Lifschitz, *Fluid Mechanics*, Pergamon Press, New York, 1959.

Langer, J. S., and T. Neal, Breakdown of the concentration expansion for the impurity resistance of metals, *Phys. Rev. Lett.*, *16*, 22, 1966.

Laval, G., R. Pellat, D. Pesne, A. Ramani, M. N. Rosenbluth, and E. A. Williams, Parametric instabilities in the presence of space-time random fluctuations, *Phys. Fluids*, *20*, 2049, 1977.

Lax, M., Hopping conductivity in random systems, in *Multiple Scattering and Waves in Random Media*, P. L. Chos, W. E. Kohler, G. G. Papanicolaou, eds., North Holland, New York, 1981.

Lichtenberg, A. J., and M. A. Lieberman, *Regular and Stochastic Motion*, Springer-Verlag, New York, 1983.

Lifschitz, E. M., and L. P. Pitaevskii, *Physical Kinetics*, Pergamon Press, New York, 1981.

Lin, R. P., D. W. Potter, D. A. Gurnett, and F. L. Scarf, Energetic electrons and plasma waves associated with a solar type III radio burst, *Ap. J.*, *251*, 364, 1981.

Lin, R. P., W. K. Levedahl, W. Lotko, D. Gurnett, F. L. Scarf, Evidence for non-linear wave-wave interactions in solar type III radio bursts, *Ap. J.*, *308*, 954, 1986.

Magelssen, G. R., and D. F. Smith, Non-relativistic electron stream propagation in the solar atmosphere and type III radio bursts, *Solar Phys.*, *55*, 211, 1977.

McDonald, S. W., Wave Dynamics of regular and chaotic rays, Ph.D. thesis, University of California, Berkeley, 1983. (Also *Phys. Rev. A*, to be submitted).

McDonald, S., and A. Kaufman, *Phys. Rev., A32*, 1708, 1985.

McKinnon, A., The scaling theory of localization, in *Localization, Interaction, and Transport Phenomena*, B. Kramer, A. Bergmann, and Y. Bruynseraede, eds., Springer-Verlag, New York, 1985.

Melrose, D. B., The emission mechanisms for solar radio bursts, *Space Sci. Rev., 26*, 3, 1980.

Melrose, D. B., G. A. Dulk, and I. H. Cairns, Clumpy Langmuir waves in type II solar radio bursts, *Astron. Astrophys., 163*, 229, 1986.

Meiss, J. D., Integrability of multiple three-wave interactions, *Phys. Rev. A., 19*, 4, 1979.

Mikhailovsky, A. B., "Drift wave instabilities," in *Handbook of Plasma Physics*, M. N. Rosenbluth, and R. Z. Sagdeev, eds., North Holland, 1983.

Mostrom, M., Ph.D. thesis, U.C. Berkeley, 1975.

Mott, N. R., and W. D. Twose, On the theory of impurity conduction, *Adv. Phys., 10*, 107, 1961.

Muschietti, L., M. V. Goldman, and D. Newman, Quenching of the beam-plasma instability by 3-D spectra of large scale density fluctuations, *Solar Phys., 96*, 181, 1985.

Nicholson, D. R., Parametric instabilities in plasma with sinusoidal density modulation, *Phys. Fluids, 19*, 887, 1976.

Nicholson, D. R., *Introduction to Plasma Theory*, John Wiley & Sons, New York, 1983.

Nicholson, D. R., and A. Kaufman, Parametric instabilities in turbulent, inhomogeneous plasma, *Phys. Rev. Lett., 33*, 1207, 1974.

O'Neil, T. M., and J. H. Malmberg, Transition of the dispersion roots from beam-type to Landau-type solutions, *Physics of Fluids, 11*, 1754, 1968.

Parker, E. N., Dynamics of the interplanetary gas and magnetic fields, *Astrophys. J., 128*, 664, 1958.

Pritchett, P. L., and J. M. Dawson, Electromagnetic radiation from beam-plasma instabilities, *Phys. Fluids, 26,* 1115, 1983.

Rickayzen, A., *Green's Functions and Condensed Matter,* Academic Press, New York, 1980.

Rose, H. A., D. F. DuBois, and B. Bezzerides, Nonlinear coupling of stimulated Raman and Brillouin scattering in laser-plasma interactions, *Phys. Rev. Lett., 58,* 2547, 1987.

Rosenbluth, M. N., Parametric instabilities in inhomogeneous media, *Phys. Rev. Lett., 29,* 565, 1972.

Sagdeev, R. A., and A. A. Galeev, *Nonlinear Plasma Theory,* W. A. Benjamin, Inc., New York, 1969.

Schmidt, G., *Physics of High Temperature Plasmas,* Academic Press, New York, 1979.

Shukla, P. K., M. Y. Yu, M. Mohan, R. K. Varma, and K. H. Spatshek, Electromagnetic wave generation in beam plasma systems, *Phys. Rev. A., 27,* 552, 1983.

Similon, P. L., A. N. Kaufman and D. D. Holm, Oscillation outer theory and ponderomotive stabilization of low-frequency plasma modes, *Phys. Fluids, 29,* 1908, 1986.

Smith, D. F., and D. Sime, Origin of plasma-wave clumping in type III solar radio burst sources,

Stephen, M. J., "Lectures on disordered systems," in *Critical Phenomena,* F. J. W. Hahne, ed., Springer-Verlag, New York, 1983.

Tamoikin, V. V., and S. M. Fainshtein, Nonlinear interaction between waves in a plasma with random inhomogeneities, *Soviet JETP, 35,* 1, 1972.

Tawel, R., and K. F. Canter, Observation of a positron mobility threshold in gaseous helium, *Phys. Rev. Lett., 45,* 2322, 1986.

Thouless, D. J., Electrons in disordered systems and the theory of localization, *Physics Reports, 13,* 3, 1974.

Thouless, D. J., "Percolation and localization," in *Les Houches Session XXX,* 1978, Ill-Condensed Matter, R. Balian et al., eds., North Holland, New York, 1979.

Tsytovich, V. N., Theory of plasma turbulence, Consultants Bureau, New York, 1977.

Van Albada, M. P., and A. Lagendijk, Observation of weak localization of light in a random medium, *Phys. Rev. Lett.*, *55*, 24, 1985.

Vollhardt, D., and P. Wölfle, Anderson localization in $d \leq 2$ dimensions: A self-consistent diagramatic theory, *Phys. Rev. Lett.*, *45*, 842, 1980.

Vollhardt, D., and P. Wölfle, Scaling equations from a self-consistent theory of Anderson localization, *Phys. Rev. Lett.*, *48*, 699, 1982.

Watson, G. M., Multiple scattering by quantum mechanical system, *Phys. Review*, *105*, 4, 1957.

Watson, G. H., P. A. Fleury, and S. L. McCall, Search for photon localization in the time domain, *Phys. Rev. Lett.*, *58*, 945, 1987.

Wegner, F. J., Anderson transition and nonlinear σ-model, *Z. Phys. B.*, *25*, 327, 1976.

Whelan, D. A., and R. L. Stenzel, Electromagnetic radiation and nonlinear energy flow in an electron beam-plasma system, *Phys. Fluids*, *28*, 3, 1985.

Yoshino, S., and M. Okazaki, Numerical study of electron localization in Anderson model for disordered systems: Spatial extension of wave-function, *Journal of the Physical Society of Japan*, *43*, 2, 1977.

Ziman, J. M., *Models of Disorder*, Cambridge University Press, Cambridge, 1979.

Plasma, Beam, and Wave Parameters for 11 March 1979. (from Lin et. al., 1986)

Solar wind plasma	
Solar wind density, n	2 cm^{-3}
Solar wind velocity, V_{sw}	480 km/s
Angle of magnetic field to solar wind, θ_B	139°
Electron temperature, T_e	2×10^5 °K
Ion temperature, T_i	4×10^4 °K
Debye length, λ_D	2.2×10^3 cm
Electron plasma frequency, f_{p-}	13 kHz
Ion plasma frequency, f_{p+}	3×10^2 Hz
Fast electrons	
Beam velocity, v_b	$\sim3.5\times10^9$ cm/s
Beam density, n_b	$\sim7\times10^{-5}$ cm^{-3}
Positive slope, $\partial f/\partial v_{\parallel}$	$\sim10^{-25}$ cm^{-3} s^2
Beam width, $\Delta v_b/v_b$	~0.1–0.2
Langmuir pump waves	
Beam resonant wave number, k_0	2.3×10^{-5} cm^{-1}
Maximum wave amplitude, $E_{0_{max}}$	~1 mV/m
Maximum normalized energy density, $W_{max} = E_0^2/8\pi n\kappa T_e$	8×10^{-7}
Long wavelength ion acoustic waves	
Wave number, k_I (typical)	1.8×10^{-5} cm^{-1}
Ion acoustic speed, c_s	5.2×10^6 cm/s
Ion acoustic frequency, f_I	15 Hz
Maximum electric field, $E_{I_{max}}$	~40 μV/m

Table 2.1

11 March 1979

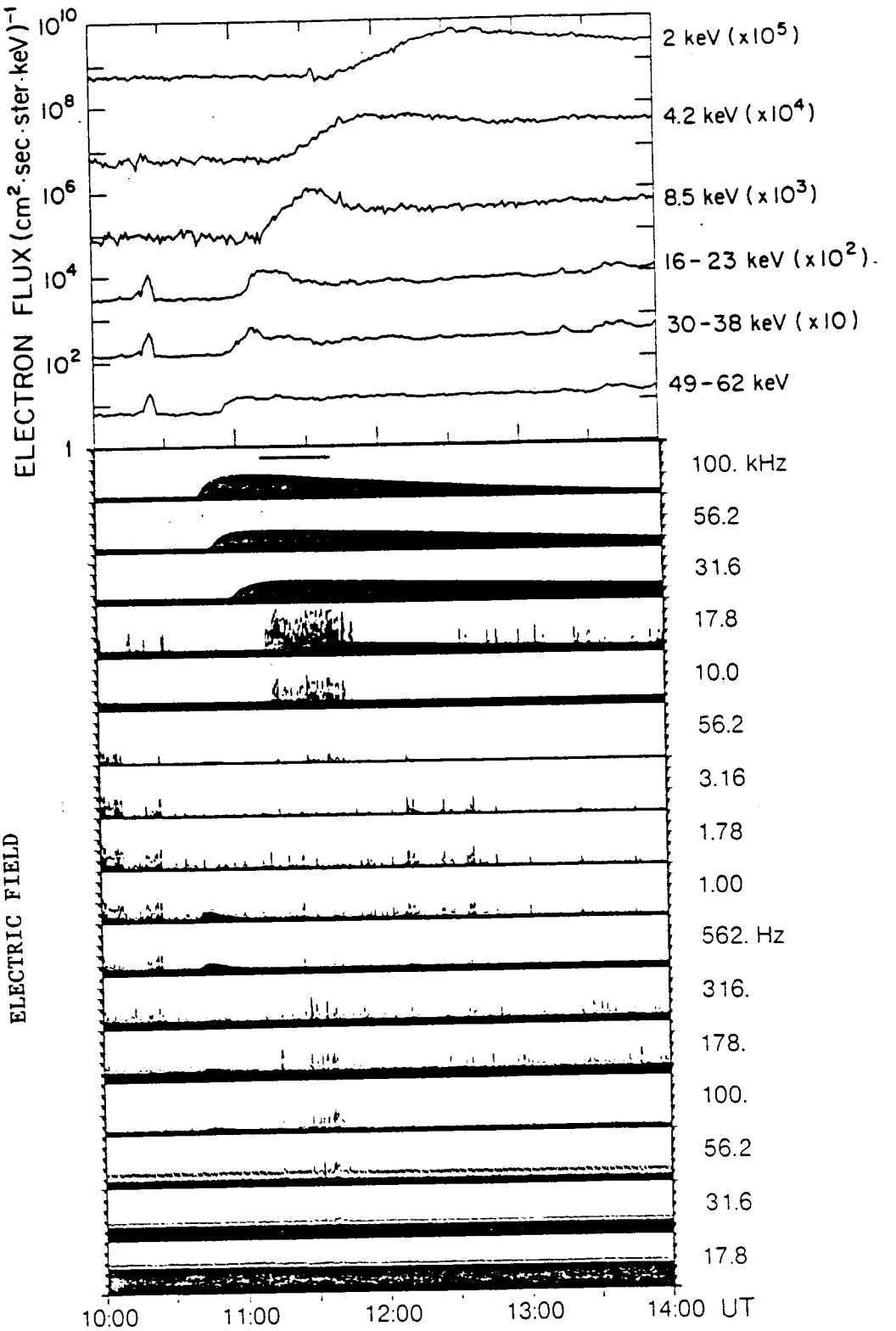

Figure 2.1 Electron flux and electric field measurements (from Lin et. al., 1986)

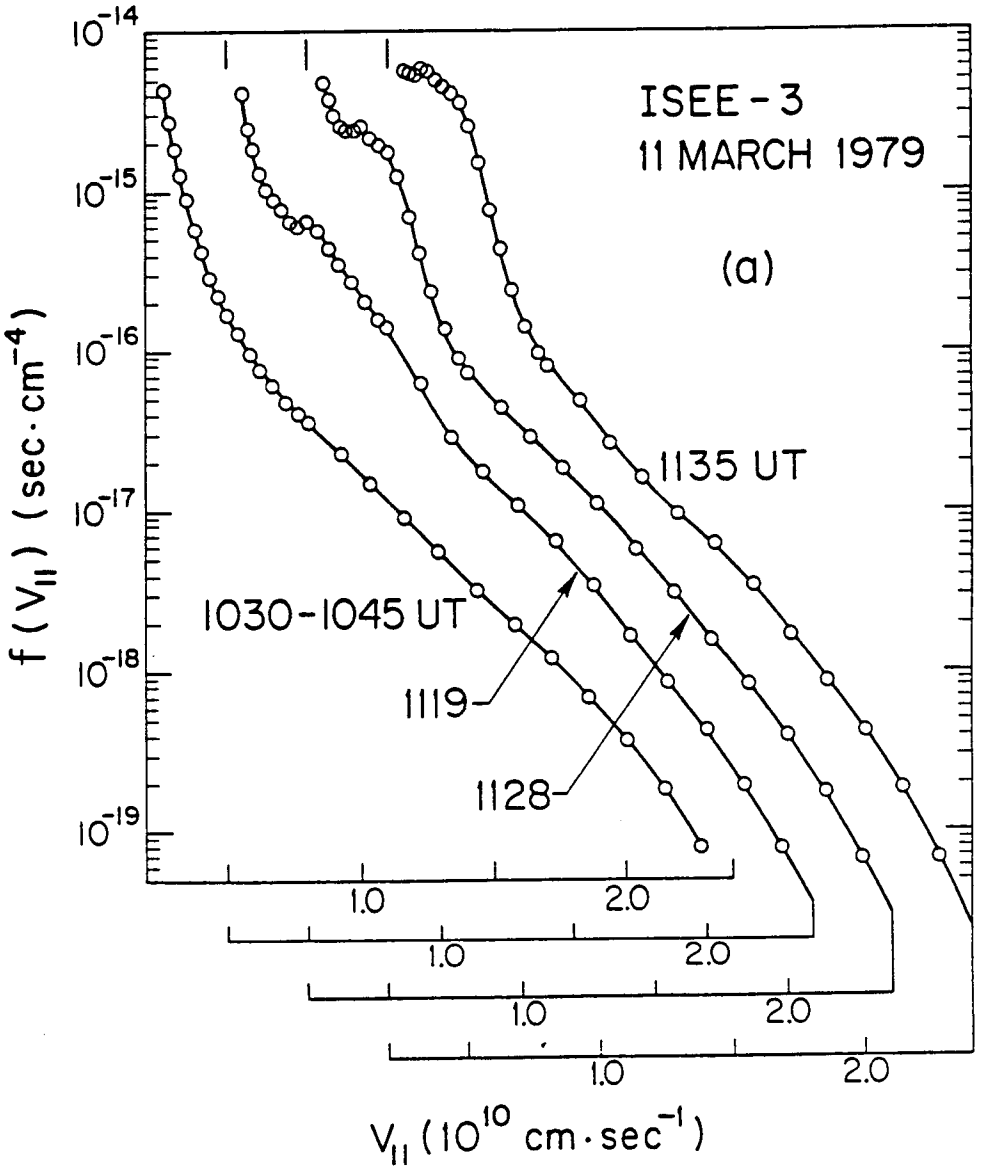

Figure 2.2 Reduced parallel electron distribution function.(from Lin et. al., 1986)

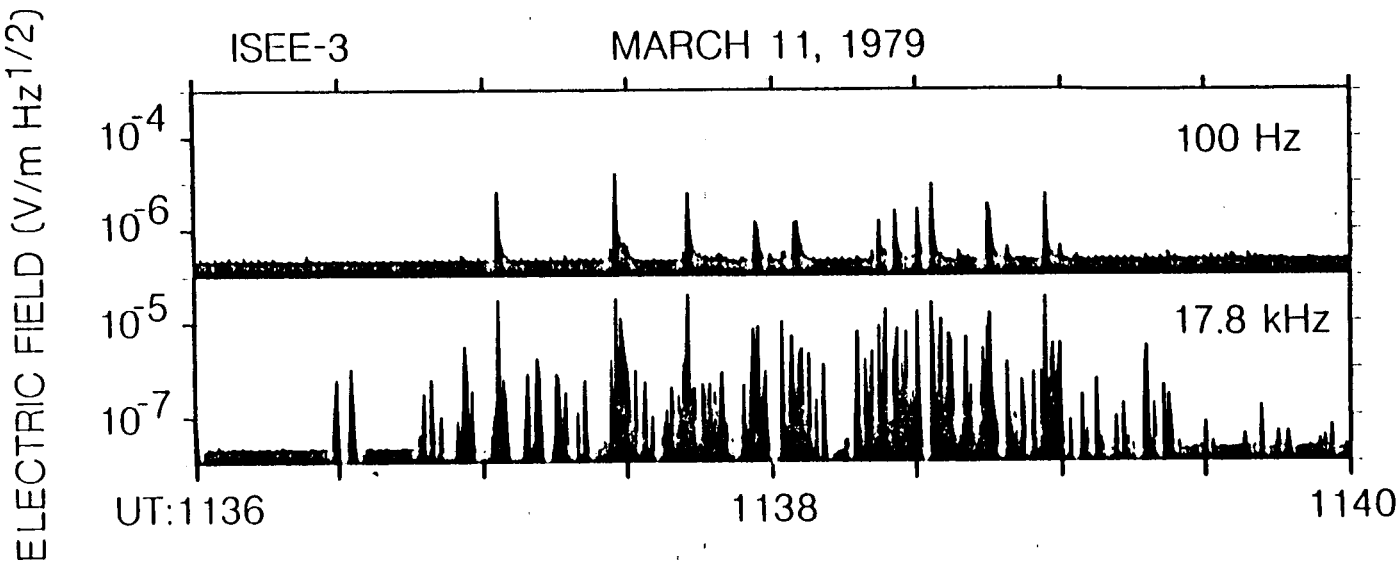

Figure 2.3 High time resolution electric field measurements. (from Lin et. al. 1986)

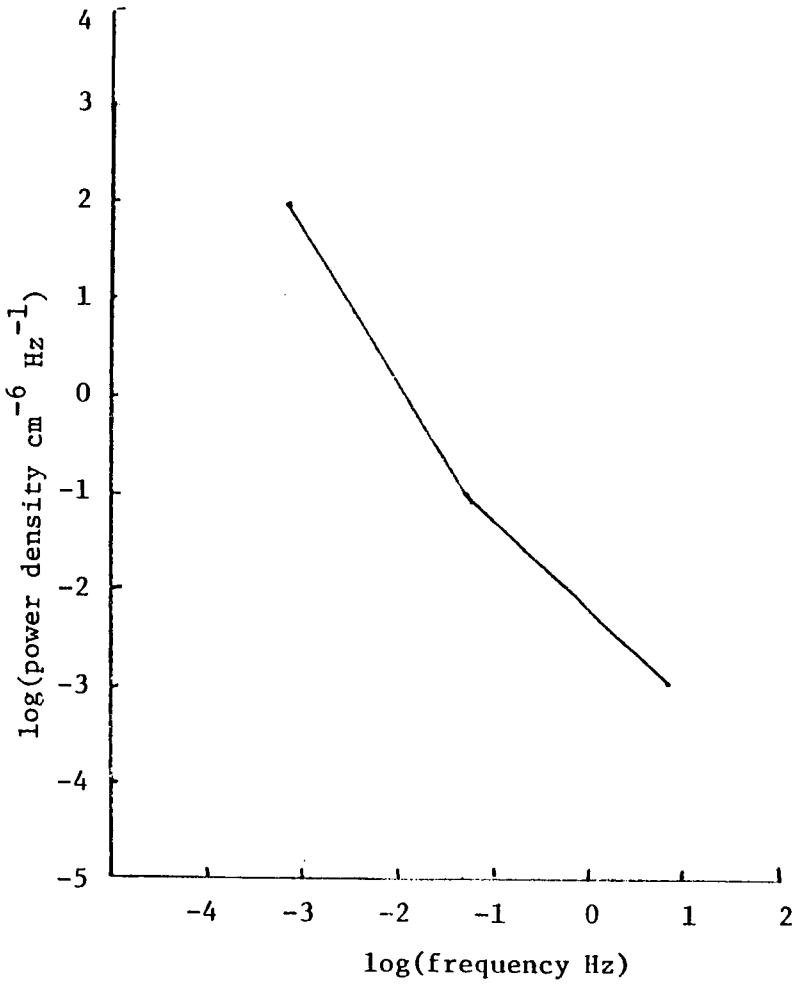

Figure 2.4 Power spectrum of solar wind density fluctuations. (from Celnikier et. al., 1981)

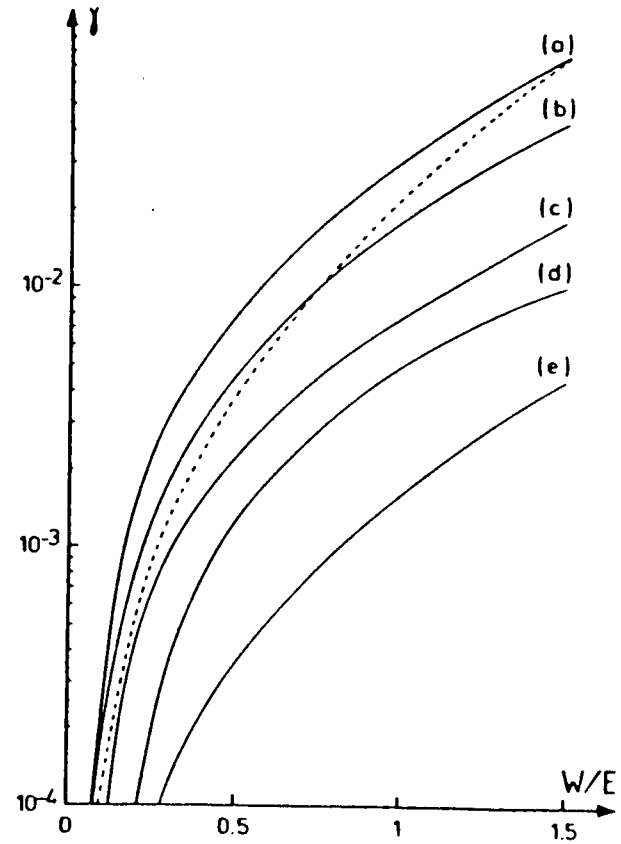

Plot of $\gamma = l_c/\xi$ vs W/E for $E = 1$ (curve a), 0.5 (curve b), 0.2 (curve c), 0.1 (curve d), and 0.05 (curve e); the dashed curve corresponds to $\gamma/2$ for $E = 5$.

(from Souillard et. al., 1984)

Figure 4.1

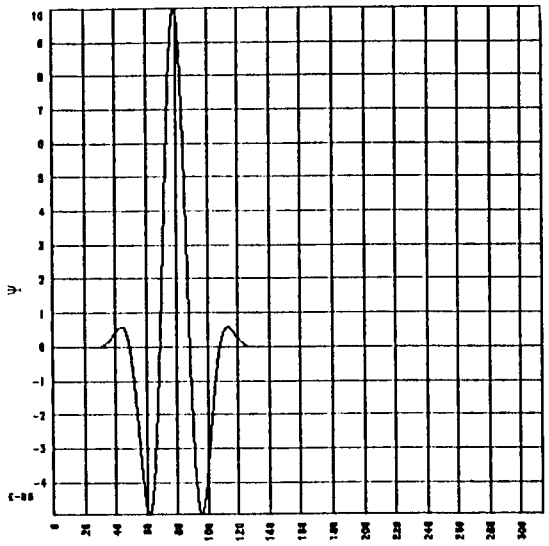

5.1.1 Ψ vs. x at t=0

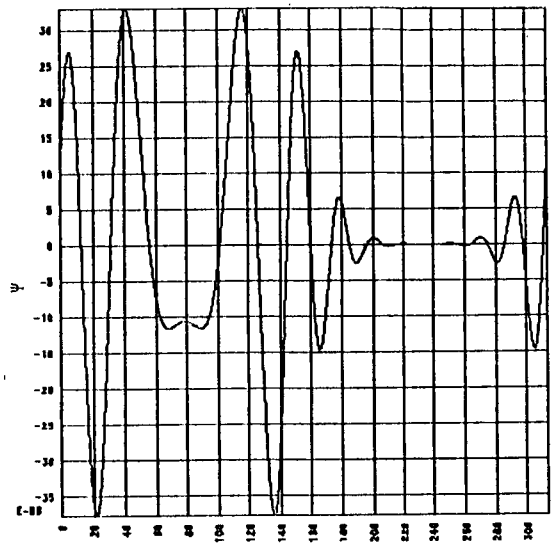

5.1.2 Ψ vs. x at t=8000

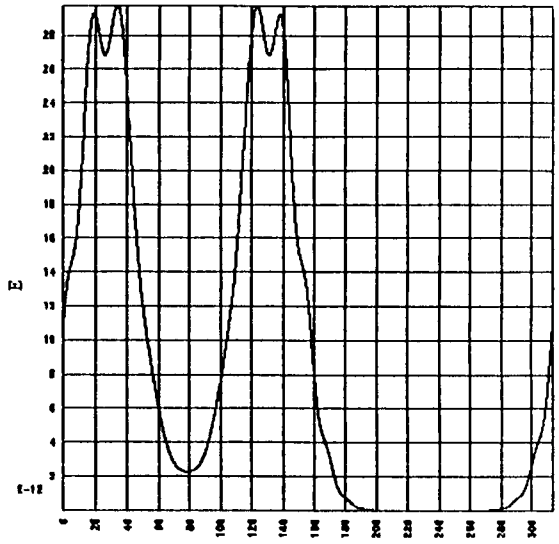

5.1.3 E vs. x at t=8000

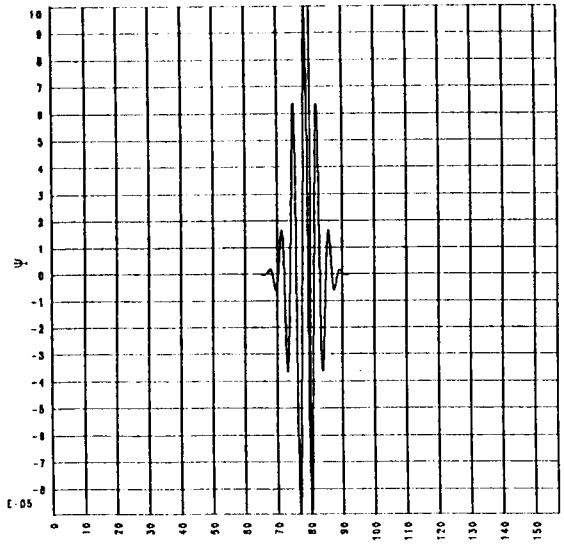

5.2.1 Ψ vs. x at t=0

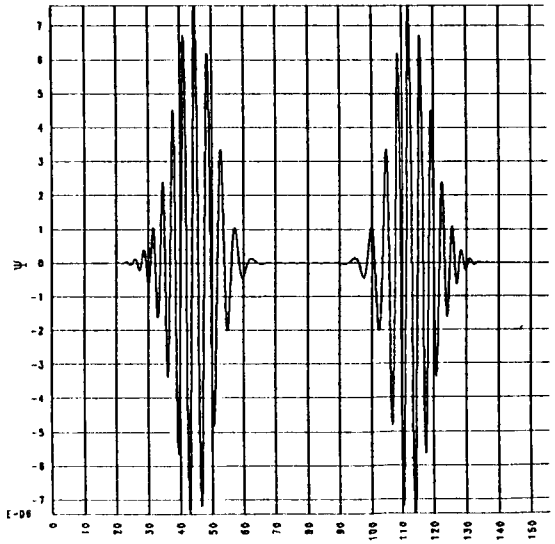

5.2.2 Ψ vs. x at t=8000

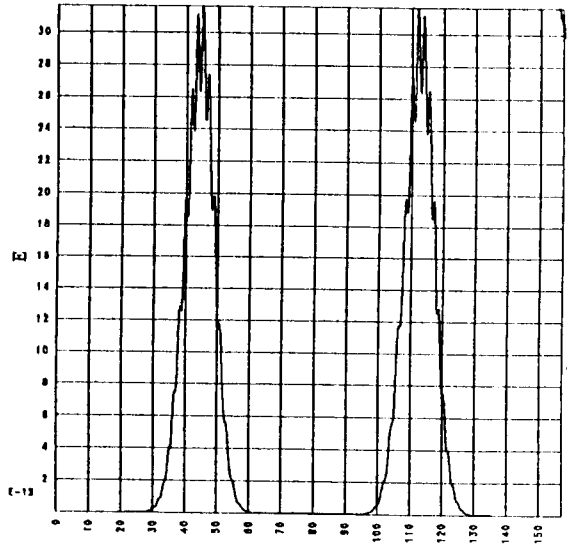

5.2.3 E vs. x at t=8000

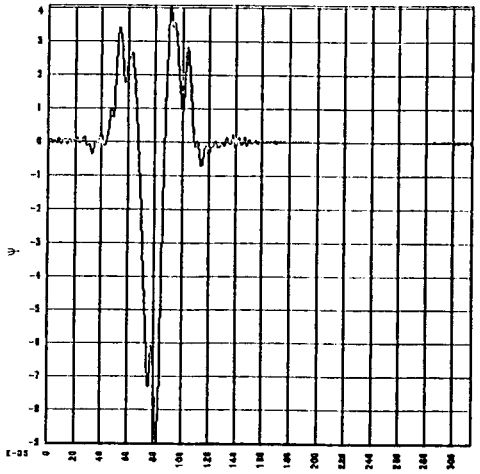

5.3.1 Ψ vs. x at t=800

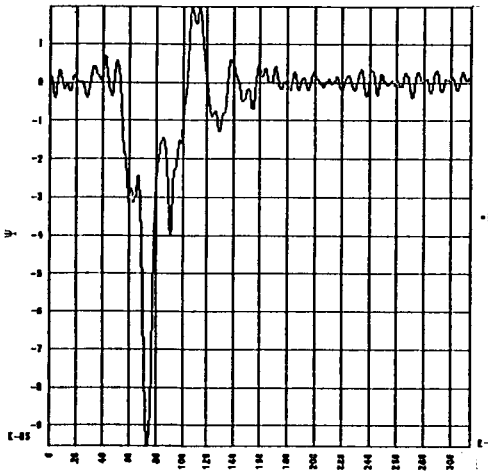

5.3.2 Ψ vs. x at t=8000

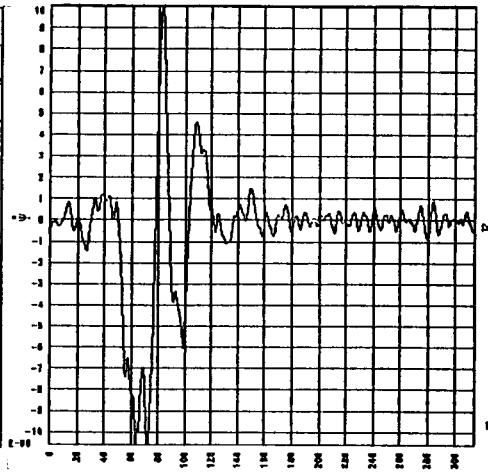

5.3.3 $\dot{\Psi}$ vs. x at t=8000

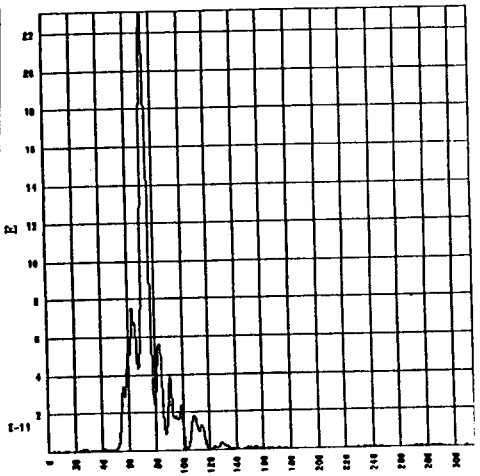

5.3.4 E vs. x at t=8000

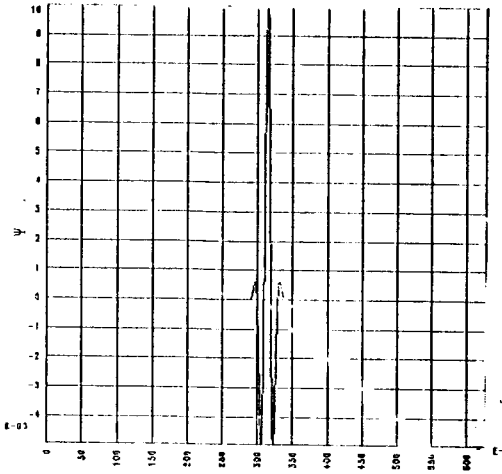

5.4.1 Ψ vs. x at t=0

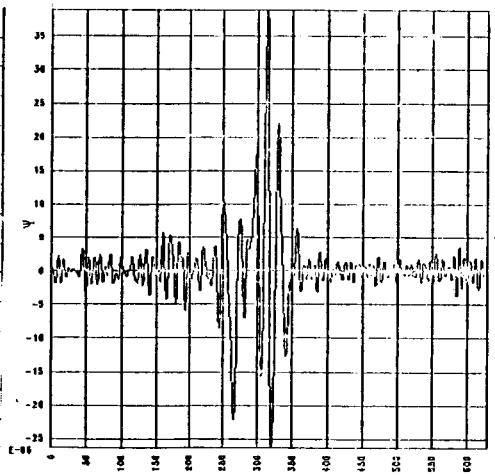

5.4.2 Ψ vs. x at t=24000

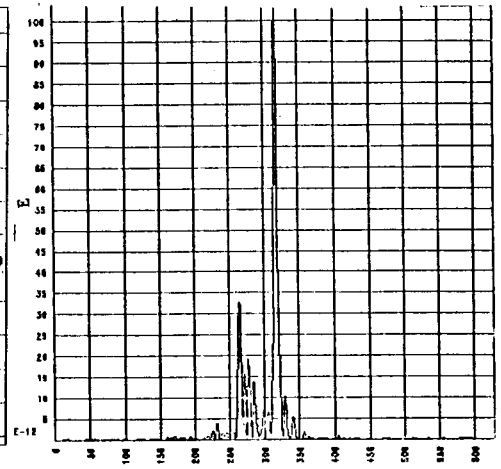

5.4.3 E vs. x at t=24000

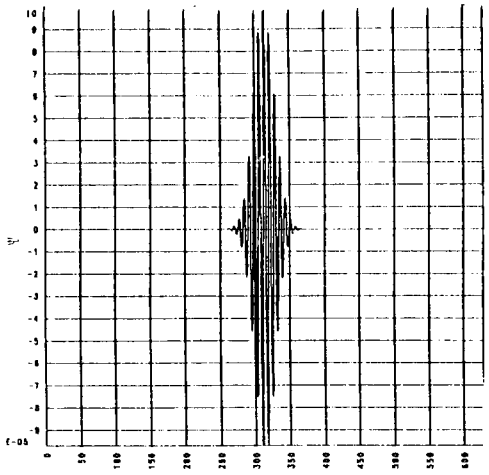

5.5.1 Ψ vs. x at t=0

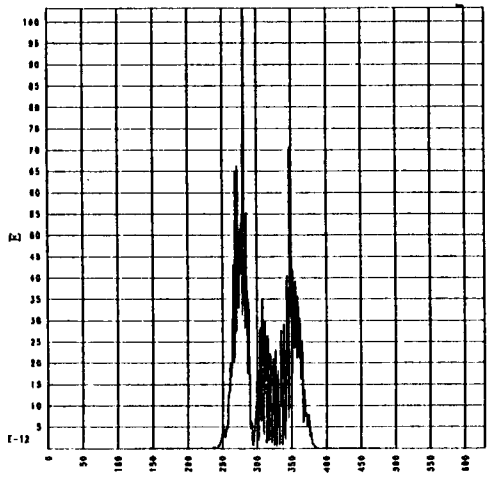

5.5.2 E vs. x at t=2000

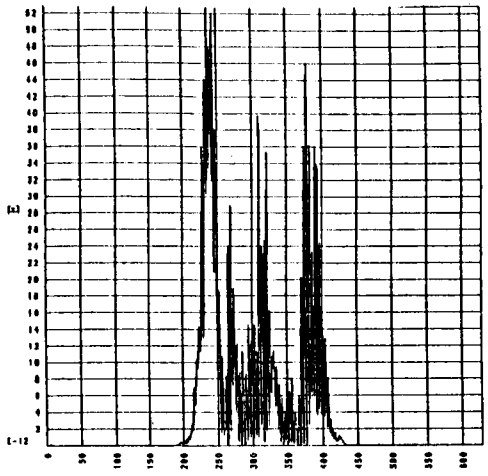

5.5.3 E vs. x at t=4000

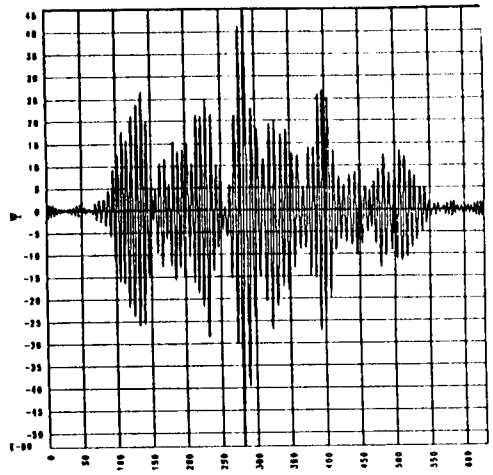

5.5.4 Ψ vs. x at t=10000

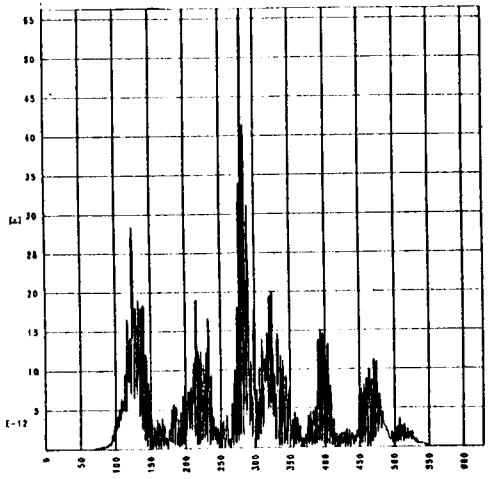

5.5.5 E vs. x at t=10000

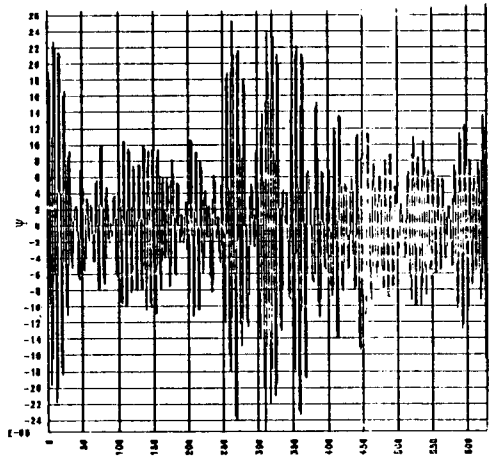

5.5.6 Ψ vs. x at t=20000

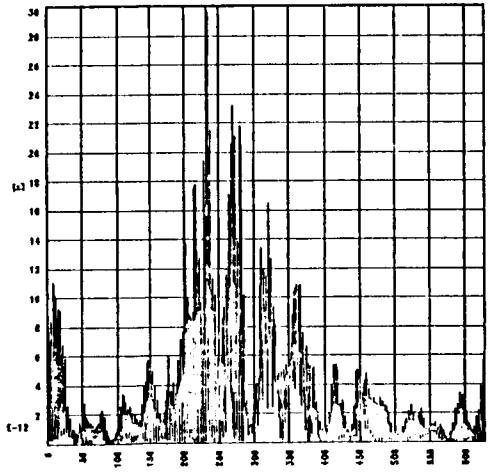

5.5.7 E vs. x at t=20000

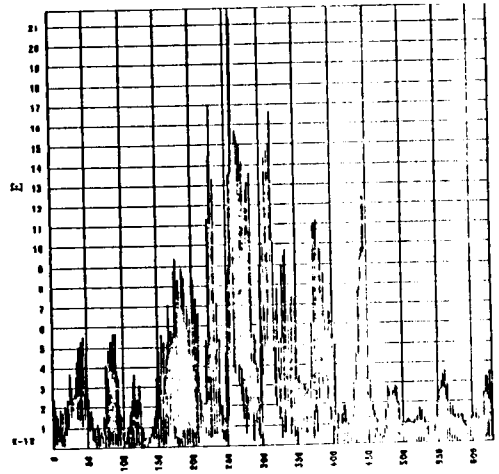

5.5.8 E vs. x at t=22000

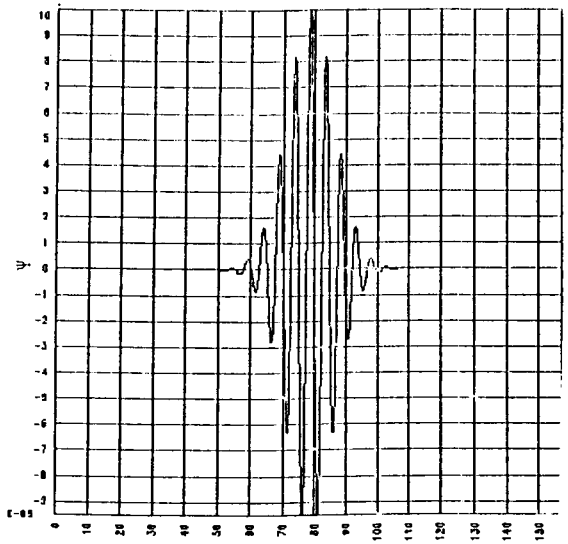

5.6.1 Ψ vs. x at t=0

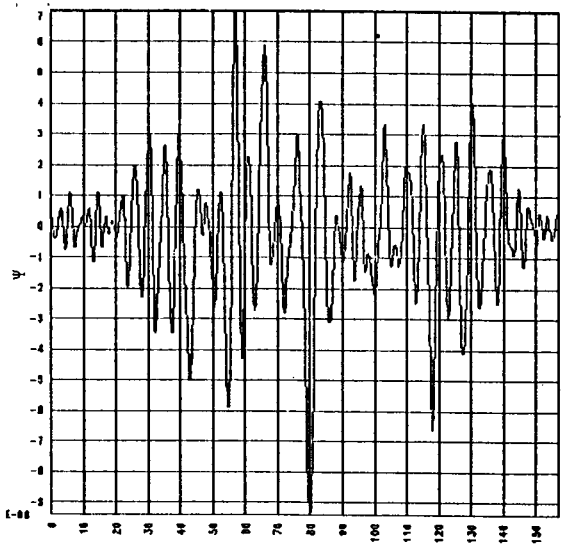

5.6.2 Ψ vs. x at t=8000

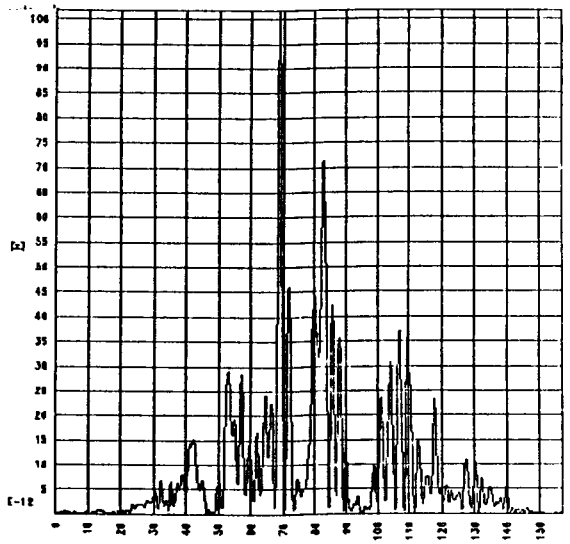

5.6.3 E vs. x at t=8000

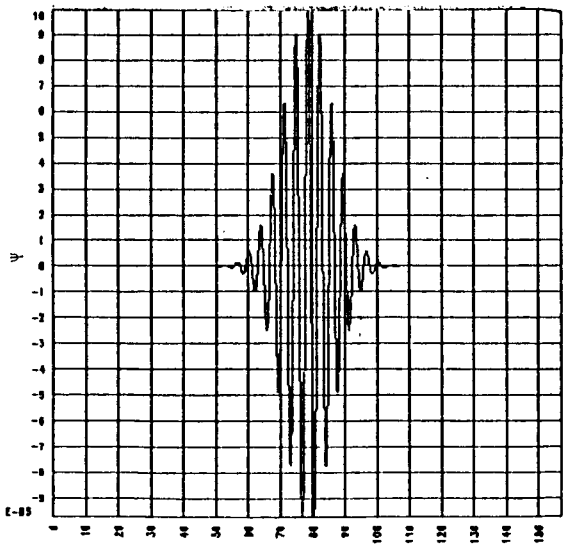

5.7.1 Ψ vs. x at t=0

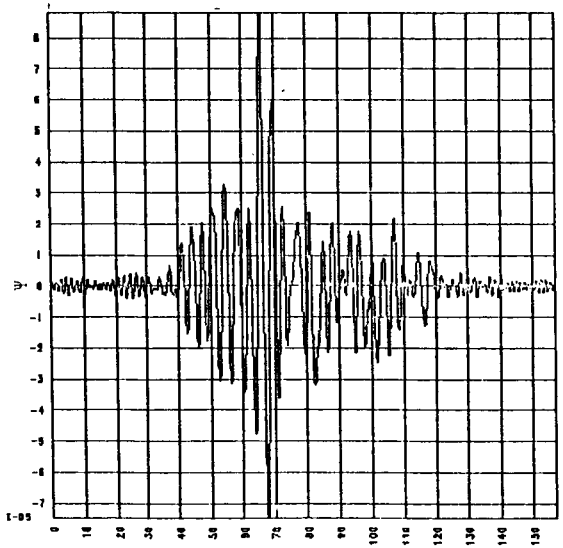

5.7.2 Ψ vs. x at t=7200

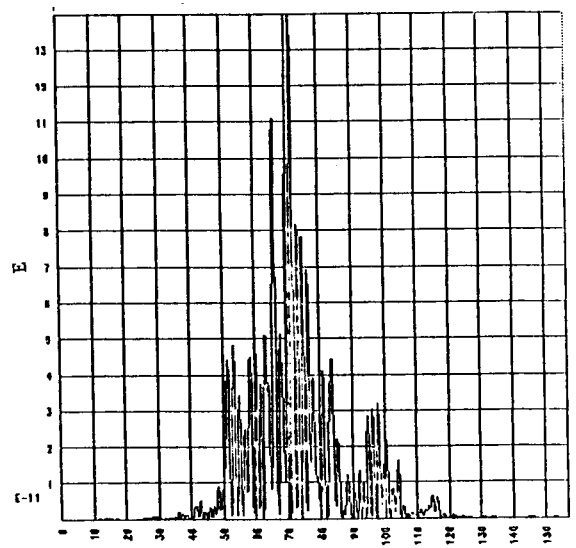

5.7.3 E vs. x at t=7200

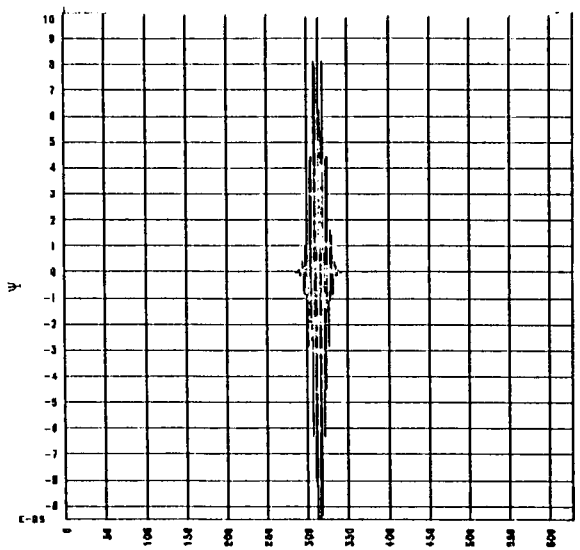

5.8.1 Ψ vs. x at t=0

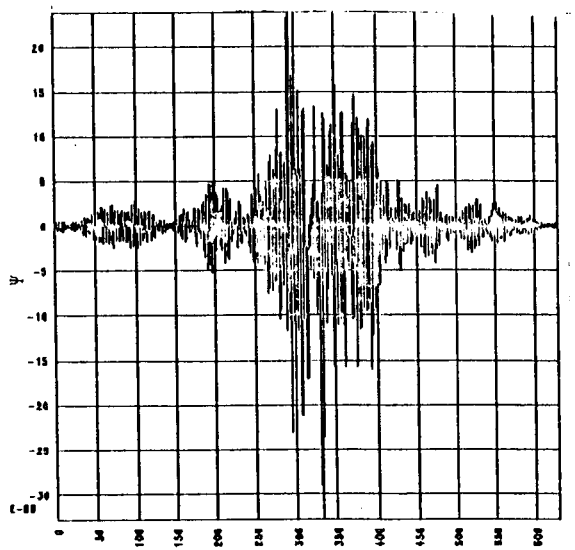

5.8.2 Ψ vs. x at t=16800

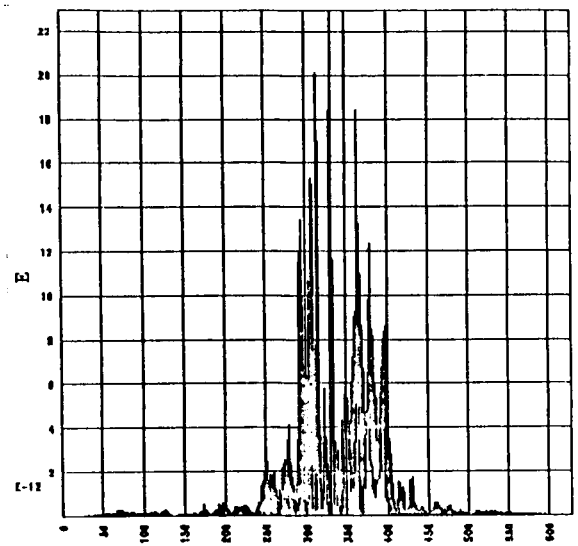

5.8.3 E vs. x at t=16800

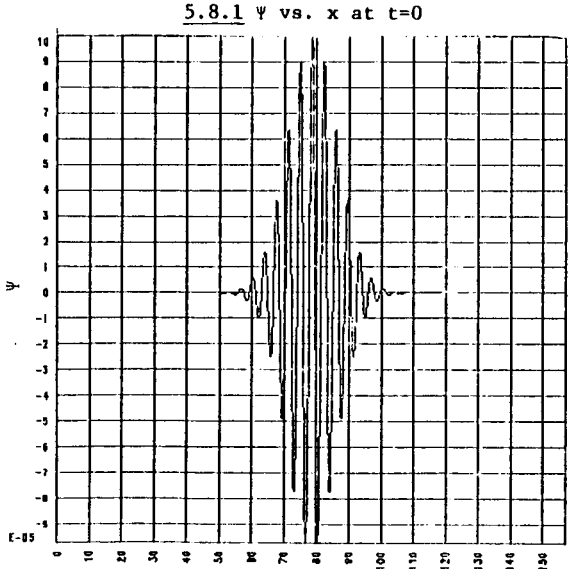

5.9.1 Ψ vs. x at t=0

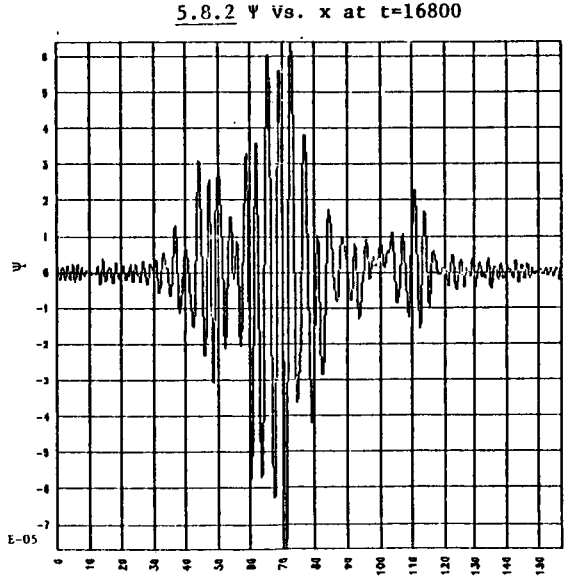

5.9.2 Ψ vs. x at t=8000

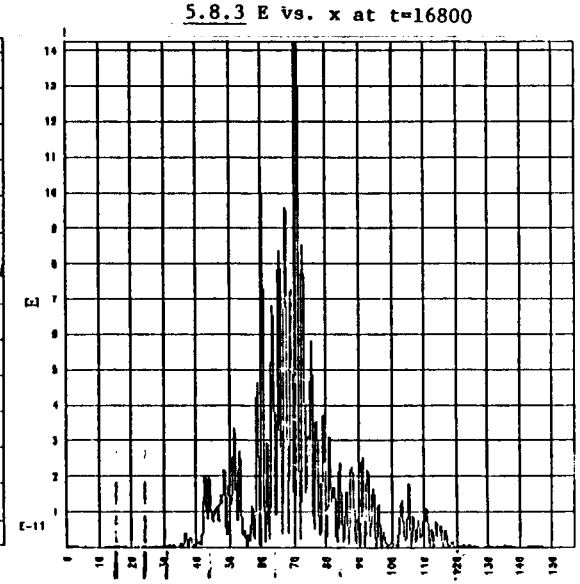

5.9.3 E vs. x at t=8000

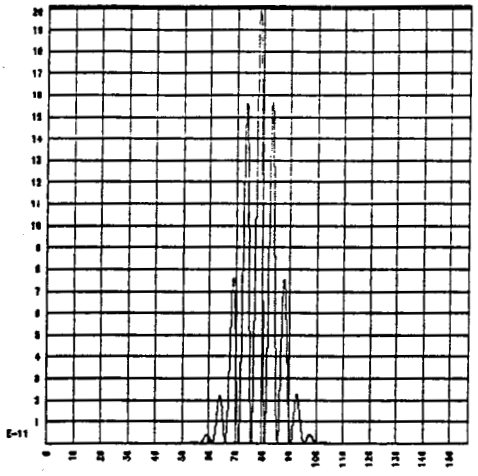

5.10.1 E vs. x at t=0

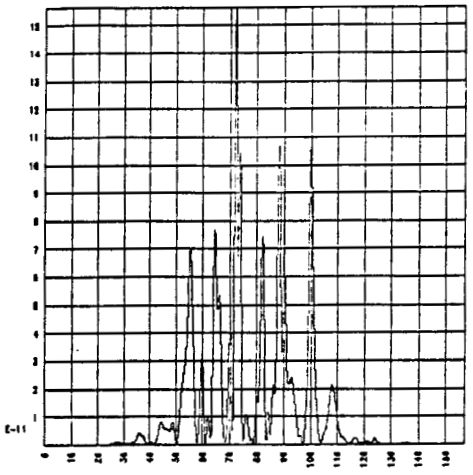

5.10.2 E vs. x at t=4000

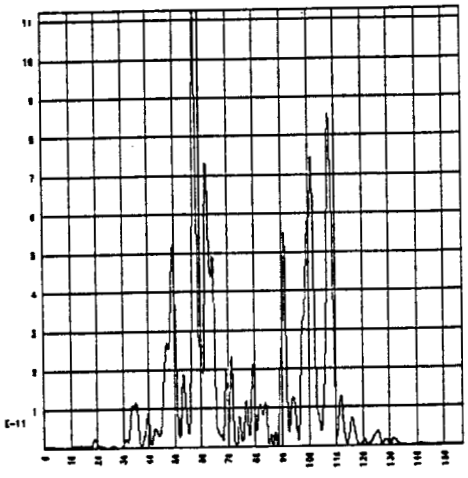

5.10.3 E vs. x at t=6800

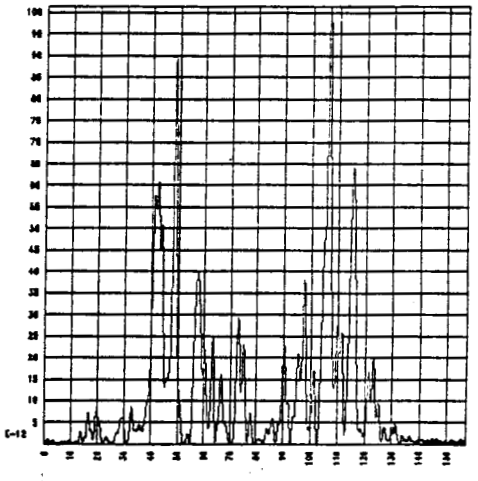

5.10.4 E vs. x at t=8000

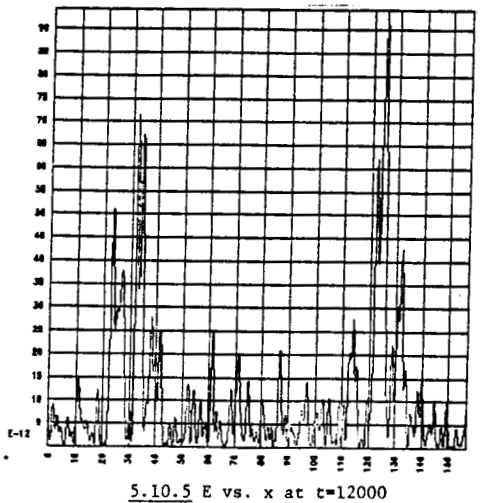

5.10.5 E vs. x at t=12000

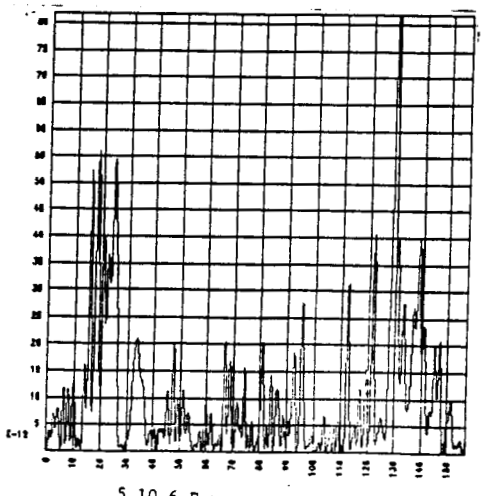

5.10.6 E vs. x at t=14000

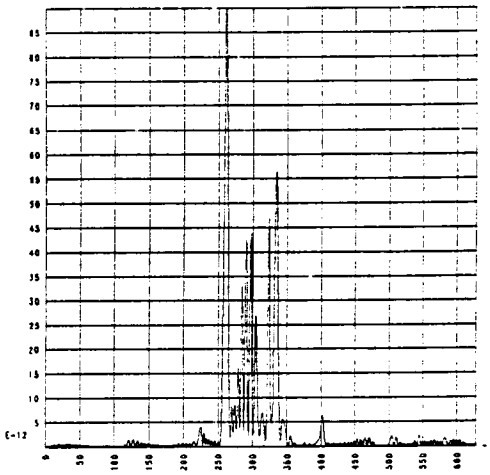

5.11.1 E vs. x at t=16000; cs=0

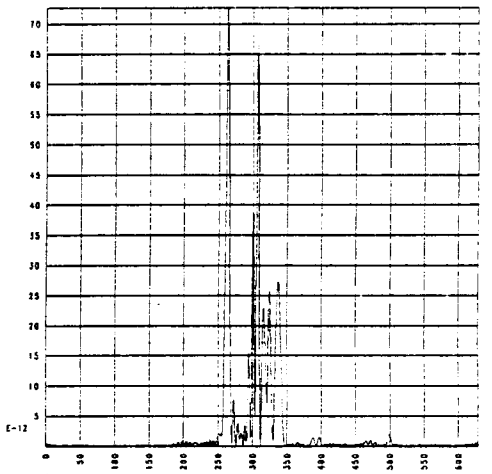

5.11.2 E vs. x at t=32000; cs=0

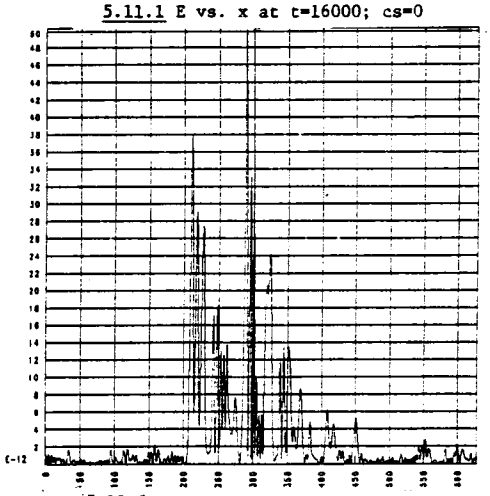

5.11.3 E vs. x at t=16000; cs=.005c

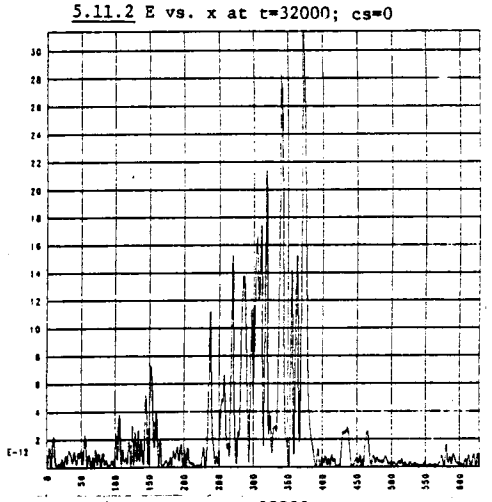

5.11.4 E vs. x at t=32000; cs=.005c

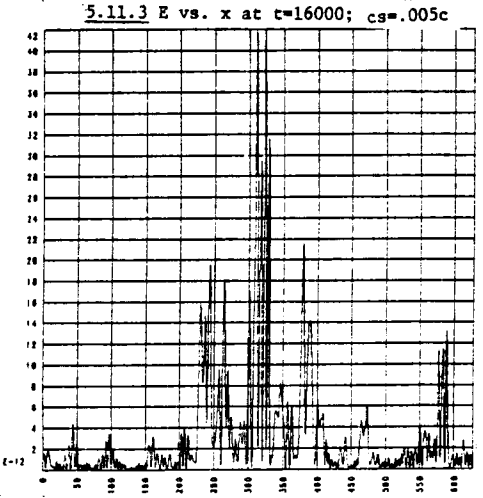

5.11.5 E vs. x at t=16000; cs=.01cc

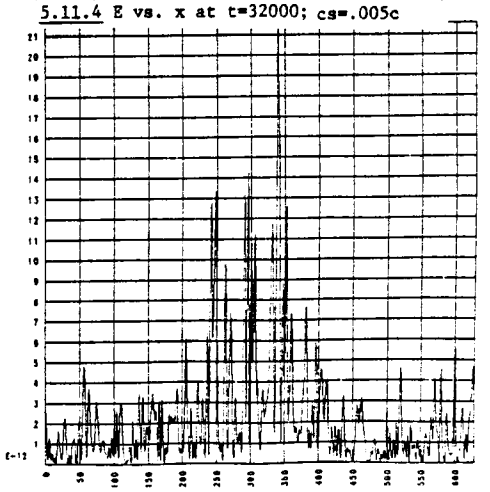

5.11.6 E vs. x at t=32000; cs=.01c

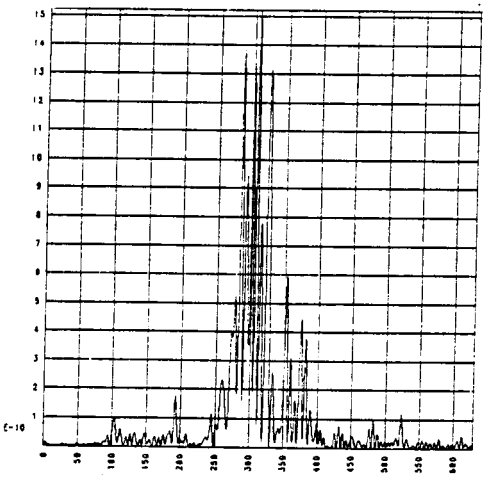

5.12a.1 E vs. x at t=6400; cs=0

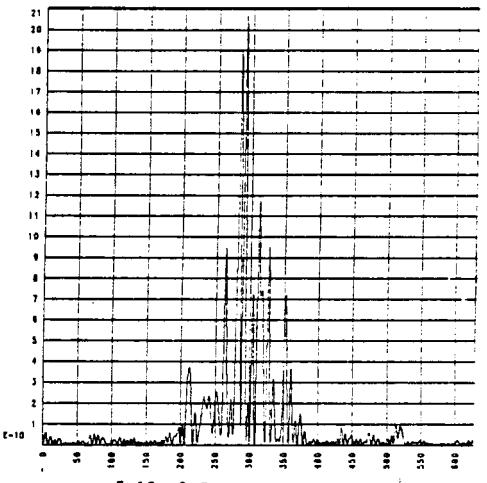

5.12a.2 E vs. x at t=9600

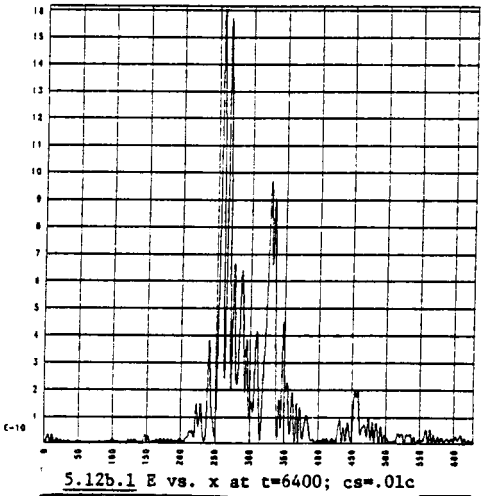

5.12b.1 E vs. x at t=6400; cs=.01c

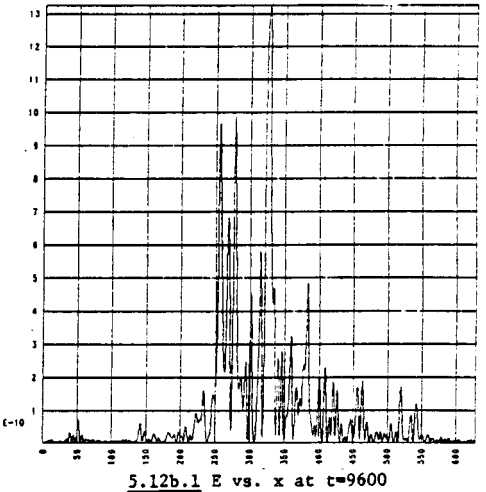

5.12b.1 E vs. x at t=9600

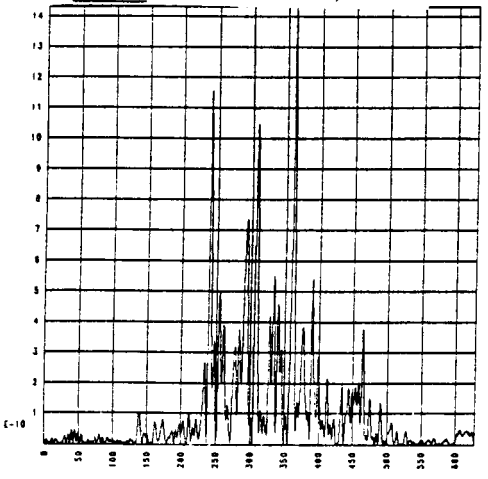

5.12c.1 E vs. x at t=6400; cs=.1c

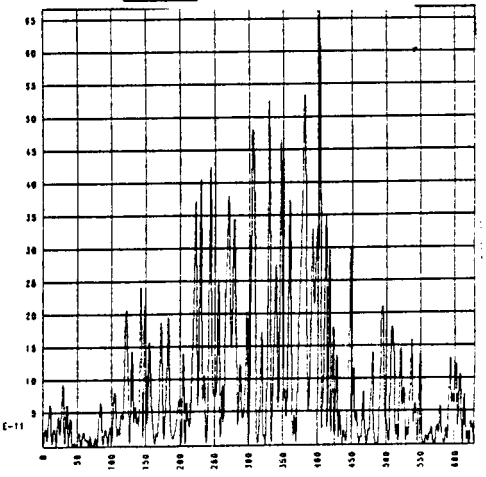

5.12c.1 E vs. x at t=9600

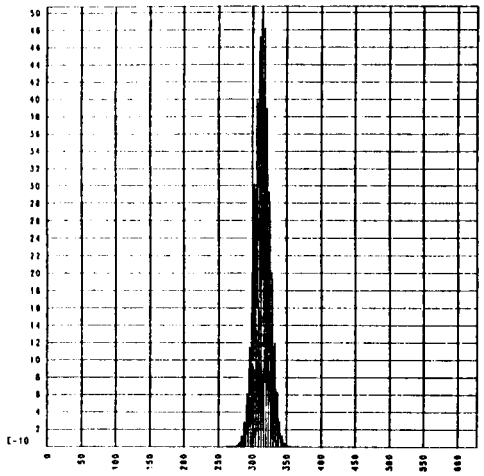

5.13a.1 E vs. x at t=0; cs=0

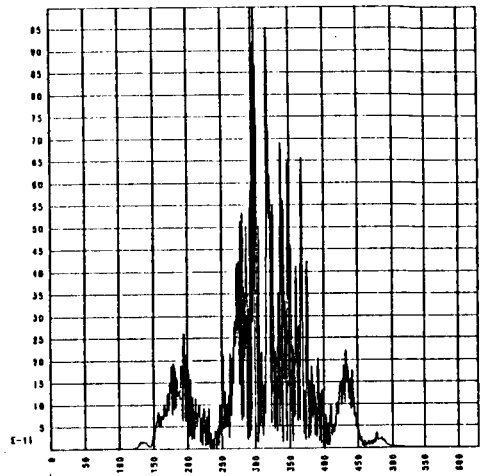

5.13a.2 E vs. x at t=3200

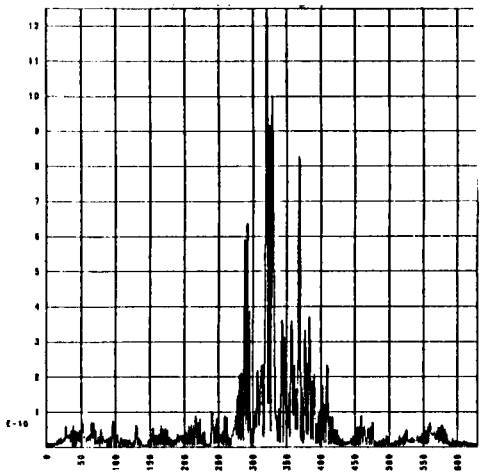

5.13a.3 E vs. x at t=6400

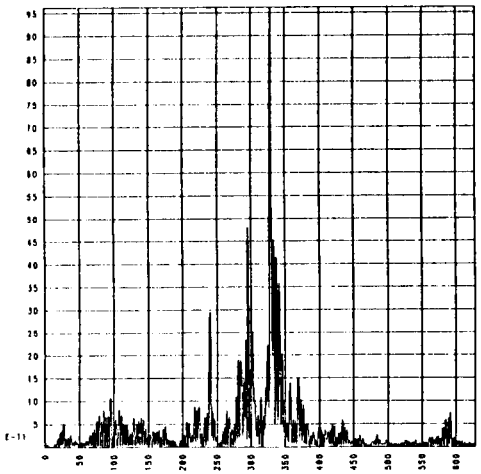

5.13a.4 E vs. x at t=12800

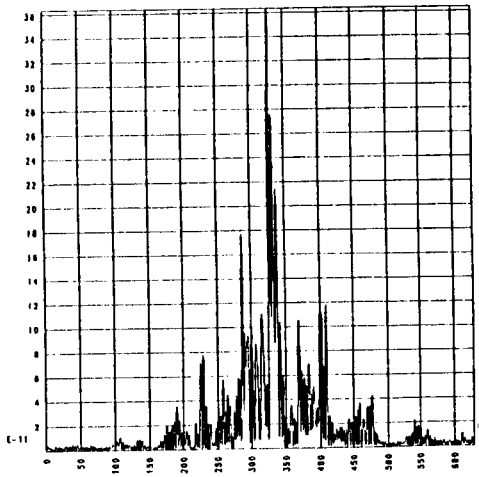

5.13a.5 E vs. x at t=22400

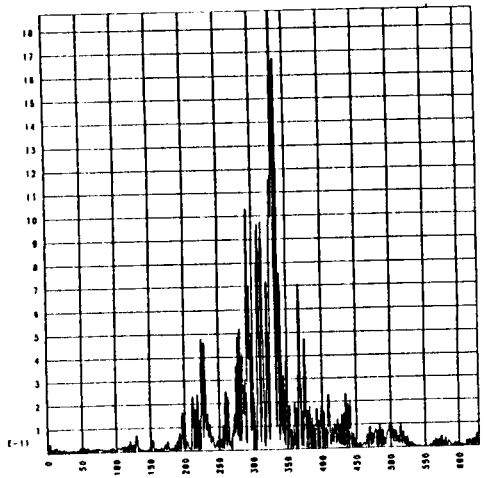

5.13a.6 E vs. x at t=32000

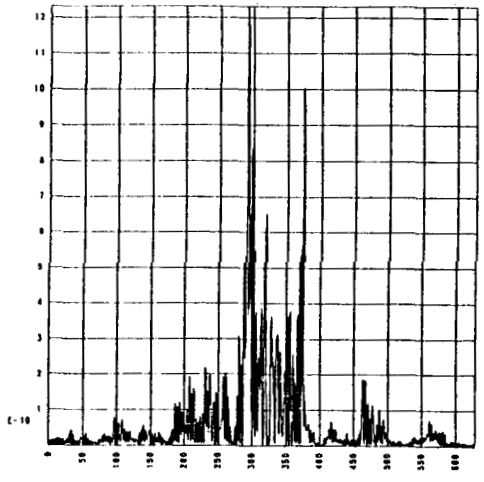

5.13b.1 E vs. x at t=6400; cs=.0025c

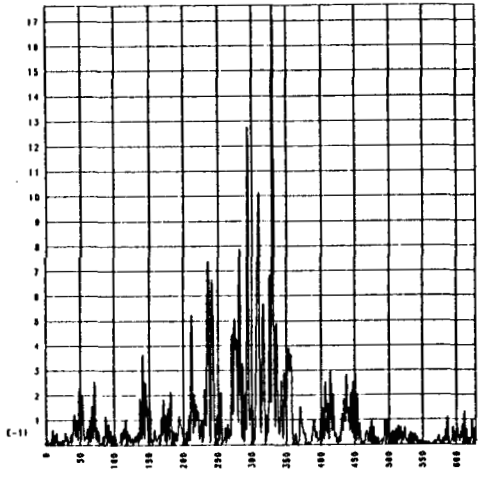

5.13b.2 E vs. x at t=19200

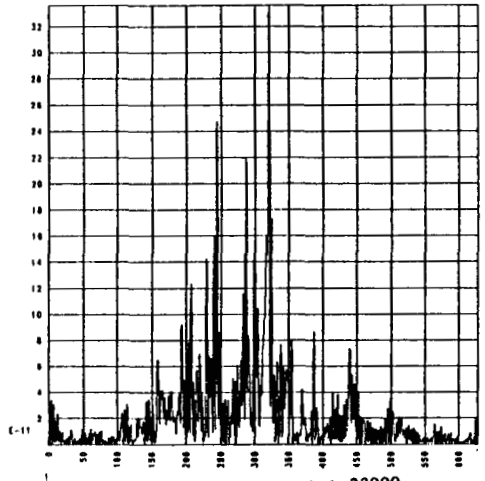

5.13b.3 E vs. x at t=32000

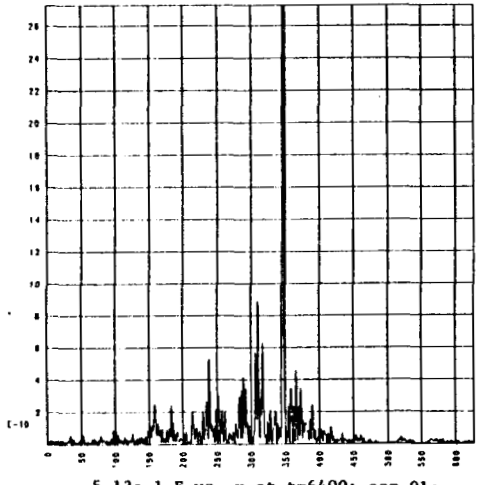

5.13c.1 E vs. x at t=6400; cs=.01c

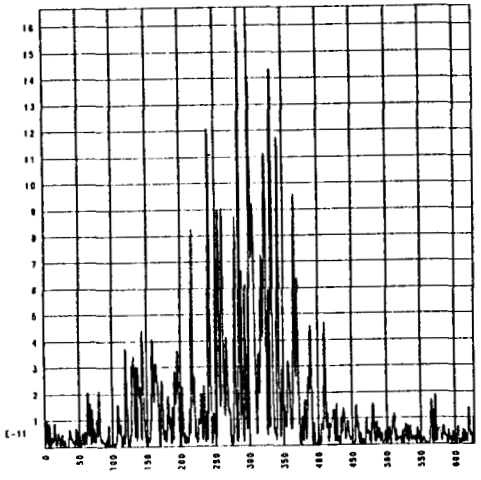

5.13c.2 E vs. x at t=19200

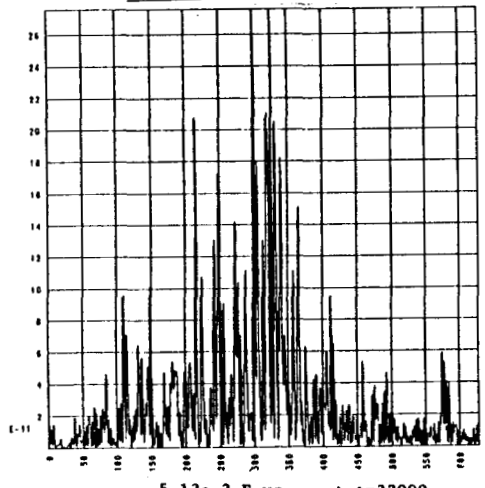

5.13c.3 E vs. x at t=32000

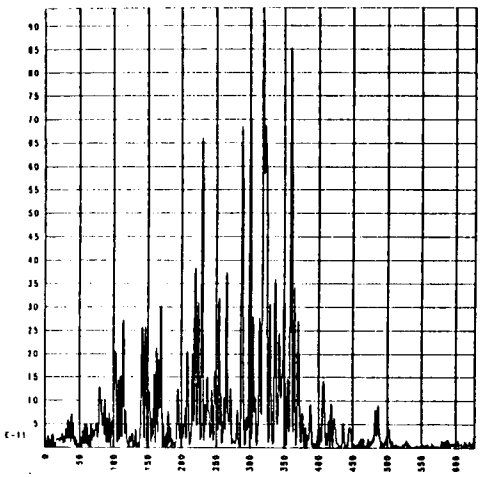

5.13d.1 E vs. x at t=6400; cs=.05c

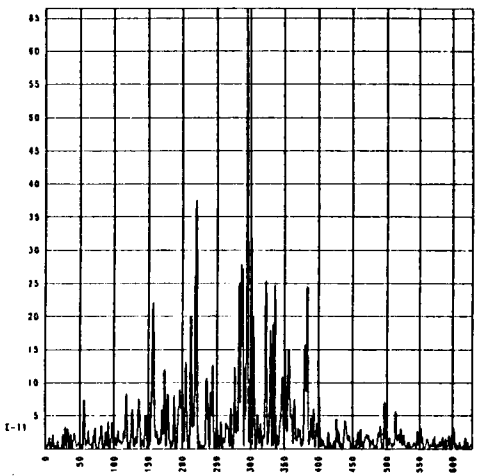

5.13d.2 E vs. x at t=19200

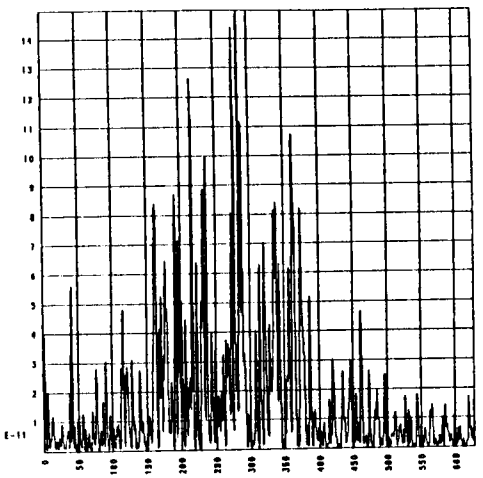

5.13d.3 E vs. x at t=32000

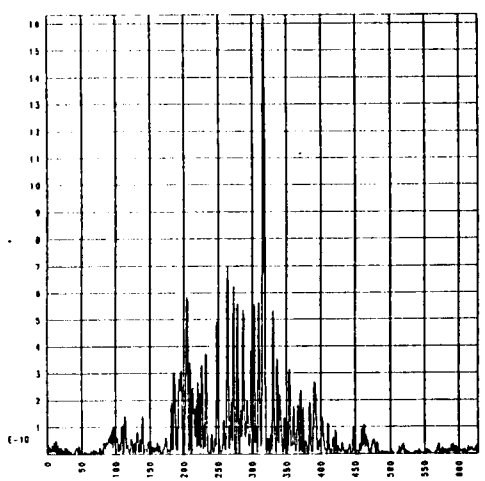

5.13e.1 E vs. x at t=6400; cs=.1c

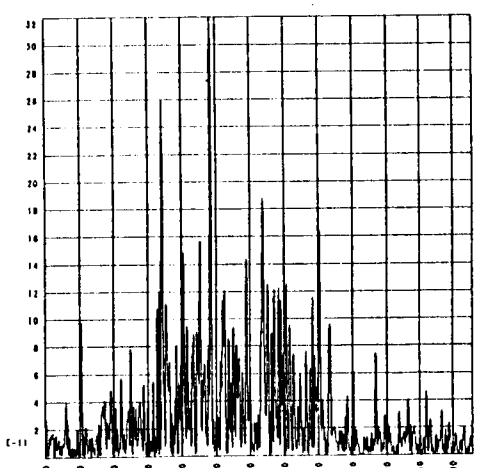

5.13e.2 E vs. x at t=19200

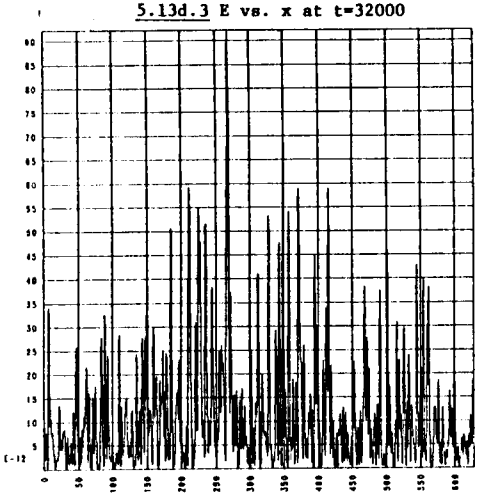

5.13e.3 E vs. x at t=32000

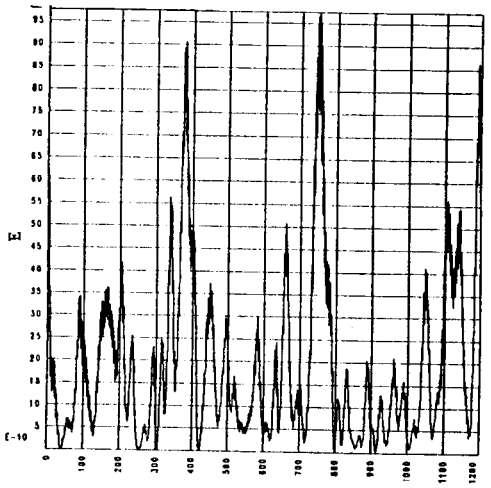

6.1.1 E vs. x at t=3000

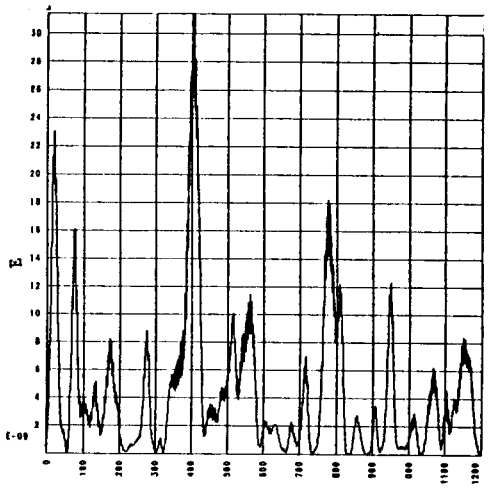

6.1.2 E vs. x at t=4800

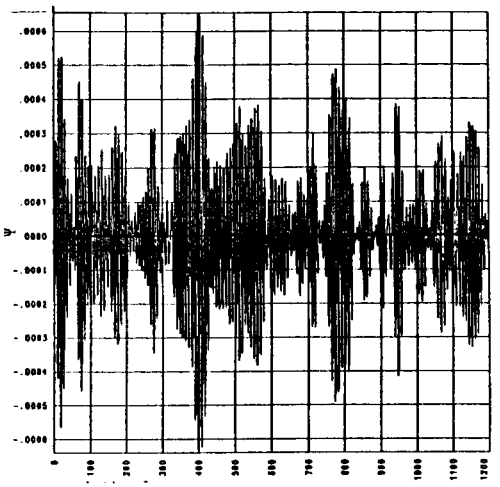

6.1.3 Ψ vs. x at t=4800

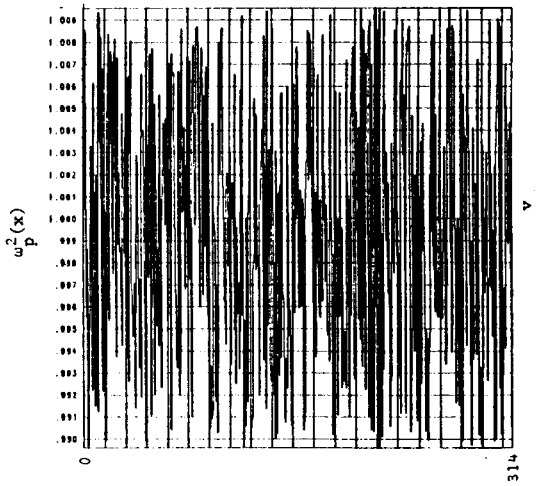

6.2.1 $\omega_p^2(x)$ vs. x

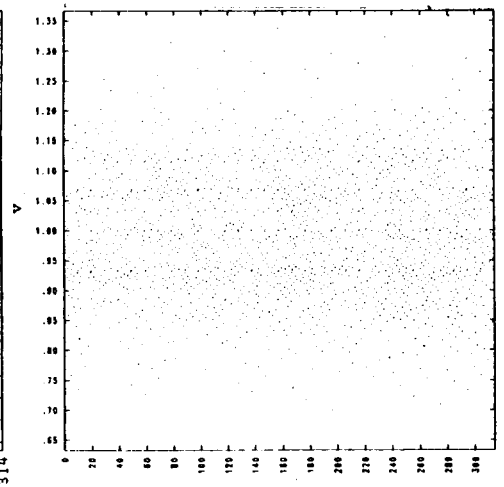

6.2.2 beam phase space; v vs. x; t=0

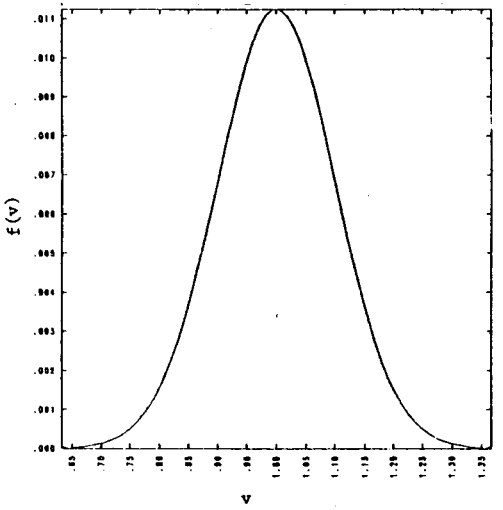

6.2.3 beam velocity distribution; t=0

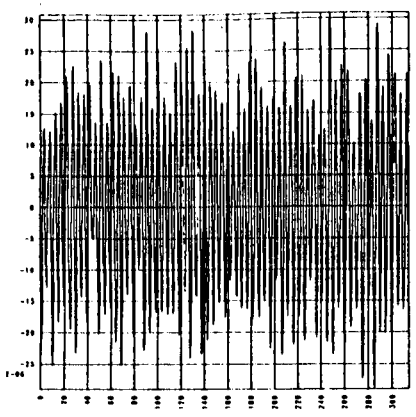

6.2.4 Ψ vs. x at t=200

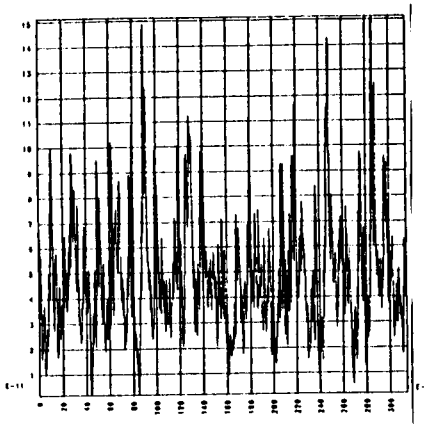

6.2.5 E vs. x at t=200

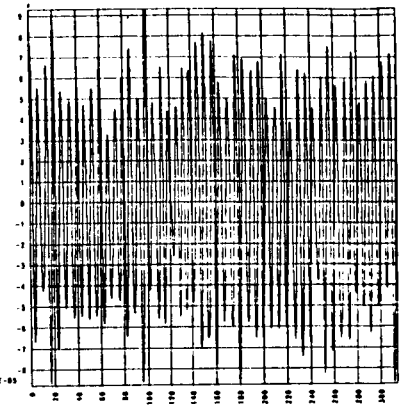

6.2.6 Ψ vs. x at t=800

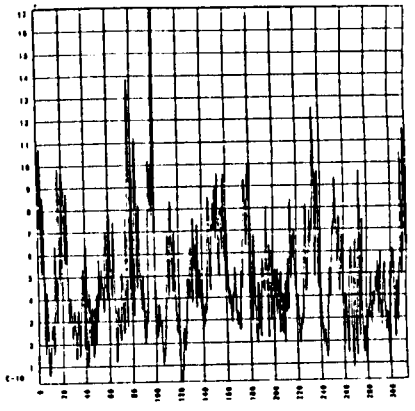

6.2.7 E vs. x at t=800

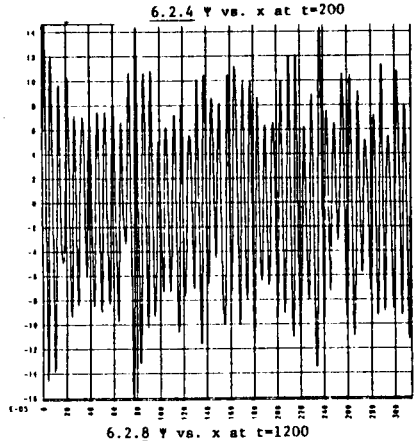

6.2.8 Ψ vs. x at t=1200

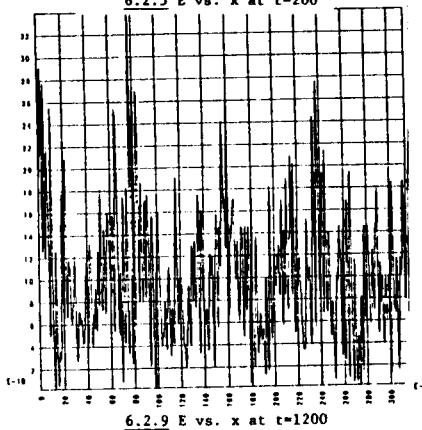

6.2.9 E vs. x at t=1200

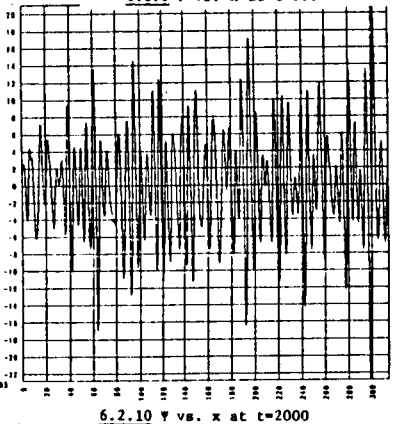

6.2.10 Ψ vs. x at t=2000

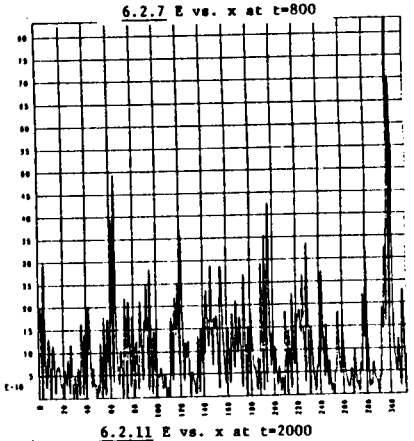

6.2.11 E vs. x at t=2000

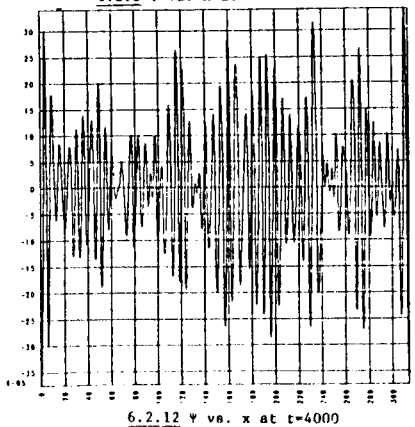

6.2.12 Ψ vs. x at t=4000

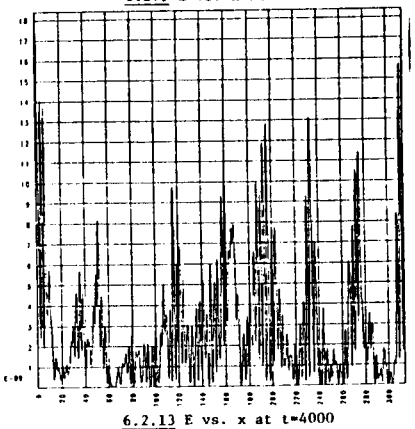

6.2.13 E vs. x at t=4000

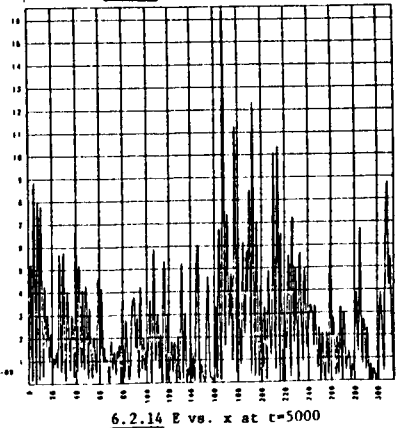

6.2.14 E vs. x at t=5000

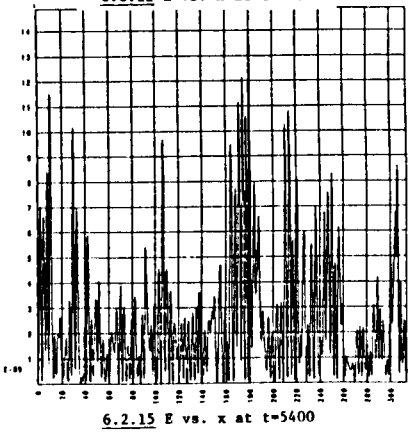

6.2.15 E vs. x at t=5400

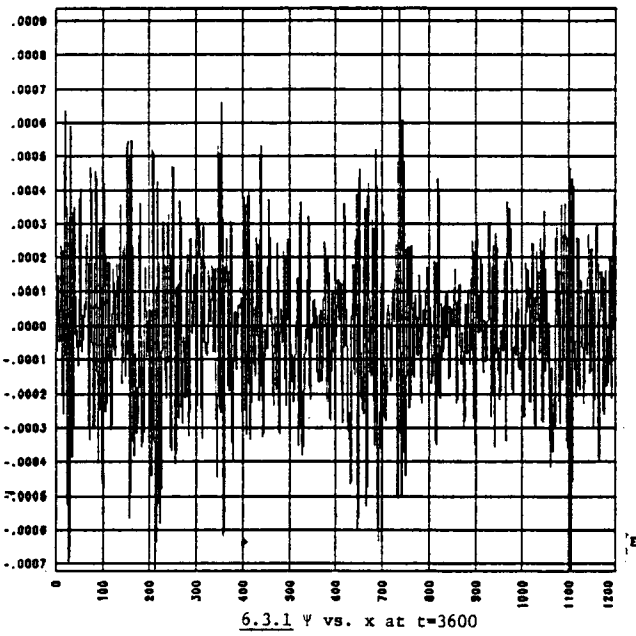

6.3.1 Ψ vs. x at t=3600

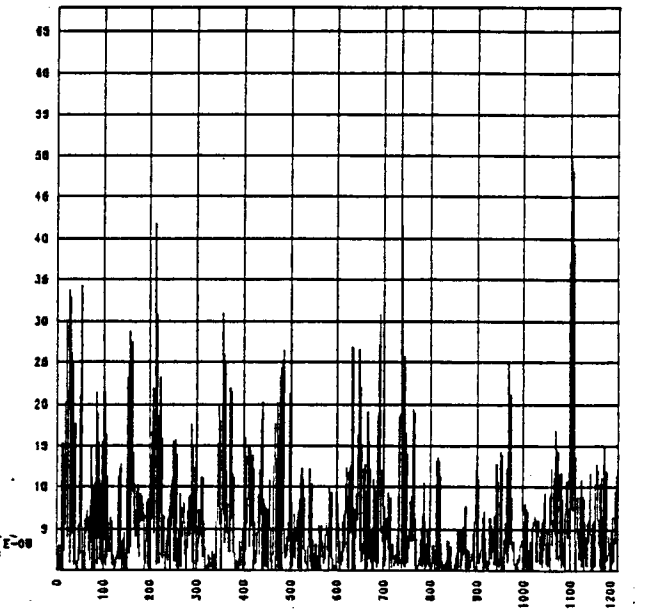

6.3.2 E vs. x at t=3600

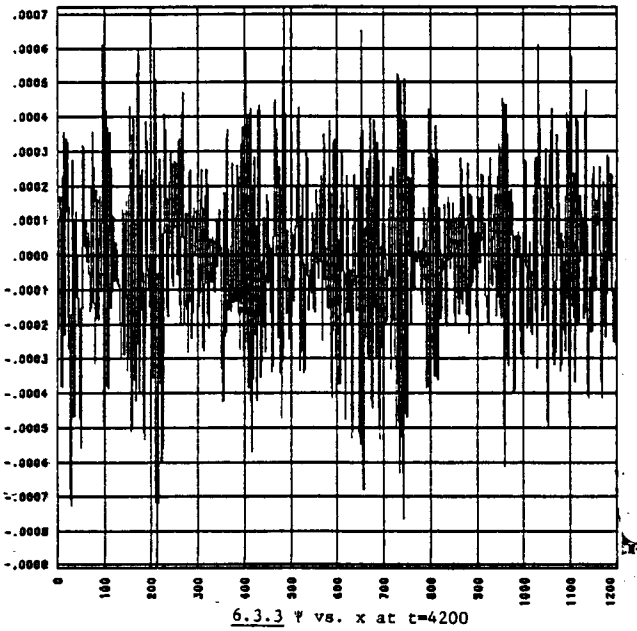

6.3.3 Ψ vs. x at t=4200

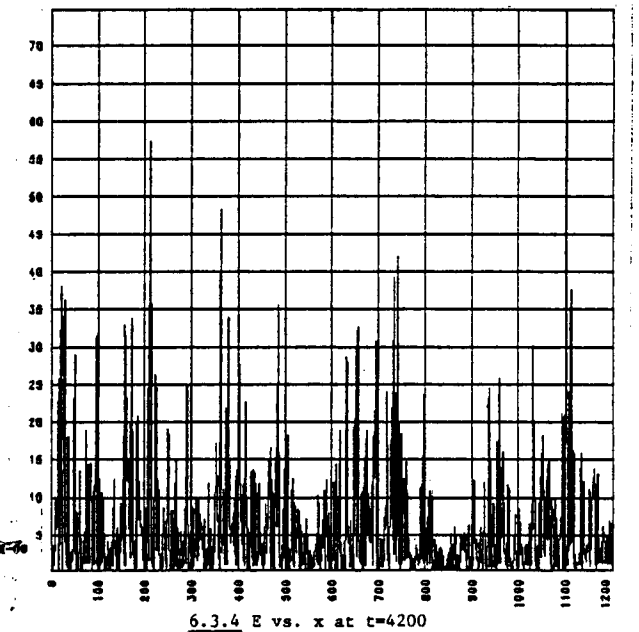

6.3.4 E vs. x at t=4200

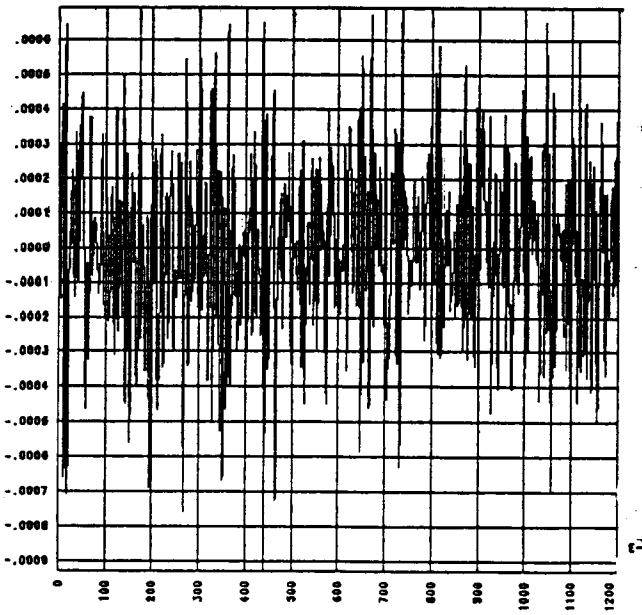

6.3.5 Ψ vs. x at t=6000

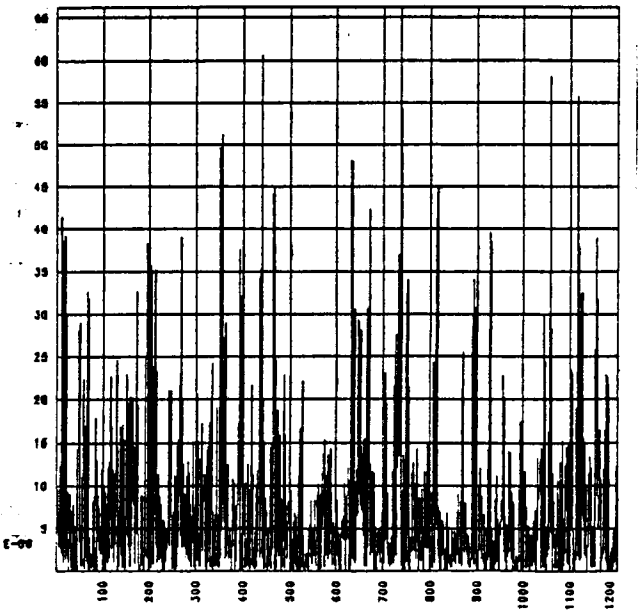

6.3.6 E vs. x at t=6000

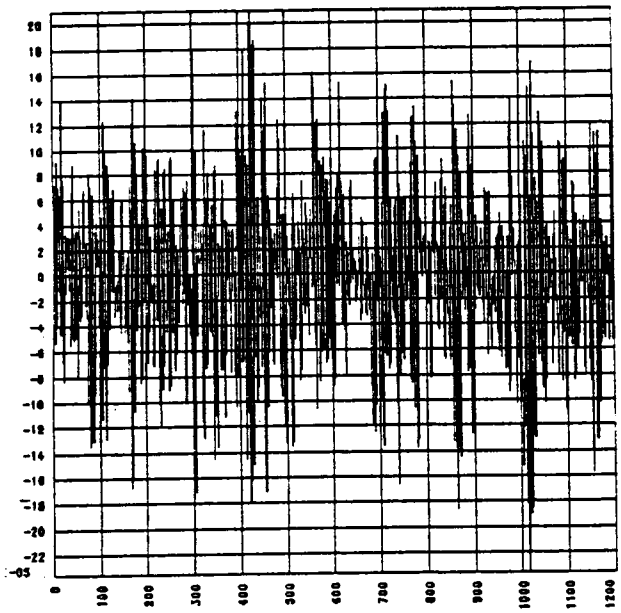

6.4.1 Ψ vs. x at t=1200

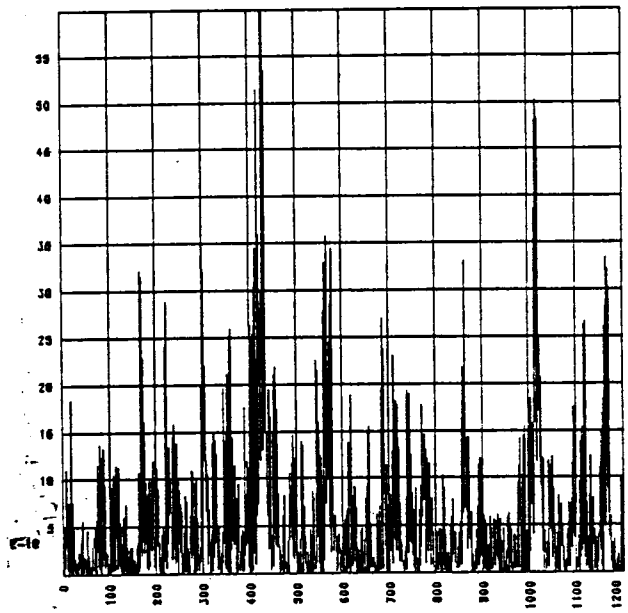

6.4.2 E vs. x at t=4200

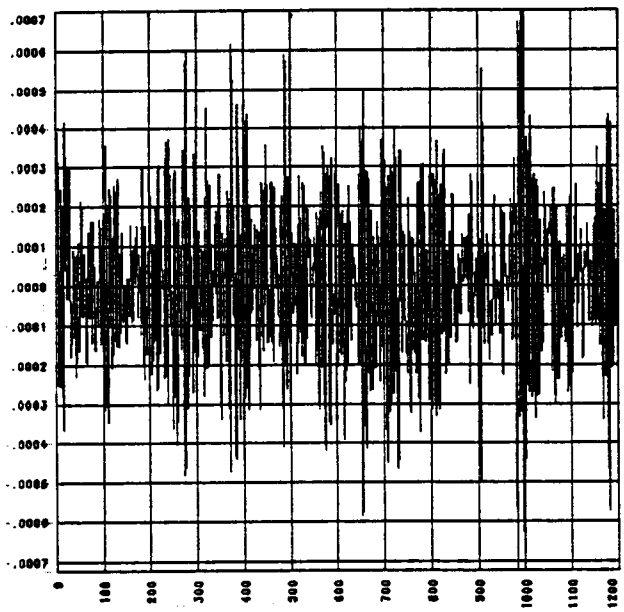

6.4.3 Ψ vs. x at t=4200

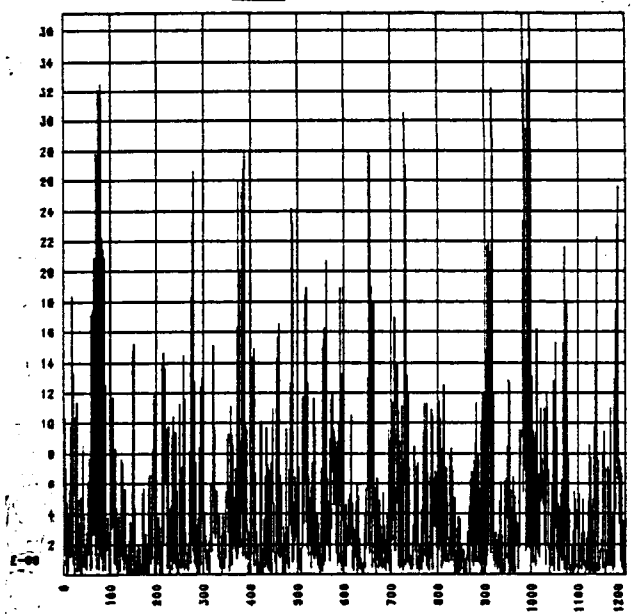

6.4.4 E vs. x at t=4200

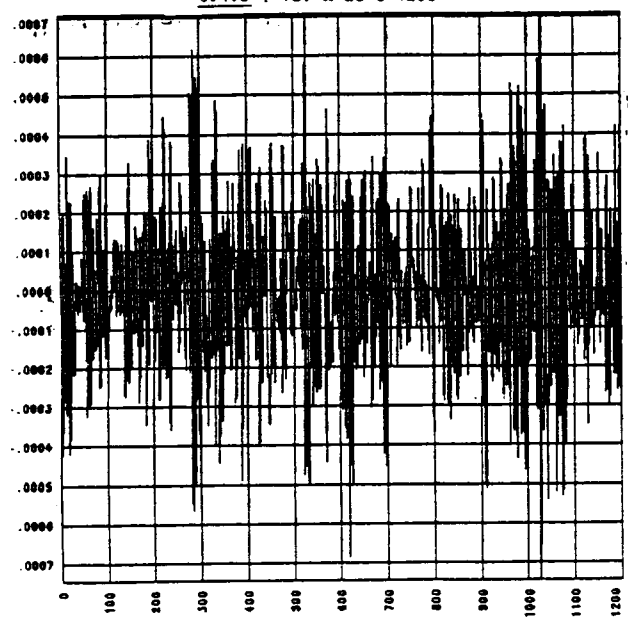

6.4.5 Ψ vs. x at t=6000

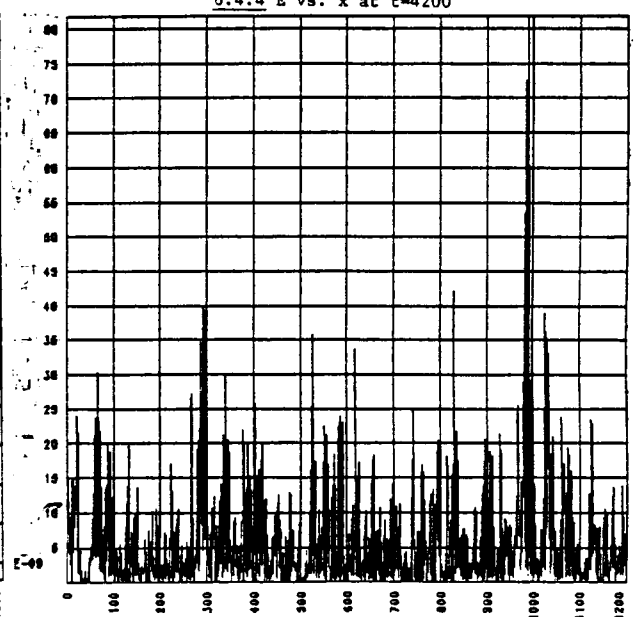

6.4.6 E vs. x at t=6000

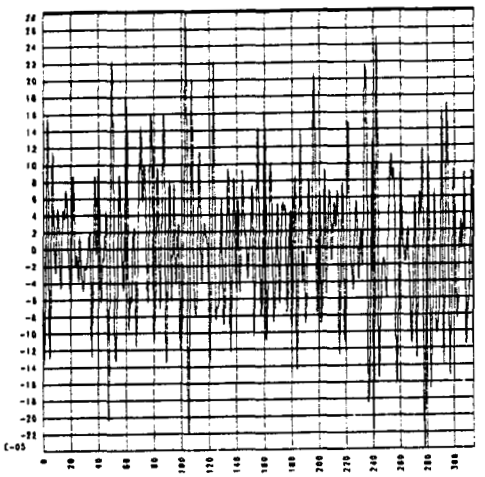

6.5.1 Ψ vs. x at t=4800

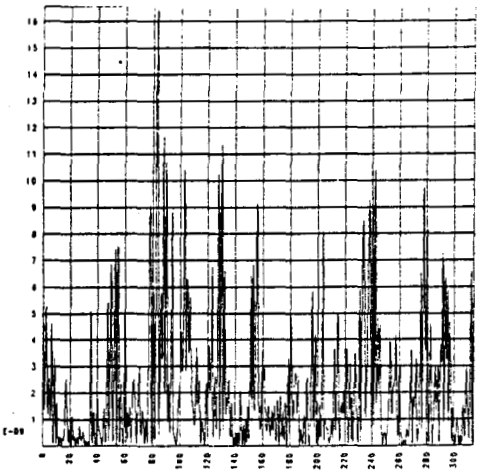

6.5.2 E vs. x at t=4800

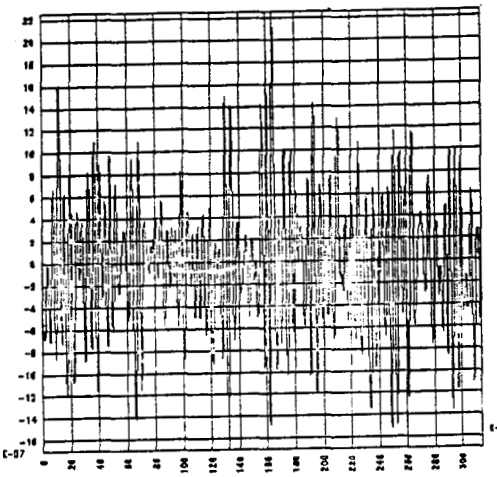

6.6.1 Ψ vs. x at t=3800

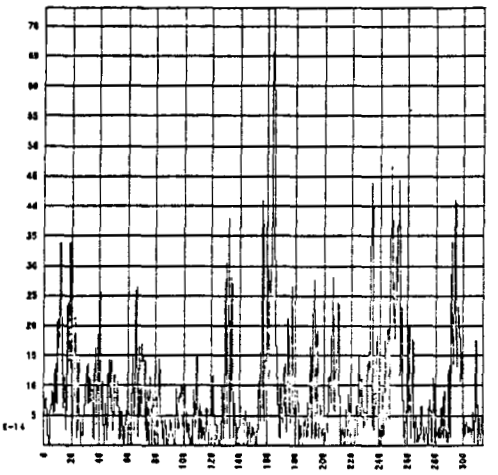

6.6.2 E vs. x at t=3800

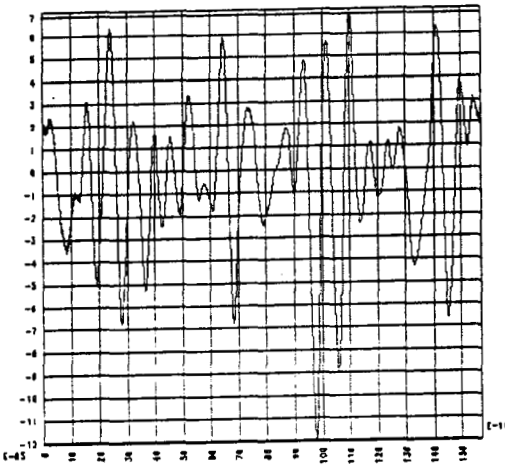

6.7.1 Ψ vs. x at t=1800

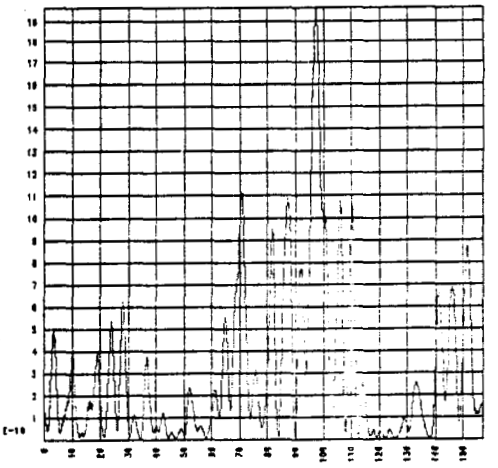

6.7.1 E vs. x at t= 1800

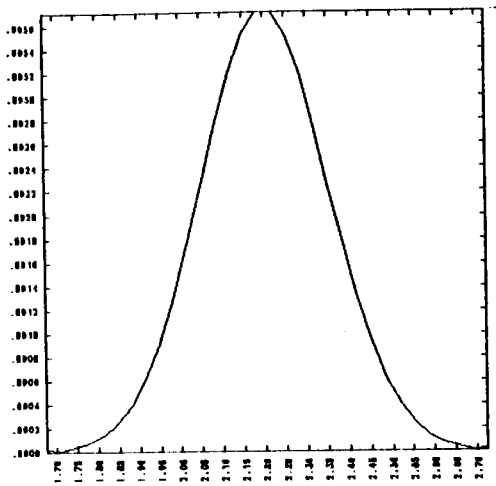

6.8.1 f(v) vs. v at t=0

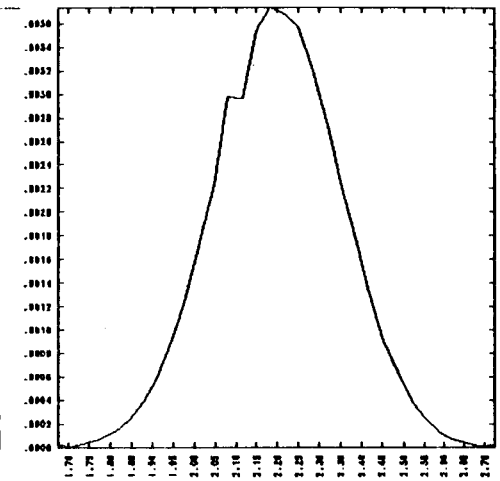

6.8.2 f(v) vs. v at t=2000

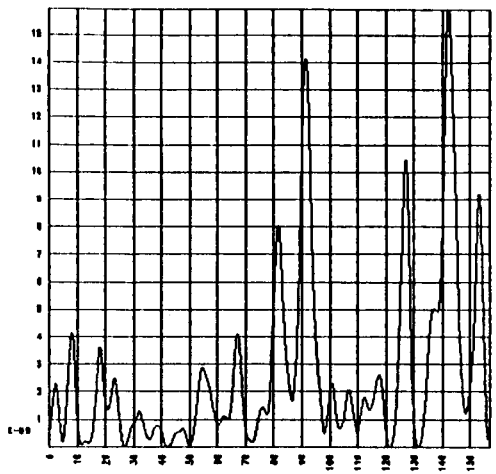

6.8.3 E vs. x at t=2000

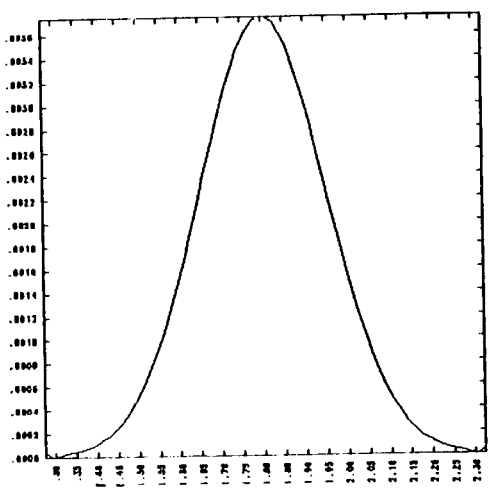

6.9.1 f(v) vs. v at t=0

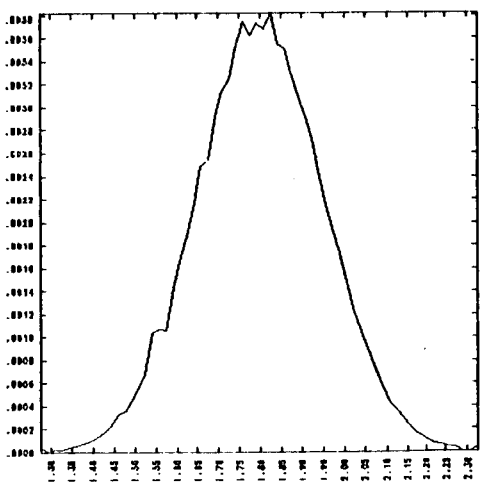

6.9.2 f(v) vs. v at t=2000

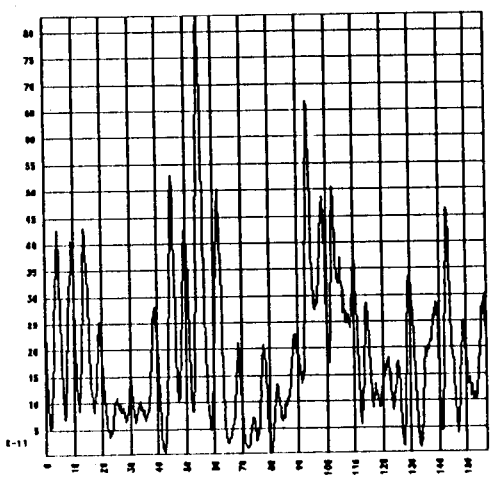

6.9.3 E vs. x at t=2000

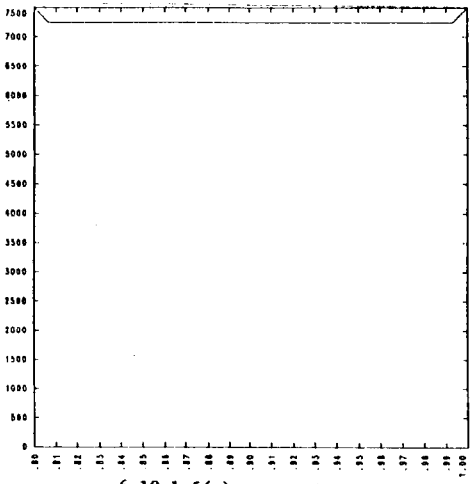

6.10.1 f(v) vs. v; initial

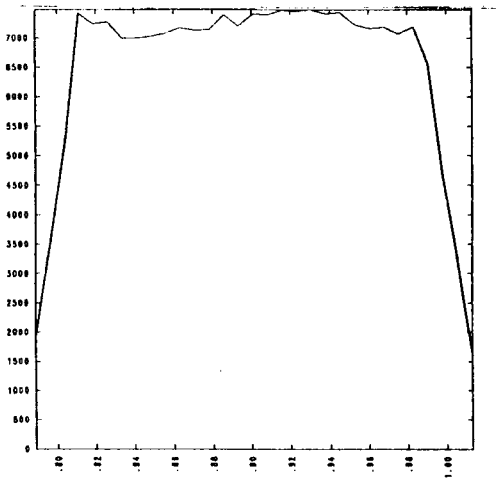

6.10.2 f(v) vs. v; κ=.1

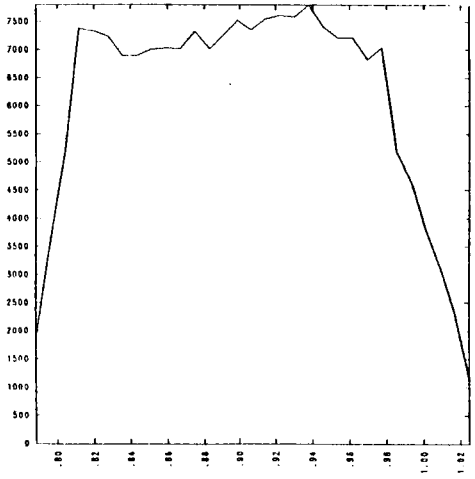

6.10.3 f(v) vs. v; κ=.2

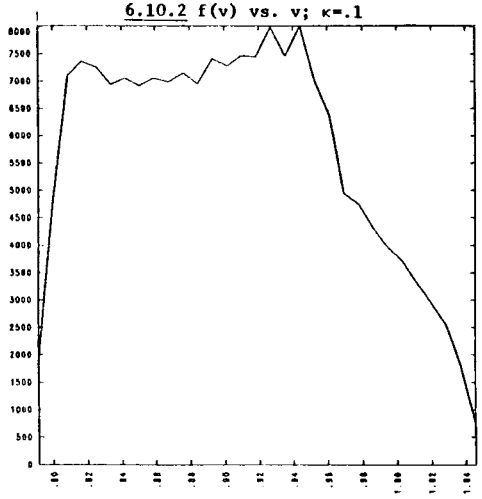

6.10.4 f(v) vs. v; κ=.4

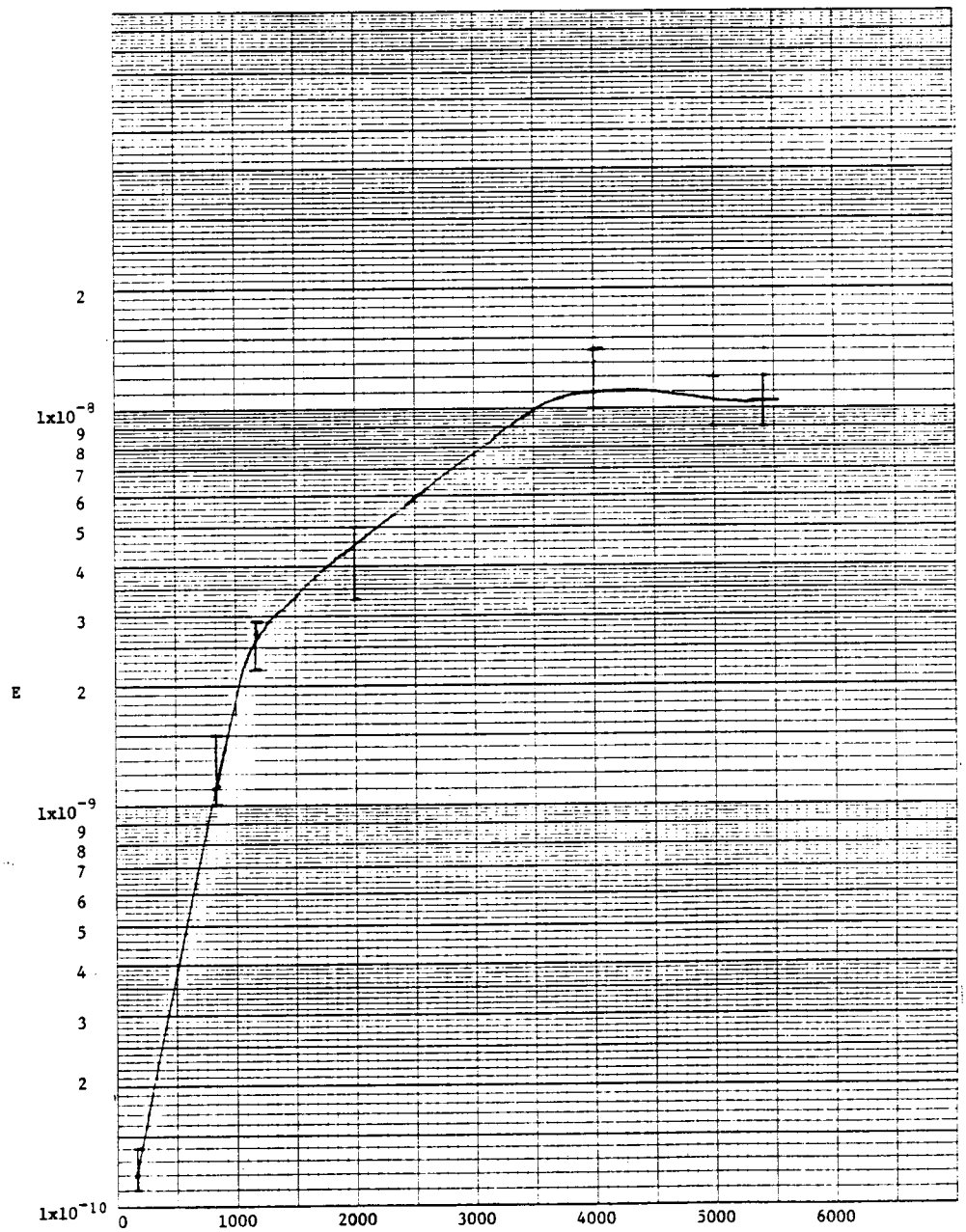

Figure 6.11 E vs. t for figures 6.2.1-6.2.15

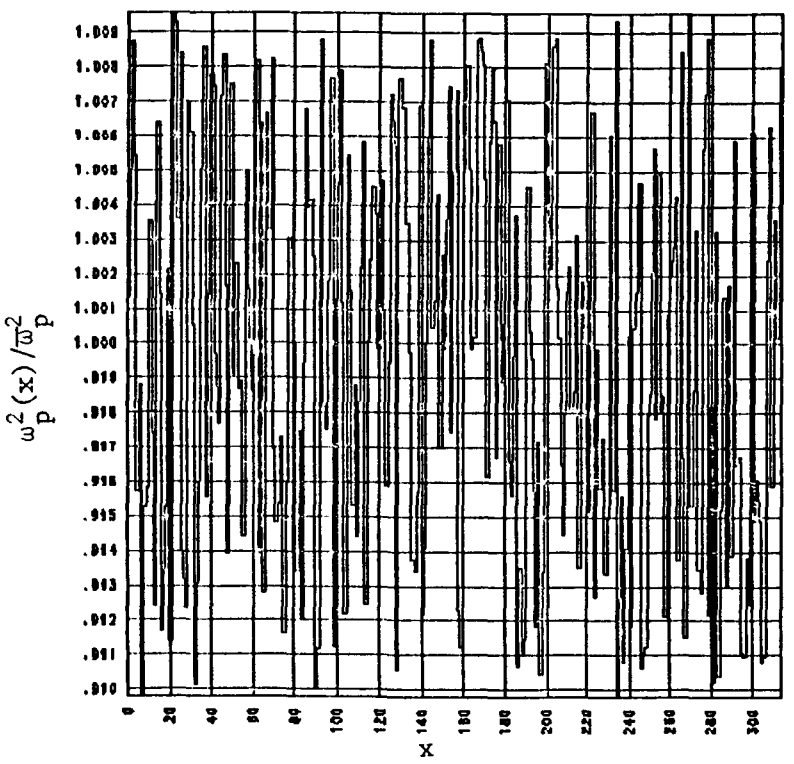

Figure B.1 Typical random density profile for simulations

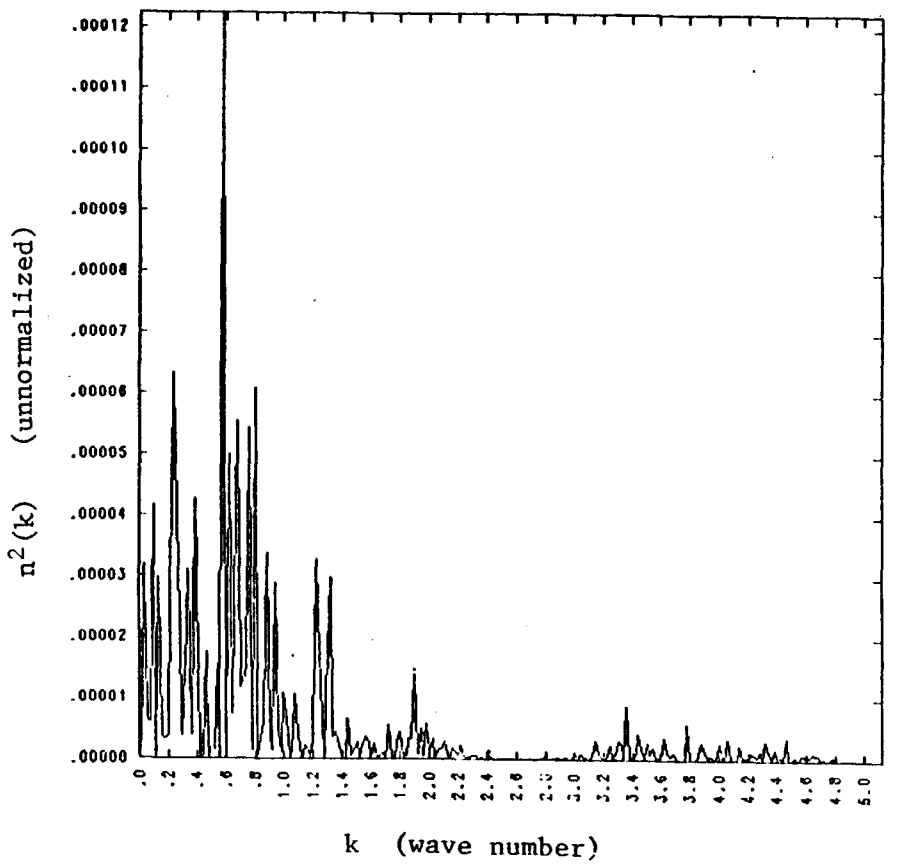

Figure B.2 Unnormalized power spectrum of the density profile of fig. B.1.